Impaired CD4 T Cell-Mediated Immunity After Sepsis

A DISSERTATION
SUBMITTED TO THE FACULTY OF
THE UNIVERSITY OF MINNESOTA
BY

Frances Victoria Sjaastad

IN PARTIAL FULFILLMENT OF THE REQUIERMENTS
FOR THE DEGREE OF
DOCTOR OF PHILOSOPHY

Thomas S. Griffith, Ph.D., Advisor

August 2020

Acknowledgements

I want to thank my advisor, Dr. Thomas Griffith, who has helped me achieve all the many successes throughout my graduate career. He always puts his students first and creates an environment where everyone succeeds together. I would also like to thank Tammy Kucaba for being so kind and always being my biggest lab cheerleader. I thank the members of my thesis committee: Drs. Kristin Hogquist, Michael Farrar, Ryan Langlois and Vaiva Vezys for their excellent advice and support. Thank you to all the members of the Center for Immunology and the Microbiology, Immunology, and Cancer Biology graduate program for providing a fun and collaborative environment to do research and learn.

Dedication

To my sister and best friend, Lucy, my parents Robin, and Victoria,

and my supportive boyfriend Matt.

Abstract

It is estimated that 1.7 million Americans suffer from sepsis every year. While improvements in intensive care over the last 30 years have reduced mortality from the initial septic event from 80% to 10-20%, sepsis survivors suffer from a functional impairment of the immune system resulting in increased susceptibility to secondary infection that can last for years. In fact, approximately 70% of sepsis related deaths are due to secondary infection that occurs after the initial septic event as result of immunosuppression. While our understanding of sepsis has grown and improved over the last several decades, there are currently no approved targeted therapies for treatment of the dysregulated host response to the initial infection or the subsequent sepsis induced immune suppression. An improvement of our understanding of the mechanisms responsible for the dysregulated host response to infection and the immunosuppression observed after sepsis will be critical for developing effective therapies and improving the survival and quality of life for septic patients.

Previous research has found that despite the transient nature of the CD4 T cell compartment depletion, recovery is uneven when looking at naïve antigen specific populations. Furthermore, it is unknown what impact this uneven recovery has on immunization responses, including CD4 T cell-dependent B cell responses, and how recovery occurs in memory populations of antigen specific CD4 T cells. In the following studies, we have investigated the hypothesis that alterations in the number and function of antigen specific populations of CD4 T cells after sublethal CLP-induced sepsis are responsible for the suppressed immunity that leads to increased mortality from secondary infection in sepsis survivors. Additionally, we have investigated inflammatory responses and CD4 T cell compartment depletion in an immune experienced mouse using various models of sepsis. Through these efforts we have uncovered

evidence of innate immune training in the cohoused immune experienced mouse which heightens inflammatory responses and reduces survival following sepsis onset.

Our rationale for these studies is that once we understand how immune experience influences inflammatory responses and cells within the adaptive immune system are affected during sepsis, we will be able to develop new and innovative therapeutic approaches to restore immune cell numbers and function in sepsis survivors.

Table of Contents

List of Figures

Chapter 2

Chapter 3

Chapter 4

Chapter 1: Background and Introduction

I. What is Sepsis?

Sepsis is defined as a life-threatening organ dysfunction caused by a dysregulated host response to infection[1,2]. Sepsis represents a significant but under acknowledged medical problem worldwide and in the United States where there are an estimated 1.7 million cases of sepsis annually resulting in 265,000 deaths, with the elderly and patients with comorbidities at particularly high risk for sepsis[3]. Furthermore, sepsis represents a significant social and economic burden costing an estimated 17 billion annually in the United States and the long-term health-related quality of life of survivors of sepsis diminished compared to that of the general population[4–7].

In the past, sepsis was understood as a predominately hyperinflammatory disease cause by an invasive pathogen. More recently it has become clear that sepsis is a highly heterogeneous disease consisting of prolonged inflammatory and immunosuppressive mechanisms occurring simultaneously and the inability for the immune system to return to homeostasis[8–12]. While sepsis is complex and variable, with both inflammatory and anti-inflammatory queues occurring in parallel, it is commonly understood to occur in two phases: the early hyperinflammatory phase and a late immunosuppressive phase. In the early phase of the disease both proinflammatory and anti-inflammatory mechanisms occur simultaneously. Despite the contrasting mechanisms of both inflammatory and anti-inflammatory signals occurring in tandem, this phase is characterized by a predominantly hyper-inflammatory state driven by proinflammatory cytokines and

chemokines in the presence of a disseminated infection[9]. In the late phase, following the initial hyperinflammatory phase, as the host recovers from the initial septic event, the immune system becomes hyporesponsive, leading to a chronic immunosuppressive state. Patients that survive the initial hyperinflammatory phase of sepsis suffer from low grade inflammation and protracted immune suppression that contribute to the majority of sepsis related deaths[9]. Early detection and advancements in critical care and life support medicine have greatly improved survival rates of patients in the 3 days following the initial injury leading to sepsis where acute death from sepsis is no longer the major cause of mortality for these patients[11]. Today, approximately 70% of sepsis-related deaths occur after the patient has recovered from the initial hyperinflammatory phase, with many patient deaths occurring weeks or months later[9]. Reduced numbers of immune cells in septic patients occur as the result of apoptotic lymphocyte death and contribute to the decreased responses to new or secondary infections and reactivation of latent viruses[2,13–21]. This sepsis-induced lymphopenia is transient but immune suppression and hypo-responsiveness after a septic event extend beyond the point of the recovery of absolute lymphocyte numbers[9,13]. This persistent immune suppression following a septic event is now considered a leading reason for the extended period of increased susceptibility to pathogens that are normally cleared in healthy individuals[4,19–21].

II. Immunopathology and Immunosuppression in Sepsis

Sepsis is commonly attributed to over exuberant immune activation in response to the loss of control of a localized infection resulting in a systemic or blood borne infection. Causes of sepsis are highly heterogeneous with the most common being

pneumonia, urinary tract infections, and intraabdominal infections with cultures positive for *Staphylococcus aureus*, *Streptococcus pneumoniae*, *Escherichia coli*, and *Pseudomonas aeruginosa*[5,22,23]. During an infection, complement is activated and cellular components of the innate immune system including macrophages, monocytes, dendritic cells, and neutrophils recognize conserved pathogen-associated molecular patterns (PAMPs) on invading pathogens using pattern recognition receptors[24]. Typically, the innate immune system can clear the infectious microorganisms quickly. However in sepsis the pathogen escapes control by the immune system resulting in excessive activation of the innate immune system through PAMPs, pro-inflammatory cytokines and chemokines including Tumor necrosis factor (TNF), IL-1β and IL-6, complement activation, and platelet activation[25–28]. These pro-inflammatory mediators are critical for activating immune mechanisms such as leukocyte recruitment, cell death, and coagulation needed to clear and prevent spread of the pathogen. However, when unleased systemically they can contribute to vascular leakage, neutrophil recruitment, disseminated intravascular coagulation (DIC), multi-organ dysfunction syndrome (MODS), and the release of damage-associated molecular patterns (DAMPs). Furthermore, the systemic inflammatory response syndrome (SIRS) results in a striking lymphocyte depletion through apoptotic mechanisms and activates a compensatory anti-inflammatory response syndrome (CARS). This response results in widespread immune suppression and enhanced susceptibility to secondary infection and viral reactivation[13,17,29–31].

Immune suppression in septic patients was first reported by Meakins *et al.* in 1977 in a publication which observed reduced delayed type hypersensitivity (DTH) responses following skin testing with various recall antigens[32]. Reduced DTH responses were associated with increased risk for secondary infection and mortality[32–34]. Following the observations of reduced DTH responses in septic patients, reports of immune suppression in septic patients became more numerous and span various cell types and immune mechanisms. Particularly in the last ten years publications on sepsis induced immune suppression have skyrocketed. Today it is well known that sepsis results in profound alterations to the immune system. These include depletion and anergy of various immune cells including dendritic cells (DCs), CD4 and CD8 T cells and B cells and expansion of immunosuppressive cell types such as regulatory T cells (Tregs) and myeloid-derived suppressor cells (MDSCs)[16,18].

Apoptosis is one of the most frequently described mechanisms involved in the loss of lymphocytes and sepsis induced immune suppression. Hotchkiss *et al.* observed apoptotic cell death in a large proportion of spleen (56.3%), colon (47.1%), and ileum (27.7%) specimens collected from septic patients[15]. In the same study, immunohistochemical staining demonstrated increased active caspase-3 in spleens from septic shock patients compared to other critically ill patients without sepsis. These findings are supported by others who have found elevated caspase activity and enhanced annexin V staining in apoptotic lymphocytes isolated from the spleens of septic patients. Blood samples from septic patients show increased lymphocyte apoptosis with some cells expressing active caspase-9 and other cells expressing active caspase-8 potentially

suggesting that both the death-receptor and mitochondrial pathway can induce lymphocyte apoptosis in sepsis[35]. Using various models such as transgenic mice and caspase-inhibitors, studies have shown that blocking of lymphocyte apoptosis improves survival in sepsis[36–39].

III. Mouse Models of Sepsis

Sepsis is a complex and widely heterogeneous syndrome with many variables, including the initial injury, location of infection, pathogen identity, immune status, patient genetics, and comorbidities. Due to the significant burden on the healthcare system, many resources have been dedicated to developing, improving, and studying various models of sepsis. However, because of the complex and heterogenous nature of sepsis, few models have managed to effectively recreate the biochemical and pathophysiological characteristics observed in septic patients.

Numerous murine models of sepsis have been developed over the last several decades. Typically these rely on one of three approaches: delivery of exogenous pathogen-derived toxins (such as zymosan, lipopolysaccharide), infectious pathogens (bacteria, viruses or fungus), or surgical disruption of barrier tissues. The surgical models include colon ascendens stent peritonitis and cecal ligation and puncture (CLP) to induce polymicrobial sepsis. In addition to these three approaches, “two-hit” models which apply two of the above approaches have been utilized in an effort to recapitulate septic outcomes as a result of secondary nosocomial infection[40].

The delivery of exogenous pathogen-derived toxins such as zymosan and lipopolysaccharide (LPS) have the advantage of being simple to administer, highly reproducible, and result in elevation of several proinflammatory cytokines found to be increased in septic patients[41]. However, because these agents rely on activation of the innate immune system through a single receptor (Dectin-1 and Toll-like receptor 4) and do not involve an infectious pathogen, they fail to recapitulate the complex nature of the proinflammatory cytokine response seen in humans including peak levels and duration. It is also important to note that unlike humans, most strains of laboratory mice are naturally endotoxin. The use of infectious pathogens to induce sepsis is more complicated than zymosan and lipopolysaccharide and requires the researcher to grow and quantify the microorganism prior to inoculation. Additionally, while this model allows for the study of the host response to a pathogen, infection with a single bacteria, virus, or fungi does not accurately recapitulate the infectious agents in septic patients, which are typically polymicrobial and derived from the hosts' microbiome. To initiate a polymicrobial sepsis derived from the hosts' microbiome, some have implemented the cecal slurry model of sepsis which involves harvesting cecal material from donor mice and preparing an injectable slurry which is injected intraperitoneally (i.p.) into recipient mice[42]. However, injection delivery of infectious pathogens does not involve tissue injury and necrosis, common and important factors in human sepsis[41].

Of the murine models used to study the complex, multifactorial pathophysiology of sepsis, the surgical cecal ligation and puncture model is one of the most popular. The CLP technique was initially developed as a porcine model of sepsis, and was rapidly

adapted to other animal model systems[43–45]. Today, this model typically involves anesthetization of a mouse, an abdominal incision, and ligation and puncture of the cecum. This results in tissue necrosis and polymicrobial sepsis secondary to autologous fecal leakage, as well as hemodynamic and biochemical responses similar to those seen in septic humans[41,43,46,47]. Additionally, a transient numerical reduction of multiple immune cell types, followed by the development of prolonged immune suppression, occurs in CLP-induced sepsis just as in humans[48]. Use of the CLP model has led to a vast expansion in knowledge regarding the intricate changes that occur within the immune system following a septic event.

In spite of extensive research into experimental models of sepsis, few effective therapies for human septic patients have been produced. While the CLP mouse model of sepsis accurately recapitulates many aspects of human sepsis, key differences between laboratory mice and humans fighting sepsis have impeded discovery of effective sepsis therapies[41,43,46,47]. One of these differences stems from the fact that humans are exposed to commensal and pathogenic microbes on a daily basis, which together with vaccination shape and mature both the innate and adaptive arms of the immune system to provide long-lasting protection against future microbial challenge. In contrast, immunological memory is minimal, equivalent to that of neonatal human, in most laboratory mice used in biomedical research due to specific pathogen free (SPF) housing conditions[49]. However, mice in the wild and available at local pet stores have increased exposure to naturally occurring murine microbes and pathogens and subsequently have more immunological memory comparable to the immune system of adult humans[50]. It

has been shown that by cohousing laboratory mice with microbially experienced pet store mice, natural pathogen transfer can alter the murine immune system to more closely resemble that seen in adult humans[50]. The maturation of the immune system in cohoused (COH) mice following microbial experience has a significant impact on immune responses[50]. Use of SPF-housed laboratory mice in the CLP sepsis model has revealed and continues to reveal a wealth of information into the pathophysiology and immunoparalysis seen during sepsis, but the use of microbially-experienced 'dirty' mice can provide sepsis researchers with another important preclinical tool for interrogating sepsis.

In Chapter 4, I will present data from COH mice illustrating how microbial exposure can enhance the innate immune response and increase the risk of immunopathology from a severe cytokine storm in various experimental models of sepsis.

IV. CD4 T Cell Loss and Dysfunction in Sepsis

CD4 T helper (Th) cells are critical for the full and proper function of various immune cell populations and are essential in eliciting a productive and protective immune response[24]. CD4 T cells have the unique flexibility of functioning in an array of immunological settings due to their plastic ability to differentiate into a variety of phenotypic subsets based on the inflammatory milieu produced in response to the infectious stimuli[51,52]. The phenotypic subsets of CD4 T cells include Th1, Th2, Th17, follicular helpers (Tfh) and Tregs[24,52]. Upon infection, CD4 T cells differentiate into

effector T cell subsets and proliferate. Differentiation is dictated by the local cytokine environment, innate immune cell contacts, costimulatory molecule signaling, T cell receptor (TCR) signal strength and Notch signaling[24,52]. Following differentiation, each T helper cell fate has a unique master transcription factor that promotes linage specific functions including cytokine production[24]. Th1 cells express IFN-γ which activates macrophages and promotes expression of major histocompatibility complex (MHC) class I[24,52]. Th1 cells are important in defending against intracellular bacteria and viruses[24]. In contrast, Th2 cells activate eosinophils and basophils though production of IL-4, IL-5 and IL-13 allowing for defense against helminth parasites[24]. Th17 cells help to eradicate extracellular bacteria and fungi by activating neutrophils and the epithelium through expression of IL-17 and IL-22[24]. Tfh express CD154 (CD40 ligand) and IL-21 and facilitate affinity maturation, proliferation, and efficient isotype switching in primary and memory B cells[24]. While the most CD4 subsets promote pathogen clearance, regulatory T cells work to regulate inflammatory responses, reduce tissue damage during infection and prevent autoimmunity, in part through the production of IL-10 and TGF-β[24]. Following pathogen clearance, the responding effector CD4 T cells contract leaving behind a small pool of memory CD4 T cells[53–55]. These memory cells are primed to respond more quickly and robustly upon secondary pathogen encounter[53–55].

CD4 T cell counts in patients with sepsis are greatly reduced, frequently to levels as low as patients with life-threatening AIDS[16,56–60]. While the lymphopenia is transient with many studies seeing recovery of circulating CD4 T cells (≥500 cells/mm^3)

by 3 or 4 weeks post sepsis, other studies have observed reductions in the number of circulating CD4 T cells (<500 cells/mm^3) in septic patients up to 6 weeks post sepsis[57,61]. Sepsis-induced depletion is observed in naïve and antigen experienced CD4 T cell populations[62–64]. CD4 T cells remaining in the periphery after CLP-induced sepsis undergo homeostatic proliferation to compensate for numerical reduction and acquire memory-like characteristics, including expression of antigen experienced or memory phenotype markers CD44, CD11a, and CD49d[62,65]. Cabrera-Perez *et al.* found that numerical recovery of the CD4 population following sepsis is not dependent on output from the thymus and that thymectomized mice have similar CD4 T cell recovery kinetics.

In addition to the numerical depletion of CD4 T cells, there are significant functional deficits in the CD4 compartment that persist after sepsis. While not solely dependent of CD4 T cells, the reduced DTH response discussed previously suggests a potential defect in CD4 T cell function as cytokine production from CD4 T cells is required for DTH responses. Splenocytes freshly isolated postmortem from septic patients and stimulated with lipopolysaccharide or anti-CD3/anti-CD28 antibodies have been found to produce little to no TNF, IFN-γ, IL-6 and IL-10[66]. Studies specifically assessing CD4 T cell function have found reduced ability to proliferate and produce IFN-γ[67,68]. Furthermore, heightened expression of inhibitory receptors including PD-1, TIM3, LAG3, 2B4 and CTLA-4 has been reported on CD4 T cells[63,66,69–71]. While most CD4 T cells subsets (Th1, Th2, Th17 and Tfh) are reduced numerically and functionally after sepsis, Tregs are not similarly impacted. Several studies have shown

that Treg numbers are increased after sepsis and cytokines made by Tregs are increased in the serum of sepsis survivors[72–74].

Studies examining sepsis-induced lymphocyte apoptosis, depletion, and dysfunction typically examine total populations of CD4 and CD8 T-cells, occasionally categorizing them by naïve and antigen experienced based on CD44 expression. While this depth of differentiation is informative, it does not adequately assess the unique characteristics of individual antigen-specific populations. Employing a peptide:MHC class II tetramer enrichment technology the Griffith lab has studied endogenous antigen-specific CD4 T cell repertoires at different time points after sepsis[31,62,64]. This work has found asymmetric depletion and recovery of antigen-specific naive CD4 T cells after sepsis. Antigen-specific populations with incomplete naive precursor recovery after sepsis correlated with reduced proliferative capacity, cytokine production and pathogen clearance during antigen-specific CD4 T cell responses. Additionally, it was found that sepsis alters TCR clonotype composition, an observation that has also been made in human septic patients[75].

To build on our current understanding of how sepsis impacts CD4 T cells, in Chapter 3 I have employed peptide:MHC class II tetramer enrichment technology to investigate how CLP-induced sepsis alters the number and function of antigen-specific memory CD4 T cells and contributes to the characteristic long-lasting immunoparalysis seen after sepsis.

V. Impact of Sepsis on B Cells and Antibody Production

Most vaccines generate immunity to viruses (Influenza, Polio, Human papillomavirus) and bacteria (diphtheria, tetanus, pertussis) in part by producing high affinity antibodies for neutralization, opsonization, antibody-dependent cellular cytotoxicity and complement activation[76–79]. Antibody responses can be classified as T cell-dependent and T cell-independent based on their requirement for CD4 T cell help. Typically, B cell responses that result in high affinity, isotype switched antibodies require T cell help. To obtain CD4 help, B cells must present antigen-derived peptides on MHC class II (p:MHCII) to a CD4 cell that has been activated by the same p:MHCII complex[24]. CD4 T cells that detect B cells presenting their cognate antigen will provide critical help to the B cell in the form of CD154 and IL-21 which allows the B cell to proliferate and undergo immunoglobulin heavy chain isotype switching[24,80,81]. The cells resulting from this proliferative burst will differentiate into plasmablasts, plasmacells, memory B cells, and germinal center (GC) cells[24,80]. Plasmablasts work to increase the levels of circulating high-affinity antibodies. Memory B cells are important for responding to a secondary infection and can generate plasmacells more rapidly than naïve B cells[82]. Some of the B cells will upregulate the transcription factor Bcl6 and travel to a primary lymphoid follicle, become GC B cells and undergo further class switching, Tfh-dependent somatic hypermutation, and affinity maturation[80]. These processes mutate the variable regions of the immunoglobulin genes and are essential for generating and selecting B cells producing the highest affinity antibodies to eliminate pathogens[24,80].

The consequences of sepsis on B cell phenotype, function, and CD4 T cell-dependent antibody responses are poorly understood and rarely studied. B cell numbers in patients with sepsis are greatly depleted due to apoptosis. Additionally, reduced lymphoid follicle area and B cell area in secondary lymphoid organs have been observed[16,56]. While there appears to be agreement across several studies that the total B cell population is reduced, there is conflicting evidence regarding other B cell population characteristics post-sepsis. One study observed reductions in the frequency of memory B cells but not naïve[83], while another group found reductions in naïve B cells but not memory[83,84]. Reduced serum levels of IgM have been observed in adult septic patients[84], while in the colon ascendens stent peritonitis and CLP mouse models of sepsis increased baseline IgM and IgG serum concentrations have been reported[85,86].

Despite the many studies examining CD4 T cell and B cell characteristics after sepsis, there is a paucity of information on the impact of sepsis on immunization and CD4 T cell-dependent antibody responses. The one study examining the impact of sepsis on immunization and CD4 T cell-dependent antibody responses found that antigen-specific antibody production was strongly impaired when mice were immunized with ovalbumin in alum 2 days post CLP-induced sepsis[86]. Specifically, the authors observed large reductions in OVA-specific IgM, IgG1 and IgG2a[86].

In Chapter 2, I present data showing that CLP-induced sepsis impacts humoral immunity by affecting the number and function of both antigen-specific B cells and CD4 Tfh cells.

VI. Concluding Remarks

Sepsis is a complex and widely heterogeneous syndrome with devastating effects on host immunity. In the following studies, we have investigated the long-term impacts of sepsis on CD4 T cell responses to immunization and secondary infection. We have also investigated inflammatory responses and CD4 T cell compartment depletion in immune experienced mice using various experimental models of sepsis. We have found that alterations in the number and function of CD4 T cells after sublethal CLP-induced sepsis are responsible for the suppressed immunity that leads to increased mortality from secondary infection. Additionally, we have uncovered evidence of innate immune training in cohoused immune experienced mice which heightens inflammatory responses to various experimental models of sepsis.

Chapter 2

Sepsis-induced Immunosuppression

Impairs Ag-Specific T Cell-Dependent B Cell Responses[1]

[1] This Chapter has been previously published. Frontiers in Immunology, Volume 9. Sjaastad FV, Condotta SA, Kotov JA, Pape KA, Dail C, Danahy DB, Kucaba TA, Tygrett LT, Murphy KA, Cabrera-Perez J, Waldschmidt TJ, Badovinac VP and Griffith TS. Polymicrobial Sepsis Chronic Immunoparalysis Is Defined by Diminished Ag-Specific T Cell-Dependent B Cell Responses, pp.2532 © 2018 Sjaastad, Condotta, Kotov, Pape, Dail, Danahy, Kucaba, Tygrett, Murphy, Cabrera-Perez, Waldschmidt, Badovinac and Griffith.

Immunosuppression is one hallmark of sepsis, decreasing the host response to the primary septic pathogens and/or secondary nosocomial infections. CD4 T cells and B cells are among the array of immune cells that experience reductions in number and function during sepsis. “Help” from follicular helper (Tfh) CD4 T cells to B cells is needed for productive and protective humoral immunity, but there is a paucity of data defining the effect of sepsis on a primary CD4 T cell-dependent B cell response. Using the cecal ligation and puncture (CLP) mouse model of sepsis induction, we observed reduced antibody production in mice challenged with influenza A virus or TNP-KLH in alum early (2 days) and late (30 days) after CLP surgery compared to mice subjected to sham surgery. To better understand how these CD4 T cell-dependent B cell responses were altered by a septic event, we immunized mice with a Complete Freund's Adjuvant emulsion containing the MHC II-restricted peptide $2W1S_{56–68}$ coupled to the fluorochrome phycoerythrin (PE). Immunization with 2W1S-PE/CFA results in T cell-dependent B cell activation, giving us the ability to track defined populations of antigen-specific CD4 T cells and B cells responding to the same immunogen in the same mouse. Compared to sham mice, differentiation and class switching in PE-specific B cells were blunted in mice subjected to CLP surgery. Similarly, mice subjected to CLP had reduced expansion of 2W1S-specific T cells and Tfh differentiation after immunization. Our data suggest CLP-induced sepsis impacts humoral immunity by affecting the number and function of both antigen-specific B cells and CD4 Tfh cells, further defining the period of chronic immunoparalysis after sepsis induction.

I. Introduction

Vaccination or infection is one of the most effective ways to generate immunity to microbes. Efficacious vaccinations and natural infection elicit antibody (Ab) production by B cells and their progeny, providing a first line of defense against subsequent microbial invasion. B cells recognize a wide variety of antigens (Ag), including proteins, lipids, polysaccharides, nucleic acids, and chemicals that bind to surface IgM or IgD[87]. While serving as a major means of protection against extracellular pathogens and the various toxins they produce, Ab are also a vital means of defense against intracellular pathogens (including viruses) because of their ability to neutralize the pathogen before they can enter a cell, preventing the spread of infection[88,89]. Ab responses can be classified as "T cell-dependent or –independent," based on the use of CD4 T cell help[90]. B cell responses to protein Ag in the absence of CD4 T cell help are weak, producing Ab with low affinity. In contrast, B cell responses generated with the help of CD4 T cells produce high affinity, class-switched Ab.

There has been considerable interest in recent years in $CXCR5^{+}PD\text{-}1^{+}Bcl6^{+}$ follicular helper CD4 T (Tfh) cells—the specialized CD4 T cell subset that provides help to B cells—and understanding the role they play in facilitating the proliferation and function of primary and memory B cells[91,92]. When Tfh cells detect B cells presenting their cognate Ag, they upregulate CD154 expression and secrete a number of cytokines to promote B cell proliferation and differentiation into plasma cells[93,94]. During the early Ab response plasma cells secrete Ab and some degree of isotype switching occurs. A few of the activated B cells return to the follicle, accompanied by Tfh cells, where they

proliferate and form a germinal center (GC) in response to the Tfh cell-derived signals. The proliferating GC B cells undergo immunoglobulin (Ig) heavy chain isotype switching, somatic hypermutation of Ab gene variable regions, and affinity maturation. Repeated exposure to their cognate Ag promotes the B cells to produce the highest affinity and most efficacious Ab for neutralization of microbes and their toxic products and differentiate into long-lived plasma cells and memory B cells[95–97].

The importance of both the humoral and cellular arms of the adaptive immune system for overall health is dramatically illustrated by individuals with immune system defects being highly susceptible to serious and often life-threatening infections. States of immune deficiency can be congenital (e.g., impaired T and/or B cell development) or acquired (e.g., HIV infection, iatrogenic (post-organ transplant) immune suppression, or surgery/trauma). The combination of quantitative and qualitative impairments to multiple compartments of the immune system that develop in the wake of a septic event lead to an acquired immune deficiency[98]. Sepsis, currently defined as life-threatening organ dysfunction resulting from the dysregulated host response to infection[2], is responsible for thousands of deaths annually[99]. As the host recovers from the initial septic event, the immune system becomes hyporesponsive, resulting in a long-lasting immunosuppressive state. Advances in critical care and life support medicine have greatly improved survival rates of patients in the initial hyperinflammatory phase of sepsis, such that the acute cytokine storm is responsible for only ~30% of the sepsis-related mortality. Today the majority of sepsis-related deaths occur after the patient has recovered from the initial hyperinflammatory phase, with many patient deaths occurring

weeks and months later[100,101]. Reduced numbers of immune cells in septic patients contribute to the decreased responses to new and secondary infections[48,102]. While the characteristic sepsis-induced lymphopenia is transient, the prolonged immune suppression that develops after a septic event and remains even once lymphocyte numbers normalize is now considered a leading cause of prolonged susceptibility to secondary pathogens normally handled by the immune system in healthy individuals[9].

Studies in human septic patients show both CD4 T cells and B cells are reduced during the hyperinflammatory phase of sepsis[16], but there is limited data detailing the long-term impact of sepsis on these cells within the context of a CD4 T cell-dependent B cell response. We have taken advantage of using peptide:MHC I or II tetramers to track the number and function of endogenous Ag-specific CD8 or CD4 T cell populations[62,64,103] to investigate how specific subsets of the T cell compartment are quantitatively and qualitatively affected in the mouse model of cecal ligation and puncture (CLP)-induced polymicrobial sepsis[47]. Similar approaches can identify endogenous Ag-specific B cells, such as B cells specific for the commonly used fluorochrome phycoerythrin (PE)[104–106]. The objective of this study was to define the mechanism(s) responsible for the impairment of primary CD4 T cell-dependent B cell responses in the septic host using the CLP model followed by immunization with an Ag containing defined CD4 T cell and B cell epitopes. Our data suggest CLP-induced sepsis impacts humoral immunity by affecting the number and function of both Ag-specific B cells and CD4 Tfh cells.

II. Materials and Methods

Mice

8 week-old female C57BL/6 mice were purchased from the National Cancer Institute (Frederick, MD) and maintained in AALAC-approved animal facilities at the University of Minnesota and University of Iowa at the appropriate biosafety level. Experimental procedures were approved by the University of Minnesota and University of Iowa Institutional Animal Care and Use Committees and performed following the Office of Laboratory Animal Welfare guidelines and PHS Policy on Human Cancer and Use of Laboratory Animals.

Cecal Ligation and Puncture (CLP)

Sepsis was induced by CLP (24). Briefly, mice were anesthetized using isoflurane (2.5% gas via inhalation) or Ketamine/xylazine (87.5 and 12.5 mg/kg, respectively, i.p.). The abdomen was shaved and disinfected with 5% povidone-iodine antiseptic. Bupivicaine (6 mg/kg s.c.) was then administered at the site where a midline incision was made. The distal third of the cecum was ligated with 4-0 silk suture and punctured once with a 25-g needle to extrude a small amount of cecal content. The cecum was returned to the abdomen, the peritoneum was closed via continuous suture, and the skin was sealed using surgical glue (Vetbond; 3M, St. Paul, MN). Meloxicam (2 mg/kg) in 1 ml saline was administered at the conclusion of surgery and the following 3 days for post-operative analgesia and fluid resuscitation. Mice were monitored daily for weight loss and pain for at least 5 days post-surgery. To control for non-specific changes from the surgery, sham mice underwent the same laparotomy procedure excluding ligation and puncture.

Immunizations

On days 2 or 30 after sham or CLP surgery, B6 mice were immunized with the following reagents: (1) influenza A virus (A/PR/8; 10^5 PFU in 100 μl PBS i.p.; obtained from Dr. Ryan Langlois, University of Minnesota); (2) 2,4,6 trinitrophenyl-conjugated keyhole limpet hemocyanin [TNP-KLH; 50 μg i.p. (Biosearch Technologies, Novato, CA)] precipitated in alum (100 μg) or mixed with CpG containing oligonucleotide 1826 (10 μg; TCCATGACGTTCCTGACGTT), followed 3 weeks later by a second immunization; or (3) 2W1S:PE conjugates [i.p. injection of 0.6 μg 2W1S peptide (EAWGALANWAVDSA; GenScript, Piscataway, NJ) conjugated to 2.4 μg PE (ProZyme; Hayward, CA) emulsified in Complete Freund's Adjuvant (CFA; Sigma-Aldrich, St. Louis, MO)][107]. The 2W1S:PE conjugate was formed by combining biotinylated 2W1S peptide with streptavidin-PE at a 4:1 ratio.

Enrichment and Analysis of Ag-Specific B Cells and CD4 T Cells and B Cells

To quantify the number of PE-specific B cells and 2W1S-specific CD4 T cells in mice following sham or CLP surgery, an enrichment protocol was used[104–106,108]. Briefly, spleens and peripheral LN (axillary, brachial, cervical, inguinal, and mesenteric) were harvested for each mouse analyzed. Pooled LN [in 1 ml of FACS buffer (PBS containing 0.1% NaN_3 and 2% FBS)] were mashed on a nylon mesh into a single-cell suspension. The spleen from the same mouse was then added, along with 1 ml of RPMI-1640 medium containing Collagenase P (0.2 mg/ml final), Dispase (0.8 mg/ml final), and DNase I (01 mg/ml final). A single-cell suspension from these pooled lymphoid tissues was then generated using a GentleMACS dissociator (Miltenyi Biotech). This suspension

was incubated in a 37°C water bath for 20 min, and then run on the GentleMACS a second time. Ten (10) ml of ice cold FACS buffer containing 5 mM EDTA was added to the dissociator tubes, which were inverted several times to wash the top of the tubes before decanting into new 50 ml conical tubes. The dissociator tubes were rinsed with an additional 5 ml of ice cold FACS buffer, which was then decanted into the corresponding 50 ml conical tubes. The cells were pelleted by centrifugation, and then resuspended in 400 µl FACS buffer containing 5 mM EDTA and anti-CD16/32 mAb (clone 93, 1:100 dilution; BioLegend) to block Fc receptors. In some cases, the single-cell suspension was divided to permit separate enrichments for the B cells and CD4 T cells from the same sample.

B Cell Enrichment

Cells were incubated with PE (1 µg; Prozyme, Hayward, CA) for 30 min on ice. After washing with 10 ml cold FACS buffer with 5 mM EDTA, the cells were then incubated with 25 µl anti-PE-conjugated magnetic microbeads (Miltenyi Biotec) for 30 min on ice. The cells were washed, resuspended in 3 ml FACS buffer, and then passed over a magnetized LS column to enrich for the PE-specific cells. The column was washed twice with 3 ml of FACS buffer, and the bound cells were eluted from the column by pushing 5 ml of buffer with a plunger.

CD4 T Cell Enrichment

I-A^b-specific tetramers containing 2W1S (EAWGALANWAVDSA) were used to identify and enrich Ag-specific CD4 T cells[108–110]. Briefly, biotinylated I-A^b molecules containing the 2W1S peptide covalently linked to the I-A^b β chain were

produced in Drosophila melanogaster S2 cell along with the I-A^b α chain[108]. The monomers were purified, and then made into tetramers with streptavidin-allophycocyanin (SA-APC; Prozyme). Tetramers (10 nM final concentration) were then added to single-cell suspensions in 300 µl tetramer staining buffer (PBS containing 5% FBS, 2 mM EDTA, and 50 µM Dasatinib, 1:50 normal mouse serum, and 1:100 anti-CD16/32 mAb). The cells were incubated in the dark at room temperature for 1 h, followed by a wash in 10 ml ice cold FACS Buffer. The tetramer-stained cells were then resuspended in 300 µl FACS Buffer, mixed with 25 µl of anti-APC mAb-conjugated magnetic microbeads (StemCell Technologies), and incubated in the dark on ice for 30 min. The cells were washed, resuspended in 3 ml cold FACS Buffer, and passed through an EasySep Magnet (StemCell Technologies) to yield an enriched tetramer positive population.

The resulting enriched fractions were stained with a cocktail of fluorochrome-labeled mAb (see below). Cell numbers for each sample were determined using AccuCheck Counting Beads (Invitrogen). Samples were then analyzed using an LSR II flow cytometer (BD) and FlowJo software (TreeStar Inc., Ashland, OR). The percentage of PE^+ or 2W1S:I-A^{b+} events was multiplied by the total number of cells in the enriched fraction to calculate the total number of PE-specific B cells or 2W1S:I-A^b-specific CD4 T cells, respectively.

Flow Cytometry

To assess the expression of cell surface proteins, cells were incubated with fluorochrome-conjugated mAb at 4°C for 30 min. The cells were then washed with FACS buffer. For some experiments, the cells were then fixed with PBS containing 2%

paraformaldeyhe. In procedures requiring intracellular staining, cells were permeabilized following surface staining using the transcription factor staining kit (eBioscience), stained for 1 h at 4°C with a second set of fluorochrome-conjugated mAb, and suspended in FACS buffer for acquisition. The fluorochrome-conjugated mAb used in surface and intracellular staining were as follows: B cell panel—FITC IgA, PerCP-eF710 IgM, AF594 IgG3, AF647 IgG2b, AF700 CD38, APC-eF780 "dump" (CD90.2, CD11c, F4-80, and GR1), BV510 IgE, BV605 IgG1, BV711 IgG2A, BV786 IgD, AF350 IgG (H+L), BUV395 B220; T cell surface panel –PE-Cy7 PD-1, AlexaFluor® (AF) 700 CD44, APC-eFluor® (eF) 780 "dump" (CD11b, CD11c, and B220), Brilliant Violet™ (BV) 421 CXCR5, BV650 CD8a, and Brilliant Ultraviolet™ (BUV) 395 CD4; and T cell ICS panel—AF488 Bcl6, BV605 Tbet, AF700 CD44, APC-eF780 "dump" (CD11b, CD11c, and B220), and BUV395 CD4.

Assessment of Ab Production After TNP-KLH or Influenza a Virus Immunization

Mice immunized with TNP-KLH were bled 7 days after the boost to collect serum to measure TNP-specific Ab levels. Mice challenged with influenza A virus were bled after 28 days to collect serum to measure anti-IAV Ab titers. Mice were anesthetized and blood was collected retro-orbitally. Blood samples were clotted and separated serum was stored at −80°C until use in enzyme-linked immunosorbent assay (ELISA) to determine the presence of Ag-specific Ab.

TNP-specific Ab were determined as follows: 96-well ELISA plates (Immulon 2, Thermo, Milford, MA) were coated with goat anti-mouse IgM (10 μg/ml; Southern Biotech, Birmingham, AL), goat anti-mouse IgG1 (5 μg/ml; Southern Biotech), or goat

anti-mouse IgG2b (5 μg/ml; Southern Biotech) in 0.05 M Tris-HCl buffer (pH 9.5) overnight at 4°C. Coated plates were blocked with 5% w/v dry milk in phosphate buffered saline (PBS). Control anti-TNP mAb (for standard curves) or serum samples appropriately diluted in 5% dry milk-PBS were added, and similarly incubated. After washing, 2μg/ml TNP-human gamma globulin-biotin diluted in 5% dry milk-PBS was added to each well, and the plates further incubated. Alkaline phosphatase streptavidin (3 μg/ml; Zymed, San Francisco, CA) diluted in 5% dry milk-PBS was added after washing. Substrate (2 mg/ml; Sigma Chemical Co., St. Louis, MO) diluted in substrate buffer [50 mM Na2CO3 and 1 mM MgCl.2 6H2O in H2O (pH 9.8)] was added to each well, and absorbance measured at a dual wavelength of 405 and 540 nm using a Microplate Autoreader EL311 (Bio-Tek Instruments, Winooski, VT). All washes between steps were performed with a 0.9% NaCl, 0.05% Tween-20 buffer (pH 7.0) and all incubation steps were done at 37°C in 5% CO2. Ab concentrations were determined from standard curves using DeltaSOFT software (Bio-Tek Instruments). Control mAb used for standard curves were 49.2 (mouse IgG2b anti-TNP mAb; Pharmingen, San Diego, CA), 4G2F8 (mouse IgM anti-TNP mAb), and 1B7 (mouse IgG1 anti-TNP mAb. 4G2F8 and 1B7 were affinity purified by passage of hybridoma culture supernatants over TNP-bovine gamma globulin-Sepharose 6B followed by elution with TNP-glycine (Sigma Chemical Co.).

Influenza-specific Ab were determined as follows: 96-well ELISA plates were coated with purified A/PR/8 Influenza A virus (50 μl/well of 2 mg/ml PBS virus) overnight at 4°C. Coated plates were blocked for 1 h at room temperature with 5% normal goat or donkey serum in PBS, followed by incubation with diluted serum samples

from IAV-challenged mice overnight at 4°C. After washing, plates were incubated with either an alkaline phosphatase-conjugated goat anti-mouse Ig (Southern Biotech) or donkey anti-mouse IgG (Jackson ImmunoResearch). Substrate was added and absorbance was measured as described above.

Statistical Analyses

Data shown are presented as mean values ± SEM. GraphPad Prism 7 was used for statistical analysis, where statistical significance was determined using two-tailed Student t-test (for 2 individual groups, if unequal variance Mann-Whitney U test was used) or group-wise, one-way ANOVA analyses followed by multiple-testing correction using the Holm-Sidak method, with $\alpha = 0.05$. *$p < 0.05$, **$p < 0.01$, ***$p < 0.005$, ****$p < 0.001$.

III. Results

Sepsis Induces a Transient Reduction in B Cells and CD4 T Cells

Patients surviving a septic event often have suppressed immune function, as data showing reduced immune cell function in critically ill sepsis patients date back over 40 years[32]. While some data suggested a phenotypic switch in CD4 T cells from Th1 to Th2[111], other data indicated that the reduced cellular activity was more likely due to a global dysfunction[67]. This idea is reinforced by decreased expression of Tbet, GATA3, and RORγt, the transcription factors regulating Th1, Th2, and Th17 phenotypes, respectively, in CD4 T cells from septic patients[112]. More recently, post-mortem assessment of T cells from patients who died from severe sepsis showed almost no production of IFNγ, TNFα, IL-6, and IL-10 after anti-CD3/CD28 mAb stimulation

compared to samples from non-septic, control patients[66]—further supporting the idea that sepsis affects general T cell function. Indirect evidence of defective CD4 T cell function has come from other studies describing altered humoral responses after sepsis, specifically in terms of Ag-specific immunity (e.g., T cell-dependent Ab responses)[86,113]. With this clinical information in mind, we wanted to further investigate how sepsis affects the generation of a primary CD4 T cell-dependent B cell response using the CLP mouse model of polymicrobial sepsis. The severity of the CLP we performed was marked by a significant, but transient, loss of weight that was recovered by 7 days after surgery (Figure 2-1A), as well as the rapid production of IL-1β, IL-6, IFNγ, and TNF detectable in the serum during the first 24 h after surgery (Figure 2-1B). Both of these parameters are consistent with previous reports[114–118]. In addition, we see a mortality rate of ~25% in the group of mice receiving CLP surgery (Figure 2-1C), which is consistent with clinical rates[119].

We initially wanted to define the numerical changes that occur within the total B cell and CD4 T cell compartments—the cells that participate in CD4 T cell-dependent B cell responses—following a septic event. B cells and CD4 T cells present in the blood and secondary lymphoid organs were enumerated by flow cytometry early (day 2) and late (day 30) after sham or CLP surgery (Figure 2-2A). B cell numbers in the blood, spleen, and inguinal lymph nodes (iLN) were significantly reduced 2 days after sepsis induction, decreasing 11-fold, 2-fold, and 6-fold, respectively, before recovering to sham levels by day 30 (Figures 2-2B and 2-2C). Interestingly, there was no reduction in B cells isolated from mesenteric lymph nodes (mLN) on day 2 and there was a slight (but

insignificant) increase in number on day 30. Similar trends were observed with CD4 T cells—transient numerical reductions in the blood (5-fold), spleens (2-fold), and iLN (3-fold) but no change in the mLN (Figures 2-2D and 2-2E). The mLN drain the gut mucosa and are located within the site of the initial polymicrobial septic insult, suggesting the proximity to the intraperitoneal inflammation may either prevent the sepsis-induced death of lymphocytes seen in the periphery and/or recruit cells from periphery through the production of inflammatory cues. However, migration of cells to mLN cannot fully account for the diminished cellularity observed in other tissues. We have previously shown dendritic cells follow the same pattern of numerical reduction, with losses in the blood, spleen, and iLN, and no change in the mLN[13], indicating cells of the lymphoid and myeloid lineages are similarly maintained numerically in the anatomical locations where the nidus of the septic event is found. Data examining the B cell and CD4 T cell compartments at the "total population" level suggest the immune system has returned to its pre-sepsis state by day 30 in terms of B cell and CD4 T cell numbers.

Sepsis-Induced Effects on Ag-Specific B Cells and CD4 T Cells

The results presented in Figure 2-2 suggest the re-establishment of a "normal" immune system within 30 days after CLP-induced sepsis. However, previous work from our group revealed distinct differences in the ability of individual Ag-specific CD4 T cell populations to numerically and functionally recover after sepsis[62]. We hypothesized that similar differences may occur for an individual Ag-specific B cell population within the total B cell compartment, prompting us to employ a system where we could directly monitor defined populations of Ag-specific B cells and CD4 T cells within the total B

cell and CD4 T cell compartments to more rigorously study the effect of sepsis on CD4 T cell-dependent B cell responses. Specifically, we used enrichment protocols to identify B cells specific for the fluorchrome phycoerythrin (PE)[104–106] and CD4 T cells specific for the 2W1S variant of peptide 52-68 from the I-E α-chain[108,120].

As a first step in this analysis, we determined how sepsis affected the number and phenotype of PE-specific B cells (Figure 2-3A). We were able to clearly detect and quantify the PE-specific B cells, as well as the $B220^{hi}IgG\ [H+L]^{int}CD38^{+}GL7^{-}$ naïve/memory B cells, $B220^{hi}IgG\ [H+L]^{int}CD38^{-}GL7^{+}$ germinal center (GC) B cells, and $B220^{lo}IgG\ [H+L]^{hi}CD38^{-}GL7^{-}$ plasma cells within the PE-specific B cell population (Figure 2-3B). Similar to the transient loss and recovery within the total B cell compartment (Figures 2-2B and 2-2C), there was a significant reduction (5.2-fold less compared to sham mice) in number of PE-specific B cells 2 days after CLP surgery that recovered by day 30 (Figure 2-3C). The number of PE-specific naïve/memory B cells decreased ~4-fold 2 days after CLP surgery, but did not fully recover by day 30 to the number found in mice that underwent sham surgery (Figure 2-3D). Interestingly, while there were ~9- and 1.5-fold reductions in number of PE-specific GC B cells and plasma cells, respectively, 2 days after CLP surgery, this was followed by a ~3-fold increase in both of these subsets by day 30 after CLP surgery (Figures 2-3E and 2-3F). In addition to determining the number of these PE-specific B cell subsets, we also evaluated how the septic event affected the Ab isotypes they produced. As expected, there were numerical reductions in several populations 2 days after CLP surgery, including $IgM^{+}IgD^{-}$ naïve/memory, $IgG1^{+}$ and IgE^{+} GC B cells, and IgA^{+} plasma cells (Figures 2-3G, 2-3H,

and 2-3I). It is also important to note several populations were increased by day 30 after CLP, namely the IgG2b-producing PE-specific naïve/memory B cells, GC B cells, and plasma cells 30 days after CLP compared to sham mice (Figures 2-3G, 2-3H, and 2-3I). IgG1- and IgG2c-producing GC B cells also increased in number by day 30 after CLP surgery. These data show sepsis can induce a variety of small numerical changes within the B cell compartment when examined at the Ag-specific level.

In contrast to the PE-specific B cells and consistent with our previous data[62], we did not observe the same numerical recovery of 2W1S:I-A^b-specific T cells after CLP surgery that was seen for the total CD4 T cell population. In fact, the number of 2W1S:I-A^b-specific CD4 T cells was reduced ~3-fold at day 2 post-CLP, which was maintained at day 30 (Figure 2-4A, 2-4B, and 2-4C). Our analysis of the 2W1S:I-A^b-specific T cells also included an assessment of CD4 T cell lineage-specific master regulators Tbet (Th1) and Bcl6 (Tfh)[121,122]. A small number of the 2W1S:I-A^b-specific CD4 T cells expressed Tbet by day 30 after CLP surgery (Figure 2-4D), but we were unable to detect any 2W1S:I-A^b-specific CD4 T cells expressing Bcl6 or PD-1 and CXCR5, indicators of Tfh differentiation, after CLP. Thus, the data in Figures 2-3, 2-4 show how sepsis affects the number of PE-specific B cells and 2W1S:I-A^b-specific CD4 T cells.

Prolonged Impairment in Primary CD4 T Cell-Dependent B Cell Responses Is Associated With Reduced Germinal Center T Follicular Helper (Tfh) Cell Differentiation

We next determined how sepsis affected the ability of the PE-specific B cells and 2W1S:I-A^b-specific CD4 T cells to respond after immunization with a CFA emulsion containing the MHC II-restricted $2W1S_{56–68}$ peptide coupled to PE[107] (Figure 2-5A).

The 2W1S-PE immunogen is internalized by the B cell receptor of PE-specific B cells, which then present 2W1S in MHC II complexes to 2W1S-specific CD4 T cells who provide the necessary help to generate a robust B cell response. This immunization method allowed us to simultaneously track the numerical and phenotypic changes among PE-specific B cells and 2W1S:I-A^b-specific CD4 T cells in the same mouse during a CD4 T cell-dependent B cell response.

Using the identical Ab panels and gating schemes that were used above (Figure 2-5B) to identify PE-specific B cells in mice that had only experienced sham or CLP surgery, we found the immunization-induced expansion for each PE-specific B cell population was greatest in the sham-treated mice (Figures 2-5C, 2-5D, 2-5E, and 2-5F). While the number of total PE-specific B cells and each subset had recovered or expanded by day 30 after CLP surgery, the response of these populations to immunization with 2W1S-PE/CFA was significantly reduced in mice subjected to CLP surgery compared to sham mice. We noted 4–6-fold fewer PE-specific naïve/memory, GC, and plasma cells in mice immunized 2 days after CLP surgery compared to sham mice, and this numerical reduction (~2-fold less) was maintained in the CLP mice immunized 30 days after surgery. Thus, the PE-specific B cell compartment showed long-lasting functional impairment in terms of cellular proliferative capacity, extending well-past the resolution of the septic event. Sepsis also affected the degree of class switching after immunization with 2W1S-PE/CFA for each subset of PE-specific B cells. In general, there were reductions in the number of multiple isotypes produced by the PE-specific B cell subsets (Figures 2-5G, 2-5H, and 2-5I). This was most evident in the PE-specific plasma cells, as

there were significantly fewer cells producing IgG1, IgG2c, IgG3, and IgA after immunization either on day 2 or 30 after CLP surgery (Figure 2-5I).

The extent of Tfh cell differentiation by the 2W1S:I-A^b-specific CD4 T cells after 2W1S-PE/CFA immunization (Figure 2-6A) was also impaired by sepsis. There were ~4-fold fewer total 2W1S:I-A^b-specific CD4 T cells in the mice subjected to CLP surgery, regardless of when the immunization occurred (day 2 or 30 after surgery), compared to sham mice (Figures 2-6B and 2-6C). Moreover, there was a significant reduction in the frequency and number (~5-fold less than sham-treated mice) of 2W1S:I-A^b-specific CD4 T cells that differentiated into GC Tfh cells, based on expression of Bcl-6 (Figure 2-6E) or CXCR5 and PD-1 (Figures 2-6F and 2-6G). The data in Figures 2-3, 2-4, 2-5, and 2-6 reveal the profound quantitative and qualitative effects of sepsis on both Ag-specific B cells and CD4 T cells, especially after immunization with a model Ag designed to elicit a CD4 T cell-dependent B cell response, that were not apparent when evaluating the bulk B cell and CD4 T cell compartments.

To bolster our findings above, we wanted to determine the impact of sepsis on Ab production during a primary CD4 T cell-dependent B cell response to a pathogen challenge commonly used to probe B cell and/or T cell response and a second model Ag classically used to evaluate the fitness of the humoral arm of adaptive immunity. B6 mice were challenged with live influenza A virus (IAV) on day 2 or 30 after sham or CLP surgery, and serum was collected 28 days later to measure the amount of anti-IAV Ab produced (Figure 2-7A). We noted marked reductions in the amount of total Ab and IgG specific for IAV in the serum of CLP-treated mice challenged on days 2 or 30 after CLP

surgery (Figures 2-7B and 2-7C). Similar results were seen after immunization with TNP-KLH, a common Ag used to test various aspect of humoral immunity (Figure 2-8). Interestingly, the sepsis-induced deficiency Ab production was most pronounced and sustained when the TNP-KLH was administered with the Th2-polarizing adjuvant alum[123,124] (Figure 2-8B). There remained a significant reduction in anti-TNP IgM, IgG1, and IgG2 even when the mice were first immunized 30 days after CLP surgery, and boosted 21 days later. By comparison, CLP-treated mice demonstrated a significant reduction in anti-TNP IgM and IgG2 when immunized with TNP-KLH mixed with Th1-polarizing adjuvant CpG[125] only on day 2, but these reductions were not maintained when immunization occurred 30 days after surgery (Figure 2-8C). The differences in response depending on the adjuvant used are intriguing, but it is important to note that our primary goal of these experiments was not to directly compare "Th1" vs. "Th2" priming conditions. Rather, we reasoned the comparison between control (sham) to CLP mice after the same duration post-surgery was more critical. Sham surgery likely causes some low-level abdominal inflammation, as the abdomen/peritoneum is surgically opened and the cecum exposed and put back into the mouse (without any needle puncture) followed by closure. While the mice received surgery at the same time, the peritoneum is going to be much different 2 days after this surgical event compared with 30 days where healing has taken place. Together, these results highlight the compromised ability to produce Ab during a primary B cell response following a septic event.

IV. Discussion

Defects in humoral immunity are associated with increased susceptibility to infection[126]. Reduced immune function after septic injury is well-documented in the clinic, and a number of mechanisms have been posited to explain sepsis-induced immune suppression[95]. Clinical data show acute reduction in both CD4 T cells and B cells in sepsis patients[16], as well as IgM levels in the circulation[127]. The reduction of these components of the adaptive immune system contribute to the increased risk of nosocomial bacterial infections and viral reactivation, and poor chances for a favorable outcome[19,66]. While there is a reasonable understanding of the numerical changes in total B cells and CD4 T cells within several days after sepsis onset, there is a paucity of information describing the qualitative long-term impact of sepsis on these cells within the context of a primary CD4 T cell-dependent B cell response. The reduced Ab response following antigenic challenge in mice that experienced CLP-induced sepsis we have described here is consistent with the recent data by Mohr et al.[86]. Further, the data we have presented importantly extend our understanding of what happens to the cellular components of the adaptive immune system following a septic event that affect the generation of a primary CD4 T cell-dependent B cells response. Our results show that following sepsis, mice subjected to CLP surgery have long-term reductions in B cell differentiation and class switching after vaccination or infection, ultimately resulting in suboptimal Ab production. The data reported here also suggest the reduced Ab production in mice challenged with Ag early during the septic event or late after sepsis

resolution is due in part to insufficient help from Tfh cells, leading to inadequate B cell differentiation and class switching.

Work reported in a number of publications have examined basic numerical and functional changes of various immune cell subsets after sepsis (almost) exclusively at the total population level. In the present study we have evaluated endogenous Ag-specific CD4 T cell and B cell populations within the context of a CD4 T cell-dependent B cell response following a septic event. Tracking Ag-specific T cells and B cells permits the most rigorous and sensitive functional analysis of these cells during the response to vaccination or infection by allowing us to identify changes at the Ag-specific level that may not be resolvable when examining the total populations[64]. Additionally, we were able to evaluate the sepsis-induced numerical and phenotypic changes in endogenous Ag-specific CD4 T cells and B cells (2W1S:I-A^b- and PE-specific, respectively) responding to the same foreign Ag (2W1S peptide covalently coupled to PE in CFA)[107]. As expected, the 2W1S:I-A^b-specific CD4 T cells expand and differentiate into Tfh cells as well as other defined CD4 T cell subsets, such as $Tbet^+$ "Th1" CD4 T cells (Figure 2-6D), in sham mice after 2W1S-PE/CFA vaccination. PE-specific B cells can then interact with the 2W1S:I-A^b-specific Tfh cells within the GC. There is robust expansion, differentiation, and class switching seen in the PE-specific B cells in this setting. Our data suggest all of these factors are affected by sepsis, even once the host has recovered from the acute hyperinflammatory response and transient lymphopenia characteristic of a septic event.

While there were a number of results that were expected, our analyses also revealed some unexpected findings. For example, the total number of PE-specific B cells was not different in the sham and day 30 CLP groups (see Figure 2-3C). There was just a redistribution among the different subsets. CLP-induced polymicrobial sepsis induces a highly inflammatory event within the peritoneum, making it possible that this inflammation can drive a small number of the PE-specific cells to differentiate into GC B cells and plasma cells. The small but significant numerical increase in PE-specific GC B cells and plasma cells 30 days after CLP, prior to 2W1S-PE/CFA immunization (Figures 2-3E and 2-3F) was surprising, and was in contrast to the reduction seen in total 2W1S:I-A^b-specific CD4 T cells (Figure 2-4C). While 2W1S:I-A^b-specific CD4 T cells recognize a defined peptide sequence presented by MHC II, PE is a 250 kD multi-subunit protein originally isolated from red algae with multiple epitopes available for Ab recognition[128,129]. Thus, while being PE-specific, the B cells we detect using the enrichment protocol are likely polyclonal in composition, and bind to different epitopes within the PE protein. One possible explanation for the increase in PE-specific GC B cells and plasma cells 30 days after CLP is that some of the PE-specific B cells cross-react with antigenic epitopes expressed by the numerous gut commensal microbes released during the CLP surgery that establish the polymicrobial peritonitis. Such cross reactivity among B cells has been observed previously; for example, gut commensal bacteria can prime for the production of antibodies specific for HIV-1 envelope gp41[130]. Similarly, CD4 T cell cross-reactivity with gut commensal bacteria can drive responses to self Ag (glucose-6-phosphate isomerase) and foreign microbes that ultimately has an impact on host health[131–134]. Future studies are needed to

investigate this interesting possibility of cross-reactivity. Despite the increases seen in the PE-specific B cell populations after CLP, sepsis dramatically reduced the ability of these cells to respond to their cognate Ag following 2W1S-PE/CFA immunization. 2W1S:I-A^b-specific CD4 T cells have reduced proliferative capacity and cytokine production after sepsis, as well has developing changes within the TCR Vβ repertoire[62]. In addition, numerical and functional deficits occur among dendritic cells following sepsis[13], suggesting the potential contribution for both T cell-intrinsic and -extrinsic factors to reduced function.

Another interesting finding was the skewing of the Ab response in the mice subjected to CLP surgery to IgG2b after immunization (and even prior to immunization). The presence of TGF-β, which has been reported to be elevated after sepsis[135], promotes switching to IgG2b and IgA[136]. While class switching to IgG2b was elevated across the board, IgA was slightly elevated only in GC B cells and plasma B cells in unimmunized mice. There is clear redundancy in regard to the ability of certain cytokines to drive IgG2 (as well as other) isotype switching in murine B cells. IFNγ and type I IFN can promote switching to IgG2, as exemplified by the presence of normal levels of induced IgG2b in mice unable to express the type II TGF-β receptor on their B cells[137]. Interestingly, it has also been reported that the absence of T cell help and presence of LPS favors switching to IgG2b[136]. Thus, given these redundancies and variety of cytokines produced during a septic event, we hesitate to suggest TGF-β (or any other single cytokine) is solely responsible for the IgG2b skewing after CLP.

While it is difficult to know how long the effects of a septic event will have on the function of the immune system, sepsis survivors have decreased 5-year survival compared to "control" patients[101,138,139]. Perturbations, such as sepsis, that result in long-term impairments to the immune system have the potential to severely diminish vaccination efficacy. Typically, adults are recommended to receive a number of vaccinations to seasonal (e.g., influenza) and non-seasonal (e.g., pneumococcus and varicella zoster virus) pathogens to develop and maintain adequate protection from infection[140]. These vaccinations work best when the host immune system is optimally functional. However, in a patient with a history of sepsis, these vaccinations may provide little-to-no protection, leaving these patients with an increased risk of secondary infection.

V. Figures

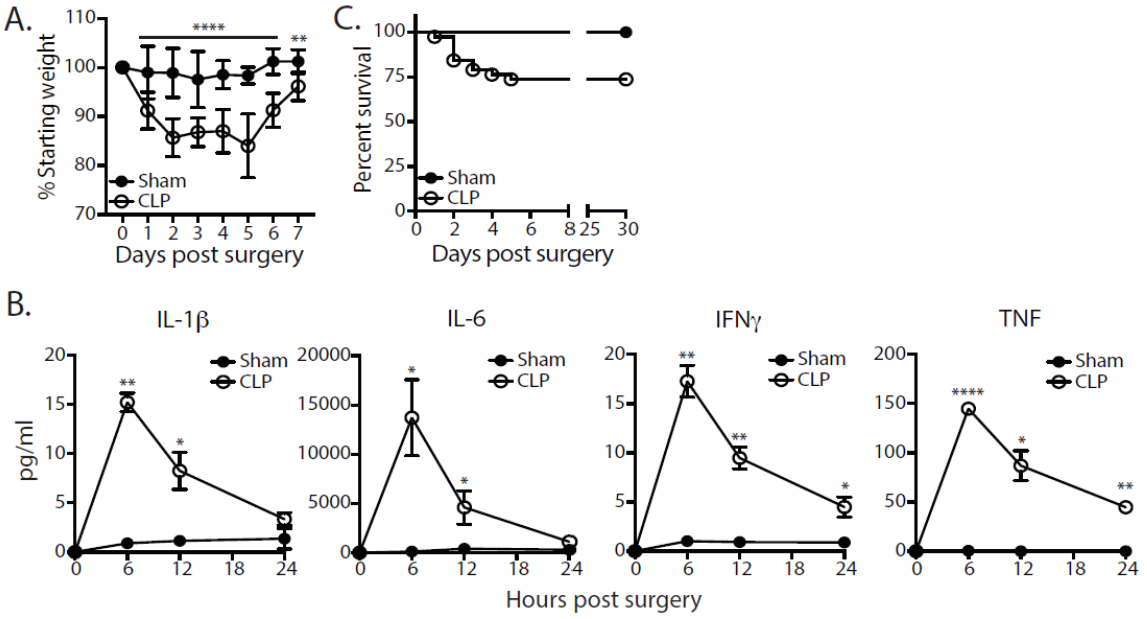

Figure 2-1. Morbidity, cytokine production, and mortality following CLP surgery. B6 mice underwent sham or CLP surgery. (A) Body weight was measured before and the 7 days after surgery. Weight loss for each was determined based on their starting weight. (B) Serum samples were collected at the indicated time points after sham or CLP surgery. The amount of IL-1β, IL-6, IFNγ, and TNF in samples was determined by bioplex. n = 11 sham and 38 CLP mice for (A,C); n = 5 mice/time point/group in (B) *p < 0.05; **p < 0.01, ****p < 0.001 for SPF—CLP vs. cohoused—CLP at the indicated time points.

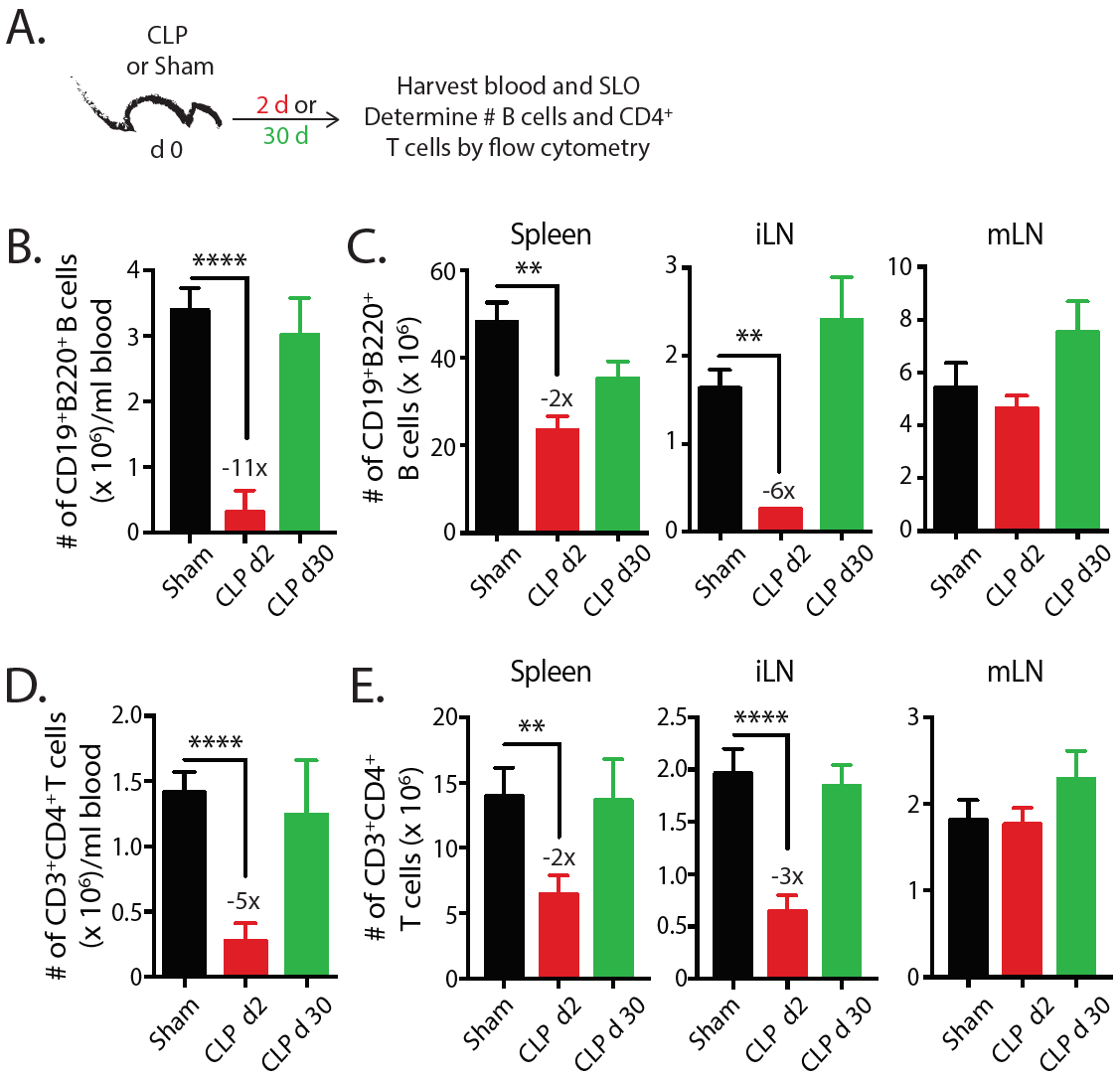

Figure 2-2. CLP induces transient reductions in the number of B cells and CD4 T cells. (A) Experimental design—blood and secondary lymphoid organs (SLO) including spleens, inguinal lymph nodes (iLN), and mesenteric lymph nodes (mLN) were harvested 2 and 30 days after sham or CLP surgery. The number of (B,C) $CD19^+$ $B220^+$ B cells or (D,E) $CD3^+$ $CD4^+$ T cells in blood (per ml), spleen, iLN, and mLN was determined by flow cytometry. n = 5–7 mice/group. $^{**}p < 0.01$, $^{****}p < 0.001$. Numbers above bars indicate the average fold change in number compared to sham mice. Data are representative of at least 3 independent experiments.

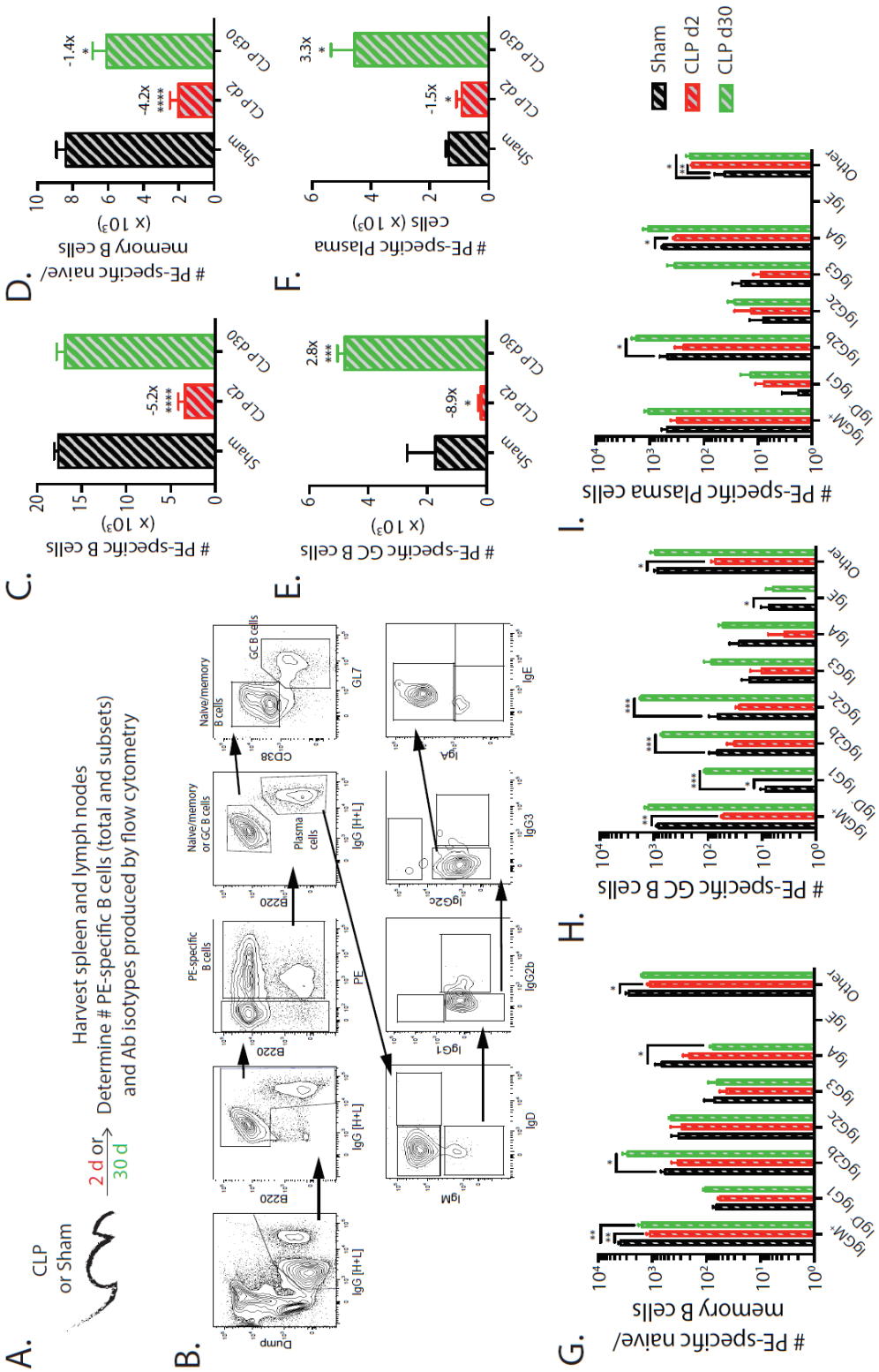

Figure 2-3. Numerical changes in PE-specific B cells after sepsis. (A) Experimental design—Spleens and peripheral lymph nodes (axillary, brachial, cervical, inguinal, and

mesenteric) were harvested from mice on day 2 and 30 post-sham or CLP surgery and combined. (B) Gating scheme used to identify PE-specific B cells, as well as the $B220^{hi}$IgG $[H+L]^{lo}$ $CD38^{+}GL7^{-}$ naïve/memory B cells, $B220^{hi}$IgG $[H+L]^{lo}$ $CD38^{-}GL7^{+}$ germinal center (GC) B cells, and $B220^{lo}$IgG $[H+L]^{hi}CD38^{-}GL7^{-}$ plasma cells. This representative scheme also shows the gating used to determine the extent of class switching within the plasma cell population, but similar gating was used on the naïve/memory and GC B cell populations. Representative flow plots are from a mouse that underwent sham surgery. The number of (C) total PE-specific B cells and PE-specific (D) naïve/memory B cells, defined as $B220^{hi}$ IgG $[H+L]^{lo}$ $CD38^{+}GL7^{-}$, (E) germinal center (GC) B cells, defined as $B220^{hi}$ IgG $[H+L]^{lo}$ $CD38^{-}$ $GL7^{+}$, and (F) plasma cells, defined as $B220^{lo}$ IgG $[H+L]^{hi}$ $CD38^{-}$ $GL7^{-}$, were determined. Numbers above bars indicate the average fold change in number compared to sham mice. (G–I) The naïve/memory B cell, GC B cell, and plasma cell subsets from the unimmunized mice were additionally subdivided based on the Ab isotype being produced. n = 5–7 mice/group. Statistical comparisons were made between sham mice and either CLP d2 or d30 mice, where *$p < 0.05$, **$p < 0.01$, ****$p < 0.001$. Data are representative of at least 3 independent experiments.

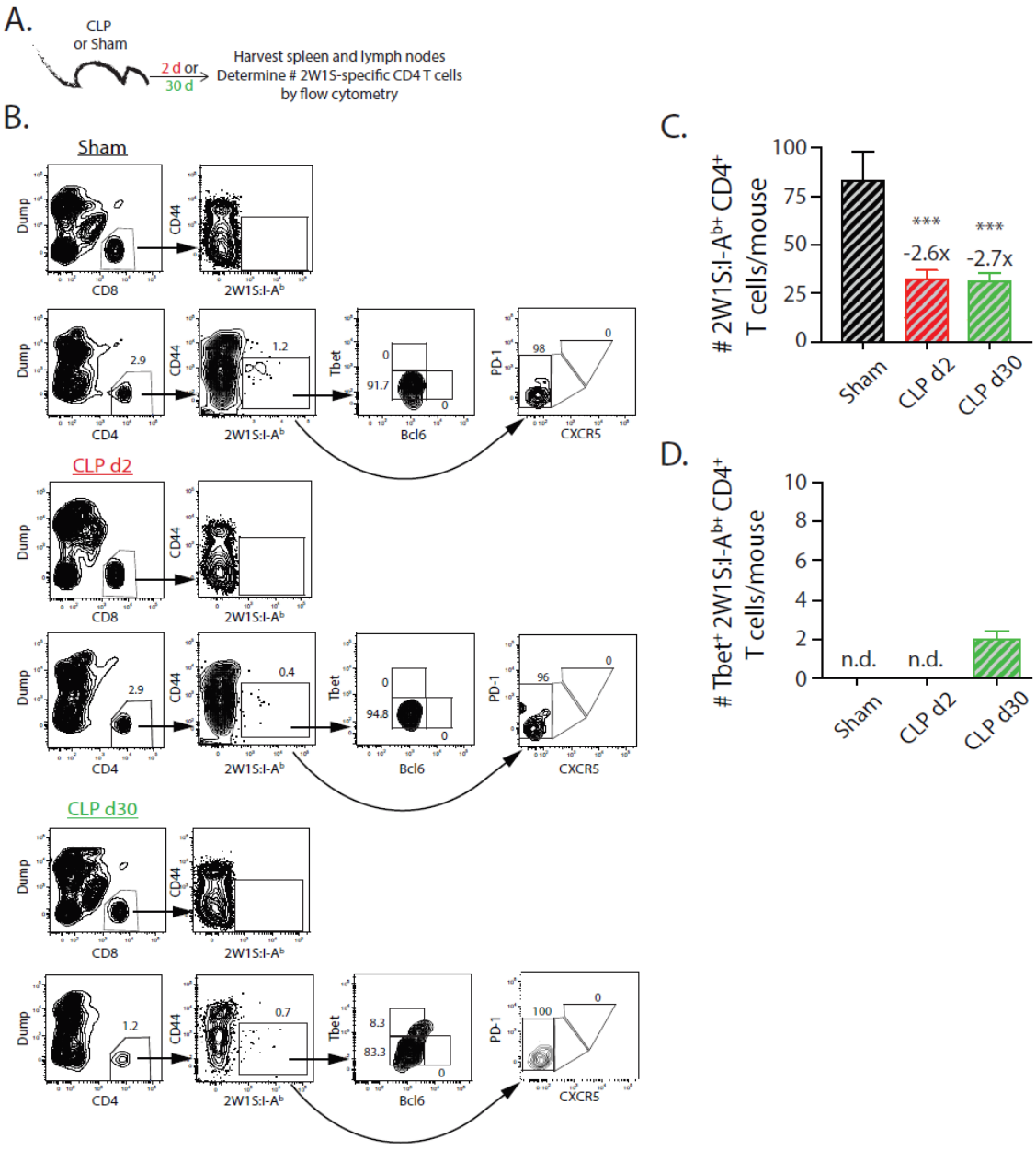

Figure 2-4. Numerical changes in 2W1S-specific CD4 T cells after sepsis. (A) Experimental design—Spleens and peripheral lymph nodes (axillary, brachial, cervical, inguinal, and mesenteric) were harvested from mice on day 2 and 30 post-sham or CLP surgery and combined. (B) Gating scheme used to identify 2W1S:I-A^b-specific CD4 T cells (CD8 T cells were used as the internal negative control for tetramer binding), as well as the 2W1S:I-A^b-specific CD4 T cells expressing Tbet, Bcl-6, or PD-1 and CXCR5. The frequency of cells within the gated populations is indicated. The number of (C) total and (D) $Tbet^+$ 2W1S:I-A^b-specific CD4 T cells was determined. n = 9–10 mice/group in (B,C). Statistical comparisons were made between sham mice and either CLP d2 or d30

mice, where ***$p < 0.005$. Numbers above bars indicate the average fold change in number compared to sham-treated mice.

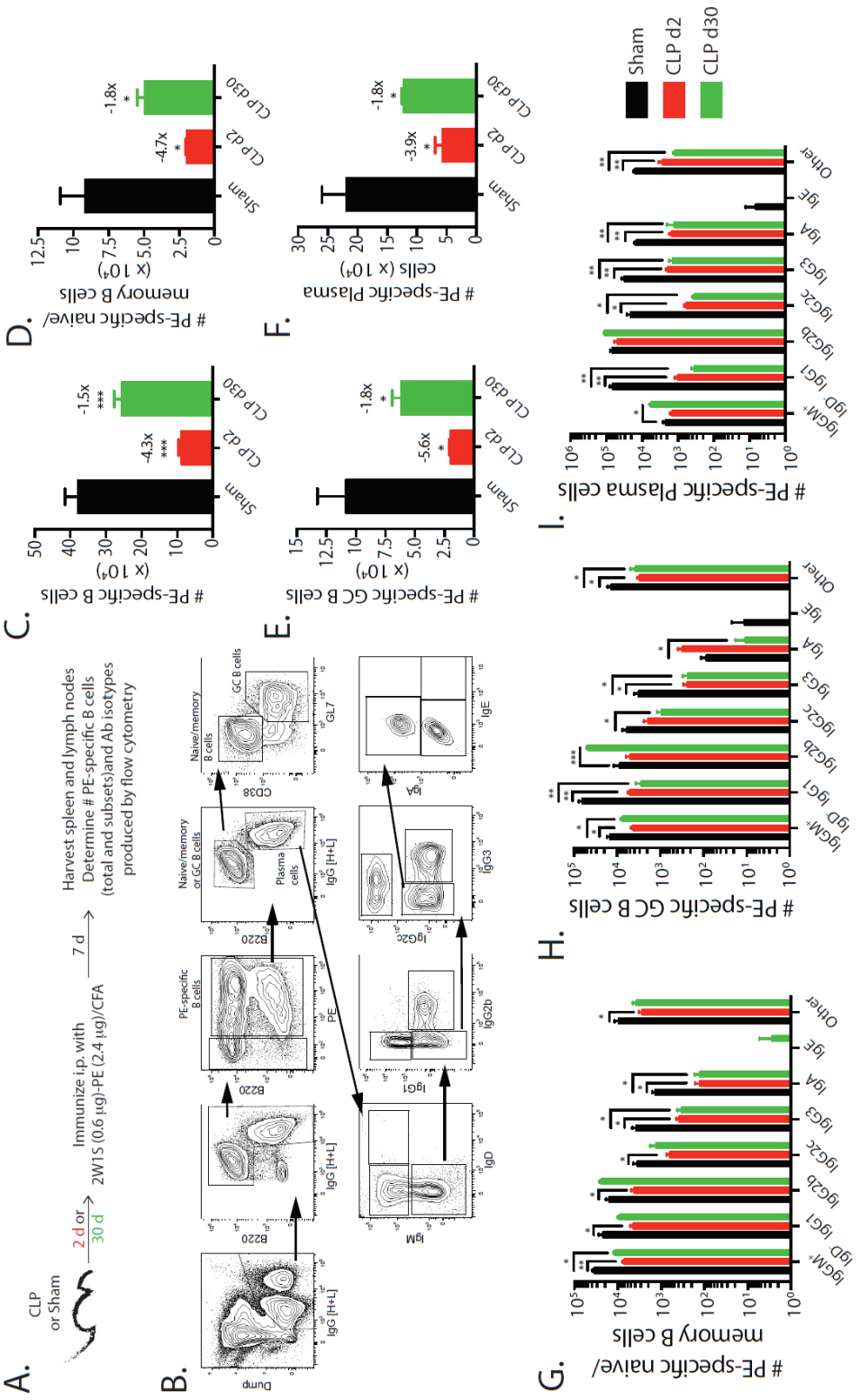

Figure 2-5. Sepsis hinders B cell differentiation and class-switching during a CD4 T cell-dependent B cell response. (A) Experimental design—mice underwent sham or

CLP surgery and were then immunized on day 2 or 30 after surgery with 2W1S-PE/CFA i.p. Spleens and peripheral lymph nodes were harvested 7 days after immunization and combined. (B) Gating scheme used to identify PE-specific B cells, as well as the $B220^{hi}IgG\ [H+L]^{lo}\ CD38^{+}GL7^{-}$ naïve/memory B cells, $B220^{hi}IgG\ [H+L]^{lo}\ CD38^{-}GL7^{+}$ germinal center (GC) B cells, and $B220^{lo}IgG\ [H+L]^{hi}CD38^{-}GL7^{-}$ plasma cells. This representative scheme also shows the gating used to determine the extent of class switching within the plasma cell population, but similar gating was used on the naïve/memory and GC B cell populations. Representative flow plots are from a mouse immunized 2 days after sham surgery. The number of (C) total PE-specific B cells and PE-specific (D) naïve/memory B cells, (E) GC B cells, and (F) plasma cells were determined. Numbers above bars indicate the average fold change in number compared to sham-treated mice. (G–I) The naïve/memory B cell, GC B cell, and plasma cell subsets from the immunized mice were additionally subdivided based on the Ab isotype being produced. n = 5–7 mice/group. Statistical comparisons were made between sham mice and either CLP d2 or d30 mice, where $*p < 0.05$, $**p < 0.01$, and $***p < 0.005$. Data are representative of at least 3 independent experiments.

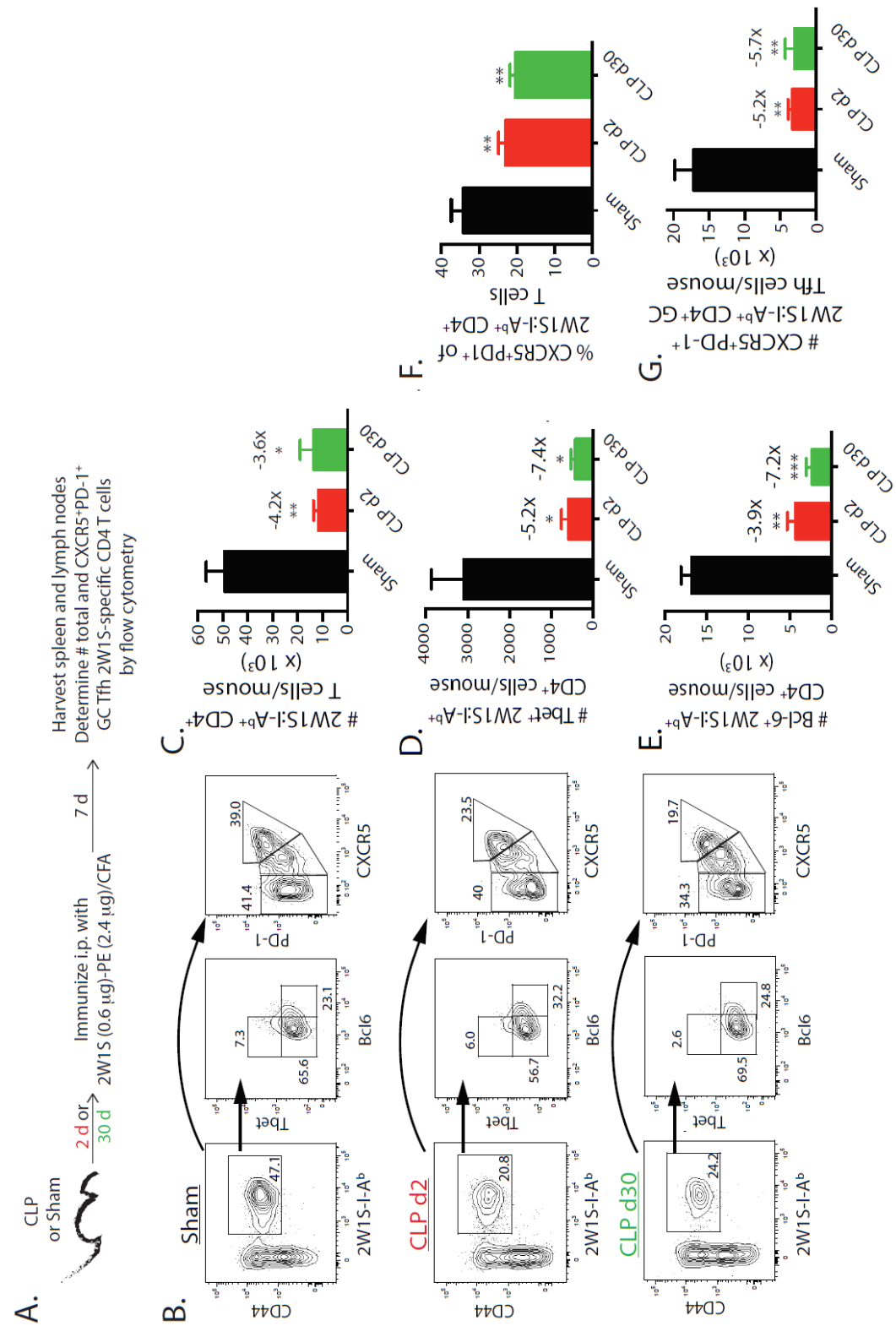

Figure 2-6. Sepsis restricts the ability of 2W1S:I-A^b-specific CD4 T cells to differentiate into Tfh during a CD4 T cell-dependent B cell response. (A)

Experimental design—mice underwent sham or CLP surgery and were then immunized on day 2 or 30 after surgery with 2W1S-PE/CFA i.p. Spleens and peripheral lymph nodes were harvested 7 days after immunization and combined. (B) Gating scheme used to identify 2W1S:I-A^b-specific CD4 T cells (CD8 T cells were used as the internal negative control for tetramer binding), as well as the 2W1S:I-A^b-specific CD4 T cells expressing Tbet, Bcl-6, or PD-1 and CXCR5. The frequency of cells within the gated populations is indicated. The number of (C) total, (D) $Tbet^+$, (E) Bcl-6^+ 2W1S:I-A^b-specific CD4 T cells, as well as (F) frequency, and (G) number of 2W1S:I-A^b-specific CD4 T cells expressing CXCR5 and PD-1, was determined. n = 5–7 mice/group. Statistical comparisons were made between sham-treated mice and either CLP d2- or d30-treated mice, where *$p < 0.05$, **$p < 0.01$, and ***$p < 0.005$. Data are representative of at least 3 independent experiments.

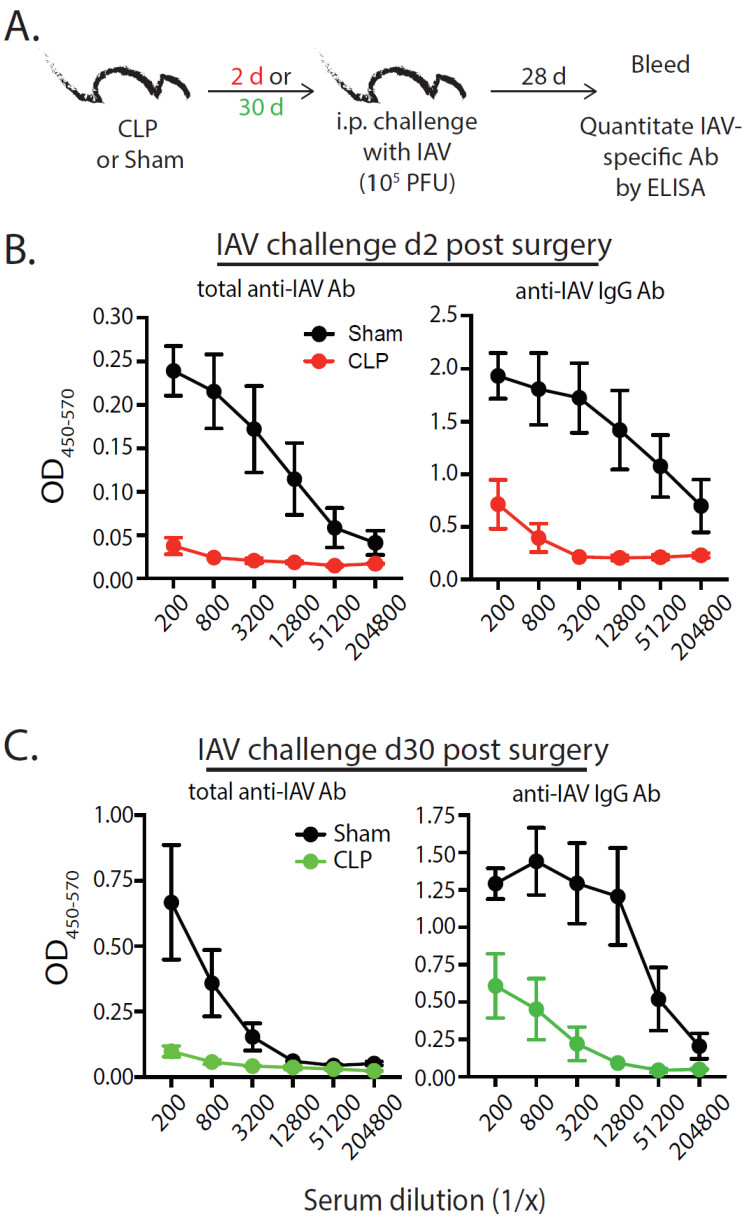

Figure 2-7. Septic mice have reduced primary Ab response following influenza A virus (IAV) challenge. (A) Experimental design—B6 mice were challenged with live IAV (A/PR/8; 10^5 PFU in 100 µl PBS i.p.) 2 or 30 days after sham or CLP surgery. Serum was collected 28 days after immunization. (B) Absorbance of total anti-IAV Ab (left) and IgG specific for IAV (right) from the indicated dilutions of serum from mice challenged 2 days after surgery. (C) Absorbance of total anti-IAV Ab (left) and IgG specific for IAV (right) from the indicated dilutions of serum from mice challenged 30 days after surgery. n = 4–6 mice/group. Data are representative of at least 2 independent experimental replicates.

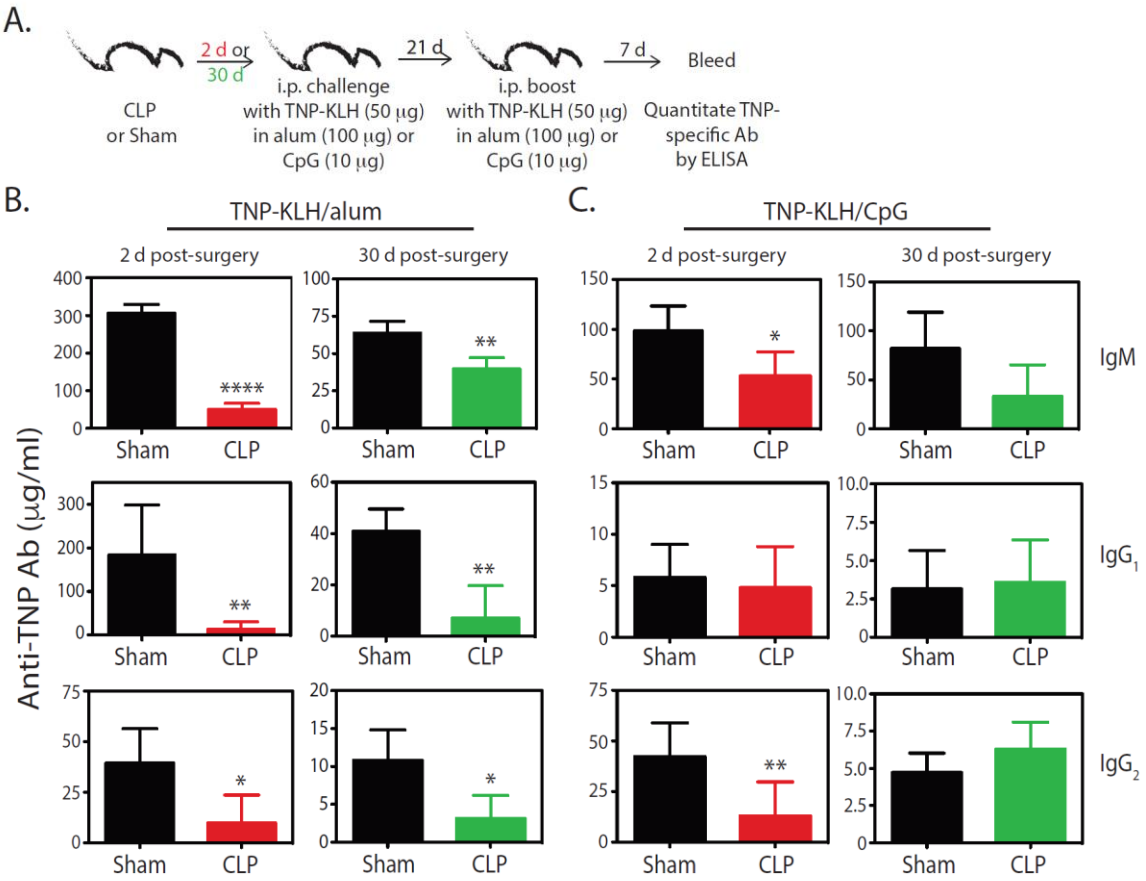

Figure 2-8. Generation of anti-TNP mAb is reduced in septic mice. (A) Experimental design—B6 mice were immunized i.p. with 50 μg TNP-KLH in alum or CpG 2 or 30 days after sham or CLP surgery. A second immunization was administered 21 days later. Blood was collected for serum 7 days after the second immunization. Serum concentrations (quantified via ELISA) of anti-TNP Ab from (B) TNP-KLH/alum- and (C) TNP-KLH/CpG-immunized mice 2 and 30 days after sham and CLP surgeries. n = 4–6 mice/group. *$p < 0.05$, **$p < 0.01$, ****$p < 0.001$. Data are representative of at least 2 independent experiments.

Chapter 3

Polymicrobial Sepsis

Impairs Antigen-Specific

Memory CD4 T Cell-Mediated Immunity[2]

[2] This Chapter has been previously published. Frontiers in Immunology, Volume 11. Sjaastad FV, Kucaba TA, Dileepan T, Swanson W, Dail C, Cabrera-Perez J, Murphy KA, Badovinac VP and Griffith TS. Polymicrobial Sepsis Impairs Antigen-Specific Memory CD4 T Cell-Mediated Immunity, pp.1786 © 2020 Sjaastad, Kucaba, Dileepan, Swanson, Dail, Cabrera-Perez, Murphy, Badovinac and Griffith.

Patients who survive sepsis display prolonged immune dysfunction and heightened risk of secondary infection. CD4 T cells support a variety of cells required for protective immunity, and perturbations to the CD4 T cell compartment can decrease overall immune system fitness. Using the cecal ligation and puncture (CLP) mouse model of sepsis, we investigated the impact of sepsis on endogenous Ag-specific memory CD4 T cells generated in C57BL/6 (B6) mice infected with attenuated *Listeria monocytogenes* (Lm) expressing the I-A^b-restricted 2W1S epitope (Lm-2W). The number of 2W1S-specific memory CD4 T cells was significantly reduced on day 2 after sepsis induction, but recovered by day 14. In contrast to the transient numerical change, the 2W1S-specific memory CD4 T cells displayed prolonged functional impairment after sepsis, evidenced by a reduced recall response (proliferation and effector cytokine production) after restimulation with cognate Ag. To define the extent to which the observed functional impairments in the memory CD4 T cells impacts protection to secondary infection, B6 mice were infected with attenuated *Salmonella enterica*-2W (*Se*-2W) 30 days before sham or CLP surgery, and then challenged with virulent *Se*-2W after surgery. Pathogen burden was significantly higher in the CLP-treated mice compared to shams. Similar reductions in functional capacity and protection were noted for the endogenous OVA_{323}-specific memory CD4 T cell population in sepsis survivors upon Lm-OVA challenge. Our data collectively show CLP-induced sepsis alters the number and function of Ag-specific memory CD4 T cells, which contributes (in part) to the characteristic long-lasting immunoparalysis seen after sepsis.

I. Introduction

The importance of a functional immune system for overall health is dramatically illustrated by individuals with immune system defects being highly susceptible to serious and often life-threatening infections. States of immune deficiency can be congenital (e.g., impaired T and/or B cell development) or acquired (e.g., HIV infection, iatrogenic (post-organ transplant) immune suppression, or surgery/trauma). Studies interrogating the events leading to acquired immunodeficiency are done with the goal of designing treatment modalities to restore immune system function and reduce the susceptibility to infection.

Sepsis causes millions of deaths annually worldwide[2]. Defined as a systemic inflammatory response syndrome during a disseminated infection[141,142], early stages of sepsis are marked by a potentially fatal hyperinflammatory state driven by proinflammatory cytokines[25,48,102]. Concurrent with this hyperinflammation is system-wide transient loss of multiple immune cell types that decreases the ability of the septic host to respond to the primary infection or secondary nosocomial infection. Advancements in critical care medicine have improved survival rates of patients following the initial sepsis-inducing injury[143–146], where acute death from sepsis is no longer the major cause of mortality for these patients. Currently, ~70% of sepsis-related deaths occur after the first 3 days of the disorder as the result of a secondary infection, with many patient deaths occurring weeks and months later[9]. Interestingly, the sepsis-induced lymphopenia is transient, and the once hyperinflammatory immune response transitions to a prolonged immunosuppressive state even though the cellular composition

of the immune system numerically returns to normal. In fact, the prolonged immune suppression that develops after a septic event is now considered a leading reason for the extended period of increased susceptibility to pathogens normally handled by the immune system in healthy individuals[9,12].

CD4 T cells are among the immune cells significantly depleted during the acute stage of sepsis[16], but gradually recover during the immunosuppressive phase[147]. CD4 T cells support the function of a variety of immune cells needed to mount a productive and protective immune response[51], and perturbations in the CD4 T cell compartment can dramatically affect overall immune system fitness. The ability to develop and sustain memory cells after infection or immunization is a hallmark of adaptive immunity and basis for protective vaccination against infectious disease[148,149]. Memory CD4 T cells possess several important features that distinguish them from naïve CD4 T cells. First, there are increased numbers of memory CD4 T cells compared to precursors, providing better coverage and a more rapid cellular response during re-challenge. Memory CD4 T cells have experienced cell-intrinsic "programming" changes that allow for rapid expression of effector cytokines, chemokines, and cytotoxic molecules. Additionally, memory CD4 T cells establish residence in both lymphoid and non-lymphoid tissues[150,151]. Finally, the number of memory CD4 T cells present at the end of the contraction phase of a primary response is maintained for the life of the host[152]. Maintenance of memory CD4 T cell responses over time is a dynamic process, depending on subsequent encounters with either cognate or non-related Ag/infections that have the potential to change their phenotype and

function[51]. Similar to the primary response, the magnitude of a memory CD4 T cell response directly correlates with the quantity and quality of memory CD4 T cells present at the time of re-challenge. Thus, changes in composition and function of naive and memory CD4 T cells can result in impaired immunity and increased susceptibility to subsequent infections[65,153]. The present study took advantage of our ability to track the number and function of endogenous Ag-specific memory CD4 T cells in the wake of a septic event (using the cecal ligation and puncture (CLP) model of polymicrobial sepsis). Our data demonstrate sepsis leads to dramatic and transient decline in pre-existing memory CD4 T cell numbers, with sustained functional impairments, which contribute to the overall increased susceptibility to secondary infections in sepsis survivors.

II. Materials and Methods

Mice

Female C57BL/6 mice (8-weeks old) were purchased from the National Cancer Institute (Frederick, MD). Female pet store mice were purchased from local pet stores in the Minneapolis-St. Paul, MN metropolitan area. All mice were housed in AALAC-approved animal facilities at the University of Minnesota at the appropriate biosafety level (BSL-1/BSL-2 for SPF B6 mice, and BSL-3 for cohoused B6 and pet store mice). SPF B6 and pet store mice were cohoused at a ratio of 8:1 in large rat cages for 60 days to facilitate microbe transfer[50,154]. In all experiments, including those using cohoused mice, mice were age-matched. Experimental procedures were approved by the University of Minnesota Institutional Animal Care and Use Committees and performed following

the Office of Laboratory Animal Welfare guidelines and PHS Policy on Human Cancer and Use of Laboratory Animals.

Cecal ligation and puncture (CLP)

Sepsis was induced by CLP[47]. Briefly, mice were anesthetized using isoflurane (2.5% gas via inhalation). The abdomen was shaved and disinfected with 5% povidone-iodine antiseptic. Bupivicaine (6 mg/kg s.c.) was then administered at the site where a midline incision was made. The distal third (~1 cm) of the cecum was ligated with 4-0 silk suture and punctured once with a 25-g needle to extrude a small amount of cecal content. After returning the cecum to the abdomen, the peritoneum was closed via continuous suture and the skin was sealed using surgical glue (Vetbond; 3M, St. Paul, MN). Postoperative analgesia and fluid resuscitation occurred at the conclusion of surgery and the following 3 days in the form of meloxicam (2 mg/kg) in 1 ml saline. Mice were monitored daily for weight loss and pain for at least 5 days post-surgery. To control for nonspecific changes from the surgery, sham mice underwent the same laparotomy procedure excluding ligation and puncture.

Experimental pathogens and infections

C57BL/6 mice were immunized with attenuated *Listeria monocytogenes*-2W1S (Lm-2W1S) or Lm-OVA (10^7 CFU i.v.) or attenuated *Salmonella enterica* serovar Typhimurium strain BRD509-2W1S (*Se*-2W1S; AroA-; 10^6 CFU i.v.) 30 days before sham or CLP surgery to generate memory CD4 T cells. In some experiments, mice received a second infection with attenuated Lm-2W1S (10^7 CFU i.v.), virulent Lm-OVA (10^4 CFU i.v.) or virulent *Se*-2W1S (10^3 CFU i.v.). In experiments where mice received a

secondary virulent Lm-OVA bacterial challenge, mice were depleted of CD8 T cells by injecting 100 μg anti-CD8 mAb (clone 2.43) i.v. 3, 2, and 1 days prior to secondary infection. In experiments where mice received a secondary virulent *Se*-2W1S bacterial infection, some of the mice were depleted of CD4 T cells by injecting 800 μg of anti-CD4 mAb (clone GK1.5) i.v. 7 days before and 400 μg i.v. 4 and 3 days before challenge. To measure the clearance of the secondary infection of virulent Lm-OVA or virulent *Se*-2W1S, livers and spleens were removed 3 or 7 days post-infection, respectively, placed in 0.2% IGEPAL solution (Sigma-Aldrich), and homogenized. Serial dilutions of the homogenate were plated on tryptic soy broth agar containing 50 μg/ml streptomycin (for Lm-OVA) or 100 μg/ml streptomycin (for *Se*-2W1S), which restricted bacterial growth to the streptomycin-resistant Lm-OVA or *Se*-2W1S used for secondary infection. Bacterial colonies were counted after 24 hours incubation at 37°C[29,64,155].

Enrichment and analysis of Ag-specific CD4 T cells

I-A^b-specific tetramers containing 2W1S (EAWGALANWAVDSA) or $OVA_{323-339}$ (ISQAVHAAHAEINEAGR) were used to identify Ag-specific CD4 T cells[108,109,156]. Briefly, I-A^b β-chains containing the 2W1S or $OVA_{323-339}$ epitopes covalently linked to the I-A^b β-chain were produced in Drosophila melanogaster S2 cells. 2W1S:I-A^b or $OVA_{323-339}$:I-A^b monomers were then biotinylated and made into tetramers with streptavidin-phycoerythrin (SA-PE; Prozyme). To enrich for Ag-specific CD4 T cells, tetramers (10 nM final concentration) were then added to single cell suspensions in 300 μl tetramer staining buffer (PBS containing 5% FBS, 2mM EDTA, 1:50 normal mouse serum, and 1:100 anti-CD16/32 mAb). The cells were incubated in

the dark at room temperature for 1 hour, followed by a wash in 10 ml ice cold FACS Buffer. The tetramer-stained cells were then resuspended in 300 µl FACS Buffer, mixed with 25 µl of anti-PE mAb-conjugated magnetic microbeads (StemCell Technologies), and incubated in the dark on ice for 30 minutes. The cells were washed, resuspended in 3 ml cold FACS Buffer, and passed through an EasySep Magnet (StemCell Technologies) to yield the enriched tetramer positive population. The resulting enriched fractions were stained with a cocktail of fluorochrome-labeled mAb (see below). Cell numbers for each sample were determined using AccuCheck Counting Beads (Invitrogen). Samples were then analyzed using a Fortessa flow cytometer (BD) and FlowJo software (TreeStar Inc., Ashland, OR). The percentage of 2W1S:I-A^{b+} or $OVA_{323-339}$:I-A^{b+} events was multiplied by the total number of cells in the enriched fraction to calculate the total number of 2W1S:I-A^{b}- or $OVA_{323-339}$:I-A^{b}-specific CD4 T cells.

In vivo peptide stimulation was used to determine Ag-specific CD4 T cell cytokine production, as previously described[62,110,156,157]. Briefly, infected mice were injected i.v. with 100 µg of the 2W1S or $OVA_{323-339}$ peptides (synthesized by Bio-Synthesis, Louisville, TX). After 4 h, spleens were harvested in media containing 10 µg/ml brefeldin A. The resulting cell suspensions were fixed, permeabilized, and stained with anti-IFNγ, -TNF, and -IL-2 mAb.

Flow cytometry

To assess the expression of cell surface proteins, cells were incubated with fluorochrome-conjugated mAb at 4°C for 30 minutes. The cells were then washed with FACS buffer. For some experiments, the cells were then fixed with PBS containing 2% paraformaldehyde. In procedures requiring intracellular staining, cells were

permeabilized following surface staining using the transcription factor staining kit (Tonbo), stained for 1 hour at 20°C with a second set of fluorochrome-conjugated mAb, and suspended in FACS buffer for acquisition. The fluorochrome-conjugated mAb used in both surface and intracellular staining were as follows: Dump gate: APC-Cy7 CD11b (clone M1/70; Tonbo), APC-Cy7 CD11c (clone N418; Tonbo), APC-Cy7 B220 (clone RA3-6B2; Tonbo), APC-Cy7 F4/80 (clone BM8.1; Tonbo), Ghost Red 780 viability dye (Tonbo). Surface staining: BV650 CXCR5 (clone L138D7; BioLegend), Brilliant Violet 510 CD44 (clone IM7; BioLegend), redFluo 710 CD44 (clone IM7; Tonbo), Brilliant Violet 711 CD8 (clone 53-6.7; BioLegend), Brilliant Ultra Violet 395 Thy1.2 (clone 53-2.1; BD Biosciences) – used as an alternative to CD3 for gating T cells, Brilliant Ultra Violet 496 CD4 (clone GK1.5; BD Biosciences), Alexa Fluor 647 CD49d (clone R1-2; BD Biosciences), FITC CD11a (clone M17/4; eBioscience), PE-Cy7 CD11a (clone M17/4; eBioscience). Intracellular staining: Alexa Fluor 488 Foxp3 (clone FJK-15S; Invitrogen), PE-Cy7 Tbet (clone 4B10; BioLegend), PE Bcl6 (clone K112-91; BD Biosciences), BV650 IFN-γ (clone XMG1.2; BD Biosciences), APC IFN-γ (clone XMG1.2; eBioscience), PE-Cy7 IL-2 (clone JES6-5H4; BioLegend), APC TNF-α (clone MP6-XT22; BioLegend), PE TNF-α (clone MP6-XT22; BioLegend), PE-Cy7 IL-2 (clone JES6-5H4; BioLegend). Gating and fluorescence thresholds were determined using fluorescence minus one (FMO) controls.

Statistical analyses

Data shown are presented as mean values + SEM. GraphPad Prism 8 was used for statistical analysis, where statistical significance was determined using two-tailed Student

t-test (for 2 individual groups, if unequal variance Mann-Whitney U test was used) or group-wise, one-way ANOVA analyses followed by multiple-testing correction using the Holm-Sidak method, with $\alpha = 0.05$. * $p < 0.05$, ** $p < 0.01$, *** $p < 0.005$, **** $p < 0.001$.

III. Results

The number of pre-existing memory CD4 T cells fluctuate after sepsis

Septic patients have reduced delayed-type hypersensitivity (DTH) responses, marked by a failure to respond to skin testing with Ag to which previous exposure is known to have occurred[32,158,159]. DTH responses are driven in large part by memory CD4 T cells – even though other immune cells such as CD8 T cells and antigen presenting cells (APCs) participate in the response – and DTH can be used as an assessment of overall immune system fitness[160]. To more directly and rigorously interrogate the long-term consequences of sepsis on memory CD4 T cells, we used a protocol where an endogenous, Ag-specific memory CD4 T cell population was generated by infection with attenuated *Listeria monocytogenes* engineered to express the I-A^b-restricted peptide 2W1S (Lm-2W1S) 30 days before performing sham/CLP surgery (Figure 3-1A). We also employed a peptide:MHC II (I-A^b) tetramer-based approach to identify the endogenous 2W1S-specific CD4 T cells before and after sham/CLP surgery. Initially, spleens were harvested from naïve mice and mice at 7, 14, and 28 days post-infection to document the expansion, contraction, and establishment of memory 2W1S-specific CD4 T cells (Figure 3-1B). The majority of memory 2W1S-specific CD4 T cells adopted a Th1 ($Tbet^+$)

phenotype (Figure 3-1C), but some cells upregulated Foxp3 suggesting their differentiation into regulatory T cells (Figure 3-1D).

Sham or CLP surgery was performed on the remaining mice 30 days post-infection, and the number of total and 2W1S-specific CD4 T cells in the spleen were determined 2, 7, 14, and 28 days post-surgery by flow cytometry (Figure 3-2A). Our version of the CLP model results in ~20% mortality within the first 4 days after surgery (Figure 3-2B). Despite this low overall mortality, the mice that underwent CLP show dramatic reductions in number of total CD4 T cells and 2W1S-specific memory CD4 T cells at 2 days post-surgery that gradually recovered by day 30 (Figures 3-2C and 3-2D), which is consistent with our previous data[31,103,117,161]. Interestingly, the numerical recovery of the $Foxp3^+$ 2W1S-specific memory CD4 T cells occurred by day 7 post-CLP, while it took longer for the number of Tbet+ 2W1S-specific memory CD4 T cells to return to sham levels (Figures 3-2E and 3-2F). Collectively, these data show pre-existing memory CD4 T cells experience a transient reduction in number during CLP-induced sepsis.

Loss and recovery of Ag-experienced memory CD4 T cells in septic 'dirty' mice

Most preclinical sepsis research done to date has used specific pathogen-free (SPF) mice, which possess an immune system equivalent to that of neonatal humans[50]. The vaccinations and infections experienced over a lifetime shape the immune system so rapid and protective functional responses can occur during new microbial encounters. Recently, we investigated the effect of sepsis on standard SPF B6 mice cohoused for 60 days with microbially-experienced 'dirty' pet store mice[154]. Cohousing laboratory SPF mice with pet store mice permits physiological pathogen transfer and matures the murine immune system to more closely resemble that seen in adult humans[50]. To determine the

effect of sepsis on multiple memory CD4 T cell populations generated following environmental pathogen/commensal exposure, we performed sham or CLP surgery on cohoused B6 mice age-matched to their SPF counterparts (Figure 3-3A). Cohousing increases the frequency of circulating memory $CD44^{hi}$ CD4 T cells (compared to age-matched SPF mice; Figure 3-3B), and the number of total CD4 T cells and $CD44^{hi}$ memory CD4 T cells dramatically decline 2 days after CLP surgery (Figures 3-3C and 3-3D). We extended this analysis of the memory CD4 T cell compartment using a second, more-stringent phenotyping to identify true "Ag-experienced" memory CD4 T cells based on the upregulation of CD11a and CD49d[162]. The cohoused mice showed a significant reduction in number of Ag-experienced (CD11+CD4d+) and naïve (CD11a-CD49d-) CD4 T cells in the spleen 2 days after CLP that returned to sham levels by day 30 (Figures 3-3B, 3-3C, 3-3D, and 3-3E), indicating entire CD4 T cell compartment is susceptible to sepsis-induced numerical reduction. Thus, the data in Figures 3-2 and 3-3 collectively show memory CD4 cells initially elicited by infection undergo a significant, but transient, numerical reduction in secondary lymphoid organs following CLP-induced sepsis.

Recall response to cognate Ag by pre-existing memory CD4 T cells is reduced after sepsis

Data in Figure 3-2 show 2W1S-specific memory CD4 T cells numerically recover by day 30 post sepsis. This result would suggest this population of Ag-specific memory CD4 T cells has returned to normal. However, the ability of pre-existing memory CD4 T cells to proliferate, accumulate, and exert effector functions after a second encounter with

cognate Ag in the post-septic host has not been rigorously defined. Thus, we first examined the ability of this population of Ag-specific CD4 T cells to proliferate in response to cognate Ag recognition during secondary pathogen encounter. To do this, B6 mice were immunized with attenuated Lm-2W1S 30 days before sham or CLP surgery. The mice were then infected a second time with attenuated Lm-2W1S on day 2 or 30 after surgery. Total numbers of 2W1S-specific CD4 T cells in the spleen were determined before and after the second Lm-2W1S infection (Figure 3-4A). When infected on day 2 post-surgery, the 2W1S-specific CD4 T cells had significantly reduced proliferative capacity compared to sham-treated mice (Figure 3-4B). Specifically, the number of 2W1S-specific CD4 T cells in the sham-treated mice expanded 44-fold during the 7 days after secondary infection, but only 6-fold in the CLP-treated mice. However, when challenged on day 30 post-surgery, the proliferative capacity of the 2W1S-specific memory CD4 T cells in CLP-treated mice had nearly recovered to what was found in sham mice (Figure 3-4C). These data indicate the ability of Ag-specific memory CD4 T cells to proliferate during a recall response to cognate Ag (such as during a secondary infection) is only transiently reduced following sepsis.

To examine the effector function of the 2W1S-specific memory CD4 T cells at 2 and 30 days post-surgery, we used in vivo peptide restimulation where the Lm-2W1S-immune mice were injected i.v. with 2W1S peptide[62,64,110,156,157]. This technique permits the evaluation of cytokine production by Ag-specific (tetramer^{+}) CD4 T cells with almost no background staining. Spleens were harvested 4 hours after 2W1S peptide injection and processed for flow cytometry to determine the frequency and number of

cytokine-producing 2W1S-specific memory CD4 T cells. Lm infection primarily generates a Th1 response[163], therefore we identified the 2W1S-specific CD4 T cells making IFNγ, TNF, and IL-2 (Figures 3-5A and 3-5B). It is important to note the gating strategy employed permits the identification and analysis of bona fide memory CD4 T cells using 2W1S:I-A^b tetramers that helps us determine the "per cell" capacity of those cells to produce cytokines. Similar to what was observed with the reduction in proliferative capacity seen 2 days post CLP-induced sepsis, the frequency and number of single or multi-cytokine producing 2W1S-specific memory CD4 T cells ($IFN\gamma^+$-, $IFN\gamma^+TNF^+$-, and $IFN\gamma^+TNF^+IL\text{-}2^+$) was significantly reduced at 2 days post-surgery (Figures 3-5C and 3-5D) and remained reduced 30 days after CLP. Interestingly, when we looked at the 2W1S-specific memory CD4 T cells only making IL-2 30 days after CLP surgery, the frequency and number of $IL\text{-}2^+$ 2W1S-specific memory CD4 T cells was similar to that seen in sham-treated mice (Figures 3-5E and 3-5F). This data is consistent with that in Figure 3-4, where we saw a restoration in proliferative capacity at day 30 post-CLP. Together, these data indicate prolonged impairment in the ability of the 2W1S-specific memory CD4 T cells to produce cytokines critical for pathogen clearing immunity when re-stimulated in an Ag-specific manner, despite recovery of cell numbers and proliferative capacity (by day 30).

Sepsis impairs memory CD4 T cell-mediated immunity to infection

Our data show 2W1S-specific memory CD4 T cells numerically recover by 30 days after CLP surgery, but their ability to produce effector cytokines after re-stimulation remains blunted, suggesting a potential lesion in protective capacity following re-

infection. To test this, we wanted to challenge post-septic mice with a virulent pathogen. Our experiments thus far have used attenuated Lm-2W1S to generate a trackable population of endogenous memory Ag-specific CD4 T cells; however, no virulent form of Lm-2W1S exists. Therefore, in the following experiments we employed two different murine models of infection using virulent bacterial strains. It is important to note that while the bacteria strains selected are pathogens not typically found in human septic patients, their use as experimental pathogens is well-established and modification to express known I-A^b-restricted epitopes allow us to examine distinct, Ag-specific CD4 T cell responses after CLP. In the first model, we generated 2W1S-specific memory CD4 T cells by infecting mice with attenuated *Salmonella enterica* engineered to express the 2W1S epitope (*Se*-2W). *Salmonella*-2W1S infection stimulates a robust Ag-specific CD4 T cell response[157,164] because the bacteria replicate in the phagosomes of dendritic cells and macrophages – the location of peptide:MHC II complex formation[155,165–168]. Moreover, mice immunized with *Salmonella* -2W1S demonstrate protective immunity to a secondary infection with virulent *Salmonella* [164]. To confirm the importance of *Salmonella* -specific memory CD4 T cells in the protection to virulent *Salmonella* infection, some of the *Se*-2W-infected mice were depleted of CD4 T cells (using the anti-CD4 mAb GK1.5) prior to a second infection of virulent *Se*-2W (Figure 3-6A). CD4 T cell-replete mice infected with attenuated *Se*-2W had significantly lower pathogen burdens after secondary virulent *Se*-2W infection compared to the CD4 T cell-depleted mice (Figure 3-6B), and had pathogen burdens comparable to that seen in naïve mice only infected with virulent *Se*-2W. We then performed sham or CLP surgery on a separate cohort of mice infected with attenuated *Se*-2W 30 days prior to surgery. On days

2 or 30 after surgery, all groups were infected with virulent *Se*-2W. Splenic bacterial titers were determined 7 days after virulent *Se*-2W infection, revealing higher burdens in the CLP-treated mice regardless of early or late secondary challenge (Figures 3-6C and 3-6D).

In the second model, naïve mice were infected with attenuated Lm engineered to express OVA (Lm-OVA) to elicit OVA_{323}-specific memory CD4 T cells[169]. We tested the ability of the OVA_{323}-specific memory CD4 T cells to provide protection against a secondary Lm-OVA infection after sepsis induction. The adaptive immune system does not confer protection against primary Lm infections after CLP[170]. CD8 T cells play prominent roles in controlling and eradicating secondary infections by intracellular pathogens that mainly localize to the cytosol of the infected cell, such as *L. monocytogenes*[171], due to the efficient production of peptide:MHC I complexes by the infected cell. However, Lm-specific CD4 T cells can provide sufficient protection to infection even in the absence of CD8 T cells[172–174]. Thus, to focus on the memory CD4 T cell-mediated clearance of Lm-OVA, CD8 T cells were depleted using anti-CD8 mAb (clone 2.43) prior to performing sham of CLP surgery (Figures 3-7A and 3-7B). Two days later the mice were infected with virulent Lm-OVA, after which pathogen burden in the liver and spleen was determined. A separate group of naïve, CD8-depleted mice were infected with virulent Lm-OVA for reference. As expected, we saw substantially reduced Lm-OVA burden in both the liver and spleen compared to infected naïve mice (Figures 3-7C and 3-7D). In contrast, the Lm-OVA burdens were dramatically higher in the CLP-treated mice compared to sham mice. To better understand the cause

for this reduced protection, we examined the impact of sepsis on the number and function of the OVA_{323}-specific memory CD4 T cells (Figure 3-7E). Just as seen with the 2W1S-specific memory CD4 T cells, CLP-induced sepsis led to a significant reduction in OVA_{323}-specific memory CD4 T cell numbers and ability to produce IFNγ after in vivo restimulation (Figures 3-7F and 3-7G). Together, the data in Figures 3-5 and 3-6 show the sepsis-induced long-lasting changes in Ag-specific memory CD4 T cell pools that ultimately impact the ability of the host to properly respond to pathogen re-infection.

IV. Discussion

Sepsis causes millions of deaths annually[2,175,176], and the incidence of sepsis has increased dramatically in recent decades. Understanding the cellular mechanisms that contribute to sepsis-induced immunosuppression is critical for developing effective therapies and improving the survival and quality of life for septic patients. CD4 T cells have the unique flexibility of functioning in an array of immunological settings due to their ability to differentiate into a variety of phenotypic subsets based on the inflammatory milieu produced at the time of primary Ag encounter[177,178]. Clinical data show considerable reduction in number of circulating CD4 T cells (along with other lymphocyte populations) in sepsis patients of all ages[16,57–59] and at the time of high pathogen burden[179,180]. Moreover, reports of decreased effector CD4 T cell function in critically ill sepsis patients date back to the 1970's with data showing impaired DTH reactions[32]. These observations and the fact that DTH is mediated in large part by CD4 T cells[181] bring into question to what extent memory CD4 T cells are numerically and functionally affected by sepsis. However, most (if not all) of the previous studies

examined the effect of sepsis on the CD4 T cell compartment in sum, which has the potential to mask some of the unique characteristics of individual Ag-specific populations[62]. In contrast to these previous publications, the present study took advantage of pathogens engineered to express defined CD4 T cell epitopes to stimulate the generation of bona fide memory CD4 T cells and reagents to identify and quantitatively and qualitatively evaluate endogenous Ag-specific memory CD4 T cells that have experienced a septic event. As a complement to the experiments using conventional laboratory mice infected with a known experimental pathogen to generate Ag-specific memory CD4 T cells, our 'dirty' mouse model allowed us to investigate how multiple populations of memory CD4 T cells are affected during sepsis in an animal with a more adult human-like immune system[50,154,182]. Together, the experimental model systems used provided a unique means by which sepsis-induced immunoparalysis of memory CD4 T cells was evaluated.

One area of sepsis research that has received considerable attention recently deals with the idea that sepsis may differentially affect naïve and memory T cells. Indeed, there is data to suggest memory CD8 T cells are more resistant to radiation-induced apoptosis than naive cells[183]. Cellular apoptotic mechanisms induced by extrinsic (i.e., death receptor) and intrinsic (i.e., mitochondrial) pathways have been suggested to be major contributors to the numerical reduction in total CD4 and CD8 T cells following sepsis[35], but the definitive molecule responsible for initiating lymphocyte apoptosis during sepsis has yet to be identified. Regardless of the mechanism by which sepsis-induced lymphopenia occurs, studies from a number of laboratories using proven

experimental infection models for eliciting Ag-specific memory T cells indicate circulating Ag-experienced memory CD8 T cells are equally susceptible to sepsis-induced attrition as naïve CD8 T cells[29,118,184,185]. In addition, the circulating memory CD8 T cells exhibit profound impairment in effector functionality (e.g, decreased Ag sensitivity, proliferative capacity, cytokine production, and inability to clear secondary infections) following a septic event[186]. The numerical and functional decrease in circulating memory CD8 T cells is not, interestingly, reciprocated in tissue-resident memory CD8 T cells after a moderate sepsis insult that leads to <10% mortality[118]. The number of tissue-resident memory CD8 T cells is maintained after sepsis, as well as their ability to produce effector cytokine after re-stimulation. In contrast to the aforementioned similar attrition of naïve and memory CD8 T cells after sepsis, it was recently suggested by Xie et al. that $CD44^{hi}$ CD8 T cells in "memory mice" (generated via *Listeria* and LCMV infection) exhibited significant attrition after CLP while this was not the case for naïve $CD44^{lo}$ CD8 T cells[63]. It was surprising to see that CLP sepsis did not lead to a reduction in $CD44^{lo}$ CD8 T cells, as such a reduction has been noted in other papers[17,36,39,103,117,147,187]. Moreover, these authors examined the bulk CD8 T cell compartment, even though peptide:MHC I tetramers were available to identify LCMV-specific CD8 T cells. The authors also detected increased expression of CD25, PD-1, and 2B4 on the memory CD8 T cells, but did not perform any studies to directly determine if and/or how these proteins may be altering T cell sensitivity to sepsis-induced attention. Needless to say, additional data is needed to conclusively determine the extent of naïve and memory CD8 T cells sensitivity to CLP-

induced apoptosis and the potential role played by intrinsic factors (e.g., CD25, PD-1, 2B4, and other proteins) in regulating this sensitivity.

Fewer studies have examined the effect of sepsis on Ag-experienced memory CD4 T cells compared to what has been done for memory CD8 T cells, driving our interest in the current set of experiments. Contrary to the increased susceptibility of memory $CD44^{hi}$ CD8 T cells (vs. naïve $CD44^{lo}$ CD8 T cells) to sepsis-induced apoptosis suggested by Xie et al.[63], data presented by these authors suggested $CD44^{hi}$ CD4 T cells were not more sensitive to attrition during sepsis compared to $CD44^{lo}$ CD4 T cells. As with their CD8 T cell data, the CD4 T cells were examined at the bulk (non-Ag-specific) level. Some of the data presented herein are consistent with the data by Xie et al., but there are some important differences in our study that are worth noting. First, our data show CLP-induced sepsis results in a transient numerical reduction of 2W1S-specific memory CD4 T cells (current study), while 2W1S-specific naive CD4 T cells suffer from prolonged numerical reduction[62]. Second, while the numerical reduction was transient, the inability of the 2W1S-specific memory CD4 T cells to produce cytokines upon peptide restimulation was evident out to day 30 post CLP, similar to what was observed in naïve cells[62]. Cytokine "help" from CD4 T cells is a hallmark of this population of immune cells, and the prolonged dysfunction in cytokine production may contribute the generalized immunoparalysis seen during sepsis. Furthermore, the in vivo peptide restimulation assay used is a more physiological way of activating the desired Ag-specific population via MHC II presentation of peptide Ag[62,110,156,157]. Third, despite their reduced ability to produce cytokines at day 30-post sepsis, 2W1S-specific

memory CD4 T cells were surprisingly able to expand upon Ag re-encounter 30 days after CLP to nearly sham levels. It is important to note that the accumulation/expansion of Ag-specific effector CD4 T cells upon Ag re-encounter is dependent on the rate of proliferation (leading to an increase in cell accumulation) and rate of death (decrease in accumulation). We did not measure either of these parameters; however, impairment is clearly seen in day 2 septic mice undergoing secondary challenge since the fold-expansion in numbers from pre-challenge level was significantly diminished (6x compared to 44x – see Figure 3-4). It is reasonable to suggest that the reduction in accumulation of memory CD4 T cells following a second encounter with cognate Ag to be due to decreased per-cell proliferation, increased death, or both. Together, our data show the 2W1S-specific memory population is similarly prone to the initial sepsis-induced depletion and prolonged inability to produce important inflammatory cytokines compared to their naïve counterparts. However, unlike naïve 2W1S-specific CD4 T cells, Ag-experienced memory 2W1S-specific CD4 T cells quickly recover numerically, as well as their ability to proliferate in response to a secondary infection. It remains to be determined how sepsis affects the number and function of tissue-resident memory CD4 T cells. Moreover, the different recovery rates between the memory and regulatory Foxp3$^+$ CD4 T cell populations could suggest additional time-dependent mechanisms that control the ability of sepsis survivors to respond to secondary infection. There have been a few reports specifically looking at the role of regulatory Foxp3$^+$ CD4 T cells in sepsis[72,188,189], and while these data hint at the participation of this CD4 T cell subset in sepsis-inducced immune suppression additional evaluation is needed to better define how regulatory CD4 T cells are maintained and function in the post-septic host.

Our data collectively show CLP-induced sepsis results in a transient numerical reduction and long-term functional deficits of Ag-specific memory CD4 T cells, which contributes to the characteristic long-lasting immunoparalysis seen after sepsis and reduced protection to secondary infection. Secondary infection after sepsis, acquired while in the hospital or after discharge, is a leading cause of sepsis mortality[19,190–192]. Lungs, blood stream, surgical site/soft tissue, and urinary tract are the most sites of secondary infection in septic patients, with *Pseudomonas spp.*, *Staphylococcus spp.*, *Candida albicans*, *E. coli*, and *Enterococcus spp.* being common secondary infection microbes[193]. We recognize that the experimental pathogens used in this study (to establish either the primary or secondary infection) are not the "typical" pathogens found in sepsis patients. We chose to use *Listeria* and *Salmonella* for the following reasons: 1) both are well-established model pathogens for examining the immune response to bacteria, where attenuated strains are available for generating memory T cells and virulent strains are available to assess the protective capacity of the memory T cells; 2) *Listeria* and *Salmonella* infection stimulates a robust Ag-specific CD4 T cell response because the bacteria replicate in the phagosomes of dendritic cells and macrophages – the location of peptide:MHC II complex formation; and 3) the recombinant *Listeria* and *Salmonella* strains express known I-A^b-restricted epitopes. Future studies could include engineering recombinant *P. aeruginosa*, *S. aureus*, and/or *S. pneumonia* to express the 2W1S (or some other) epitope that will enable testing of the 2W1S-specific memory CD4 T cell response in CLP-treated mice given a secondary infection with a clinically-relevant pathogen after recovery from the initial septic event. It is also important to note that while our study exclusively examined the in vivo function of memory CD4 T cells after sepsis,

other publications have shown the environment is also a critical factor in sepsis-induced suppression of T cells[13]. Following sepsis, a number of CD4 T cell extrinsic factors have been found to suppress the activity of CD4 T cells, including the reduced APC function and TNF signaling[13,188]. Sepsis also leads to dysfunction of the innate immune system, including impaired bacterial clearance by neutrophils, leading to increased susceptibility to *P. aeruginosa* and *S. aureus*[170,194]. Future studies could investigate the extent to which sepsis impairs innate immune responses, especially those related to trained innate immunity, in microbially-experienced mice containing a high frequency of Ag-experienced memory T cells.

In summary, our experiments have uncovered differences in recovery and function within the endogenous memory CD4 T cell compartment compared to what has been detected at the "bulk" CD4 T cell level. The data presented here will serve as the foundation for a number of future studies examining the behavior of endogenous, Ag-experienced memory CD4 T cells in the septic host, as well as methods of reversing the immunoparalysis typically observed within this population of immune cells vital to overall immune system fitness.

V. Figures

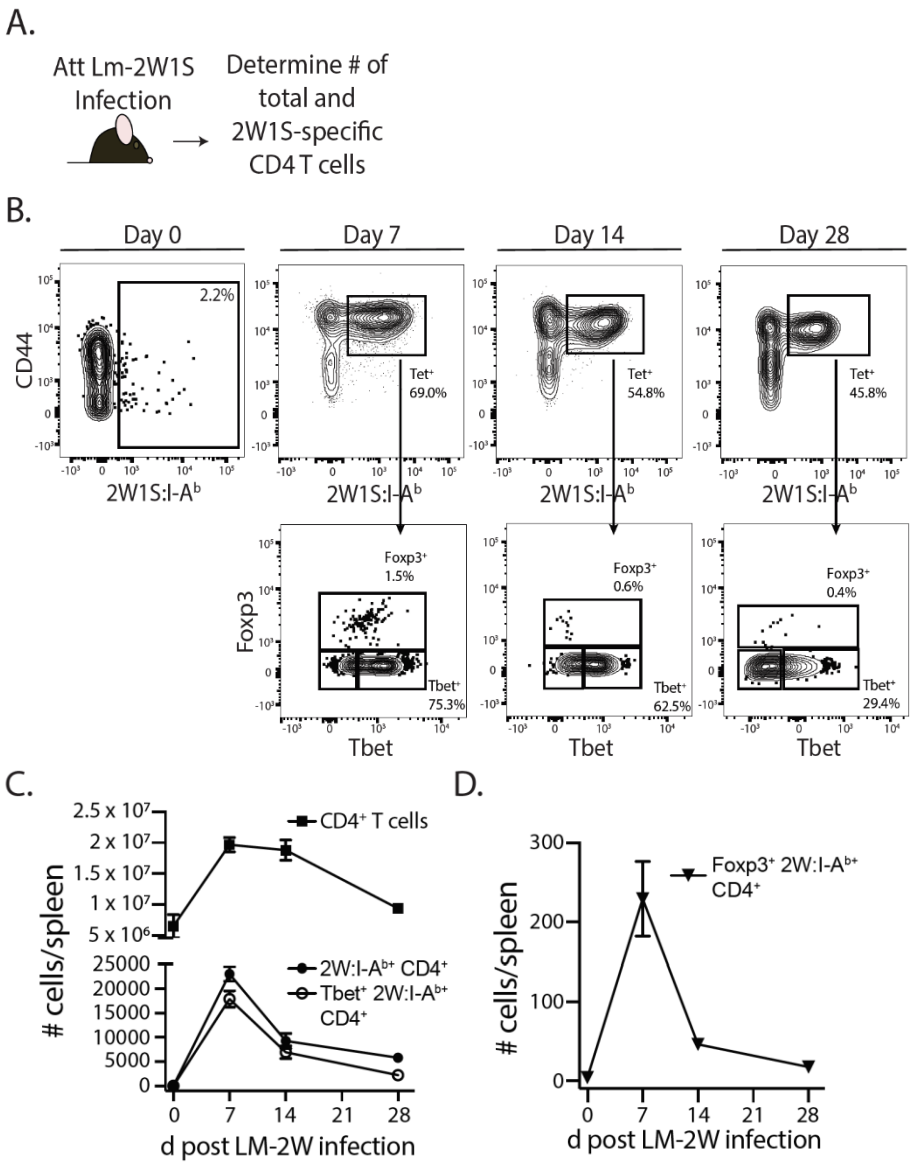

Figure 3-1. Generation of Ag-specific memory CD4 T cells following attenuated *Listeria monocytogenes*-2W1S infection. A. Experimental design – B6 mice were immunized with attenuated *Listeria monocytogenes*-2W1S (10^7 CFU i.v.). The number of 2W1S-specific CD4 T cells were determined before and after infection. B. Representative flow plots show the gating strategy used to identify 2W1S:I-A^{b+} cells first identified as being $CD3^+$ and $CD4^+$. From the tetramer+ gate, cells expressing the transcription factors Tbet (Th1 phenotype) or Foxp3 (regulatory T cell phenotype) were then identified. Positive and negative gating determined using FMO controls. C-D. The number of (C) total CD4 T cells, 2W1S-specific CD4 T cells, $Tbet^+$ 2W1S-specific CD4 T cells, and (D)

Foxp3^{+} 2W1S-specific CD4 T cells in the spleen was determined 7, 14, and 28 days after attenuated LM-2W1S infection. Data shown are representative from 3 independent experiments, with at least 3 mice/group/time point in each experiment.

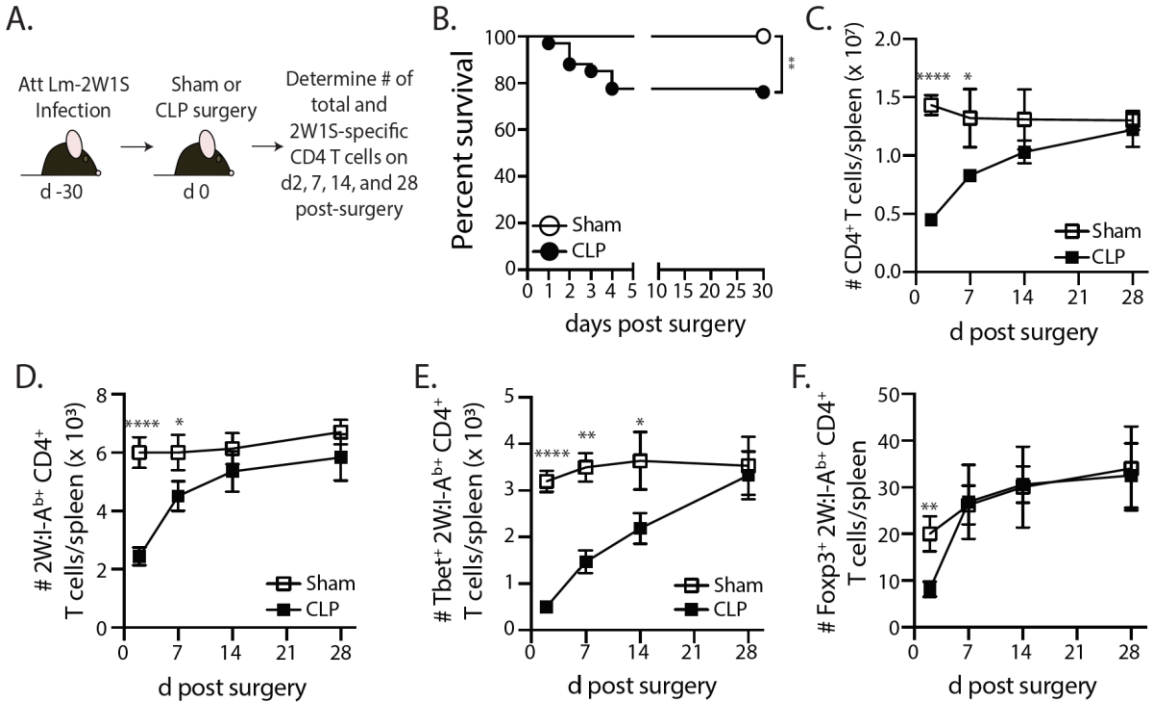

Figure 3-2. Loss and recovery of 2W1S-specific memory CD4 T cells following CLP-induced sepsis. A. Experimental design – B6 mice were immunized with attenuated *Listeria monocytogenes*-2W1S (10^7 CFU i.v.) 30 days before sham or CLP surgery. The number of 2W1S-specific CD4 T cells were determined after surgery. B. Survival of LM-2W-infected B6 mice after sham and CLP surgery (n = 29 sham; n = 67 CLP). C-F. The number of (C) total CD4 T cells and (D) 2W1S-specific CD4 T cells in the spleen was determined 2, 7, 14, and 28 days after sham or CLP surgery by flow cytometry. In addition, the 2W1S-specific CD4 T cells were subtyped based on (E) Tbet (Th1 phenotype) and (F) Foxp3 (regulatory T cell phenotype) expression. Data shown are cumulative from 3 independent experiments, with at least 3 mice/group/time point in each experiment. * $p < 0.05$, ** $p < 0.01$, ** $p < 0.005$, ** $p < 0.001$.

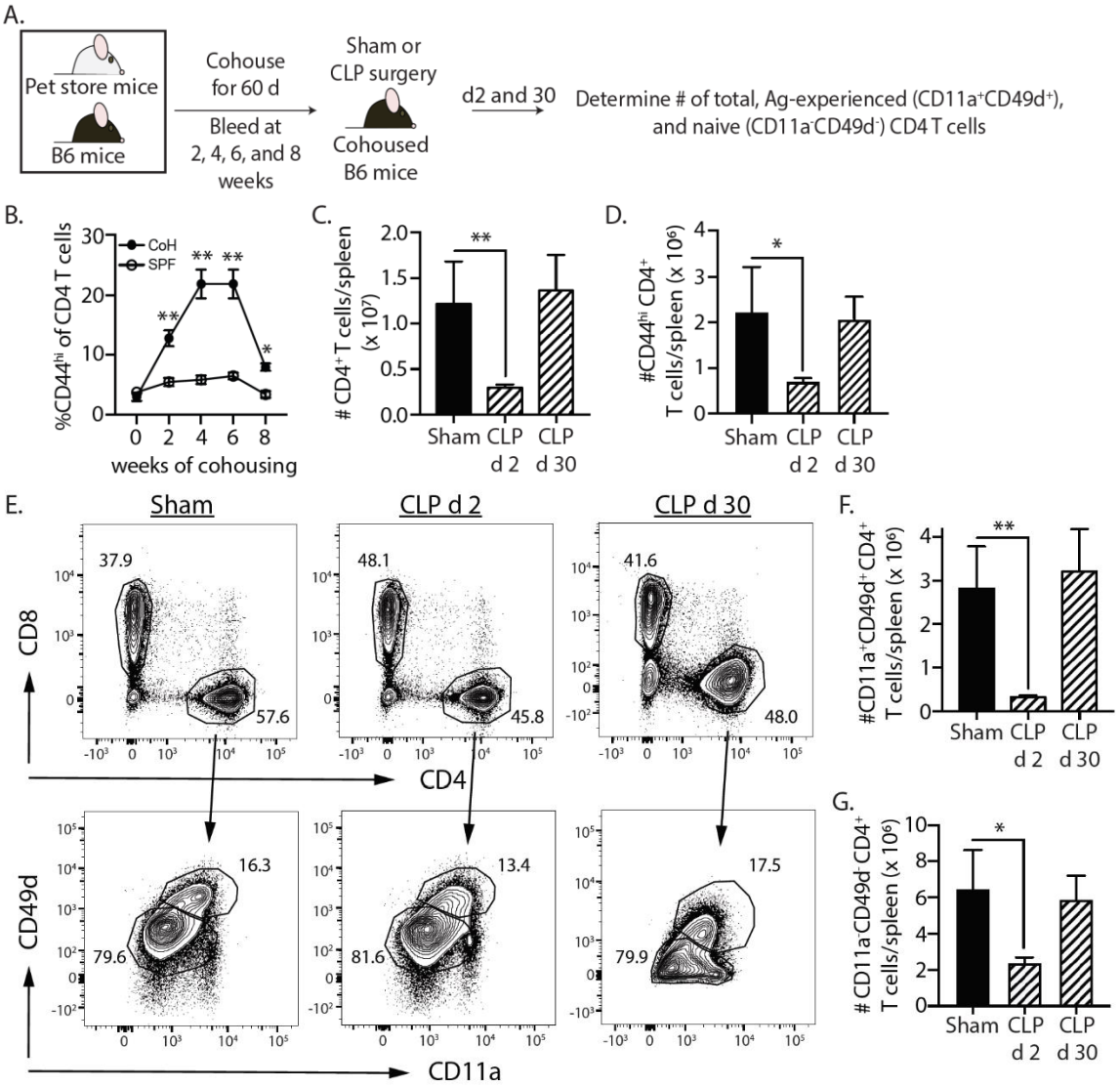

Figure 3-3. Sepsis induces transient loss in number of pre-existing "Ag-experienced" CD4 T cells in microbially-experienced 'dirty' mice. A. Experimental design – SPF B6 mice were cohoused with pet store mice for 60 days to permit microbe transfer and immune system maturation. B. Age-matched SPF and cohoused (CoH) mice were bled prior to and at 2, 4, 6, and 8 weeks after cohousing to determine the frequency of $CD44^{hi}$ CD4 T cells. C-G. Sham or CLP surgery was performed on cohoused B6 mice. The number of total, $CD44^{hi}$, $CD11a^{+}CD49d^{+}$ "Ag-experienced", and $CD11a^{-}CD49d^{-}$ naive CD4 T cells in the spleen was determined 2 and 30 days post-surgery by flow cytometry. E. Representative flow plots show gating strategy. Positive and negative gating determined using FMO controls. The number of (C) total, (D) $CD11a^{+}CD49d^{+}$, and (E) $CD11a^{-}CD49d^{-}$ CD4 T cells was determined. Data shown are representative of 2 independent experiments, with at least 4 mice/group in each experiment. * $p < 0.05$, ** $p < 0.01$.

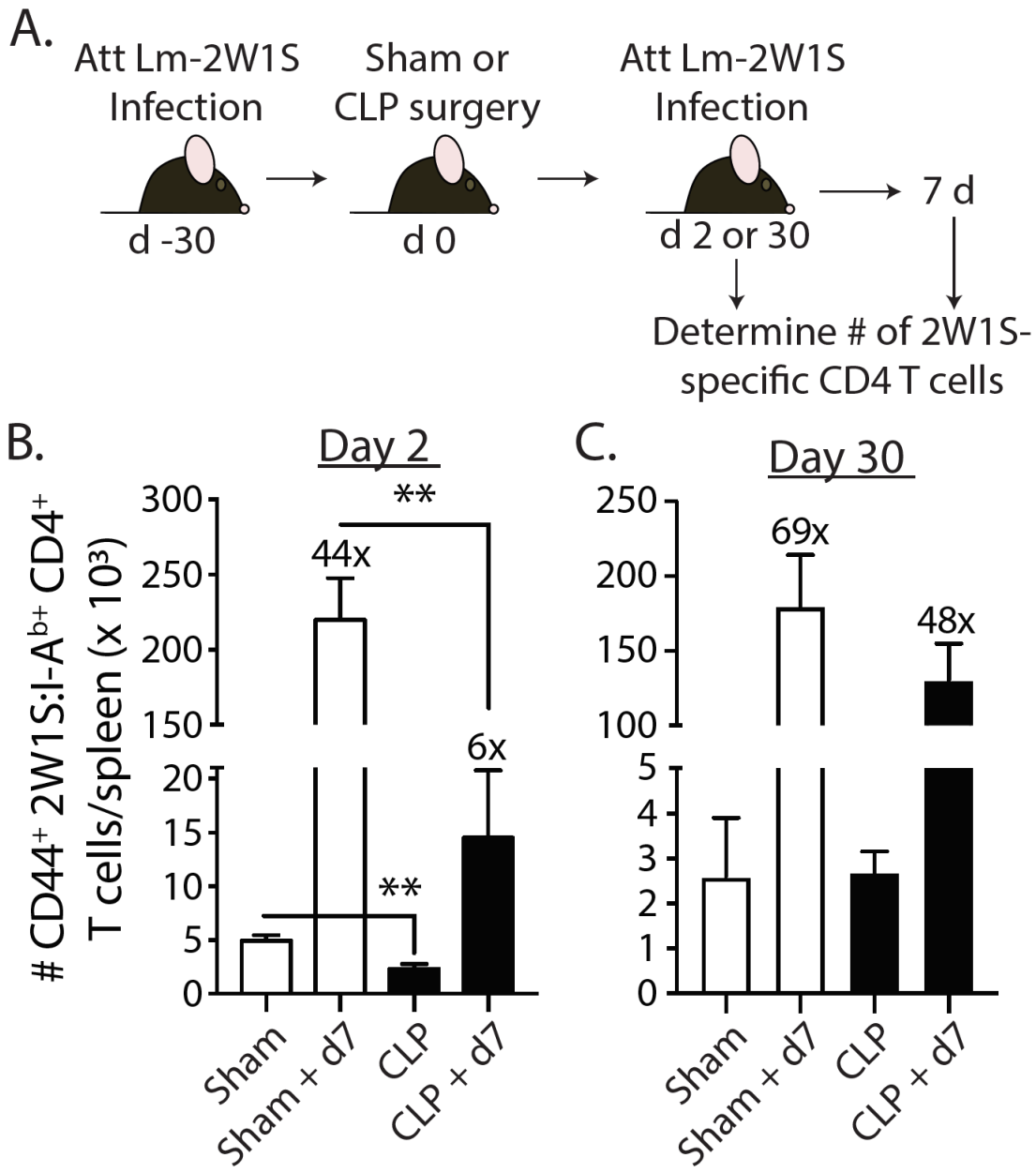

Figure 3-4. Sepsis impairs the recall response by pre-existing 2W1S-specific memory CD4 T cells to cognate Ag. A. Experimental design – B6 mice were immunized with attenuated *L. monocytogenes*-2W1S (10^7 CFU i.v.) 30 days before sham or CLP surgery. The mice were given a second infection with attenuated *L. monocytogenes*-2W1S (10^7 CFU i.v.) 2 or 30 days after surgery. B. Total number of 2W1S-specific CD4 T cells in the spleen was determined the day of and 7 days after the second LM-2W1S infection (10^7 CFU i.v.) . The fold increase in cell numbers at day 7 post-secondary infection is indicated. Data shown are representative of 2 independent experiments, with 4 mice/group in each experiment. ** $p < 0.01$

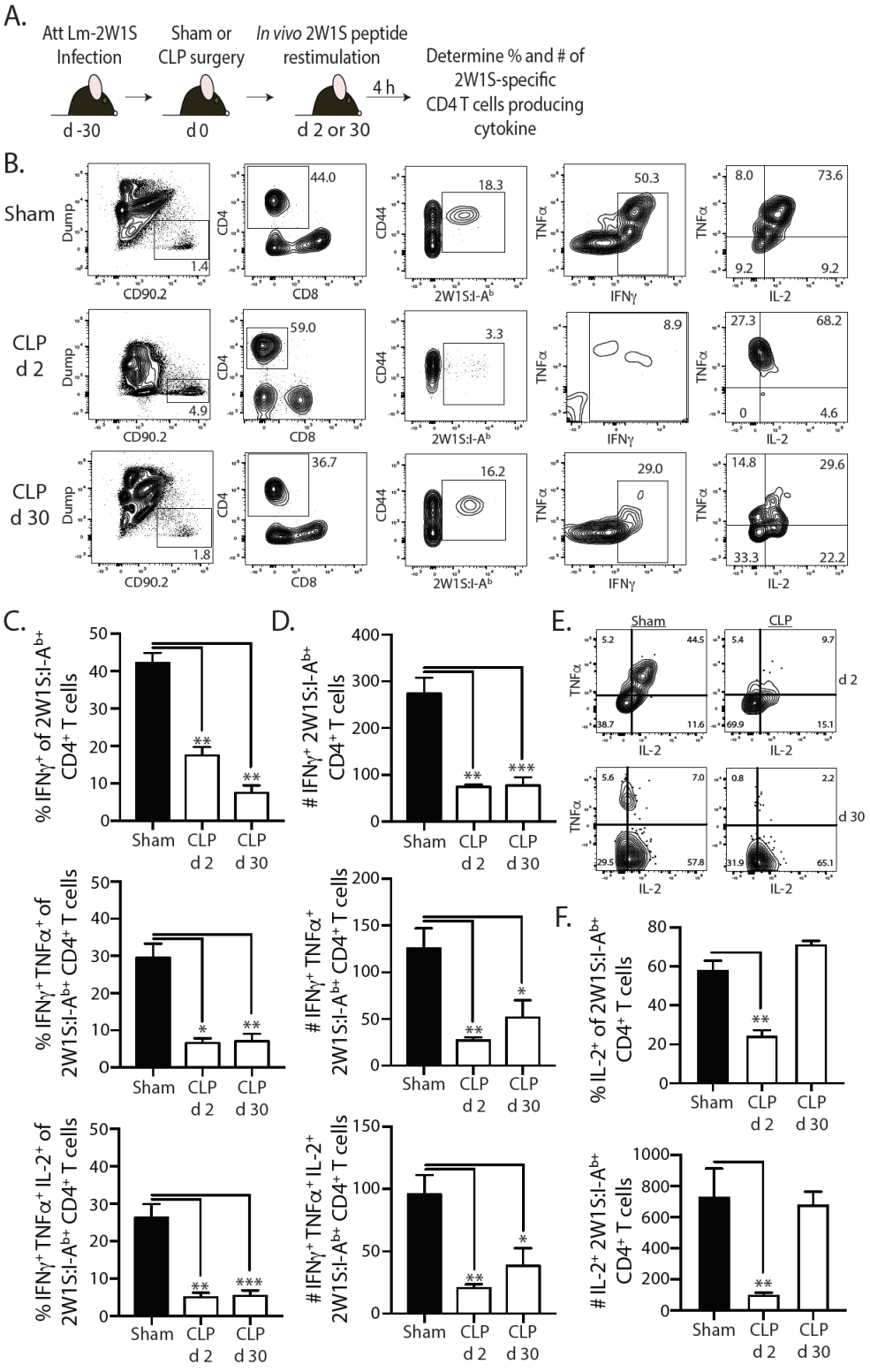

Figure 3-5. Sepsis impairs the ability of 2W1S-specific memory CD4 T cells to produce effector cytokines after in vivo cognate Ag restimulation. A. Experimental

design – B6 mice were immunized with attenuated *L. monocytogenes*-2W1S (10^7 CFU i.v.) 30 days before sham or CLP surgery. Mice were injected with 2W1S peptide (100 μg i.v.) 2 or 30 days after surgery to restimulate the 2W1S-specific memory CD4 T cells. Spleens were harvested 4 hours later, and the frequency and number of $IFN\gamma^+$, $IFN\gamma^+TNF\alpha^+$, and $IFN\gamma^+TNF\alpha^+IL\text{-}2^+$ 2W1S-specific CD4 T cells was determined by flow cytometry. B. Representative flow plots of intracellular IFNγ, TNFα, and IL-2 detection in $CD44^{hi}$2W1S:I-A^{b+} CD4 T cells after in vivo peptide restimulation. Plots show cells gated from 2W:I-A^b-enriched CD4 T cells from sham- or CLP-treated mice. Positive and negative gating determined using FMO controls. Frequency (C) and number (D) of $CD44^{hi}$2W1S:I-A^{b+}-specific CD4 T cells in the spleen producing IFNγ, IFNγ/TNFα, and IFNγ/TNFα/IL-2. E. Representative flow plots of intracellular IL-2 detection in $CD44^{hi}$2W1S:I-A^{b+} CD4 T cells after in vivo peptide restimulation. Plots show cells gated from 2W:I-A^b-enriched CD4 T cells from sham- or CLP-treated mice. Positive and negative gating determined using FMO controls. F. Frequency and number of $CD44^{hi}$2W1S:I-A^{b+}-specific CD4 T cells in the spleen producing IL-2. Data shown are representative of 2 independent experiments, with at least 4 mice/group in each experiment. * $p < 0.05$, ** $p < 0.01$, *** $p < 0.005$

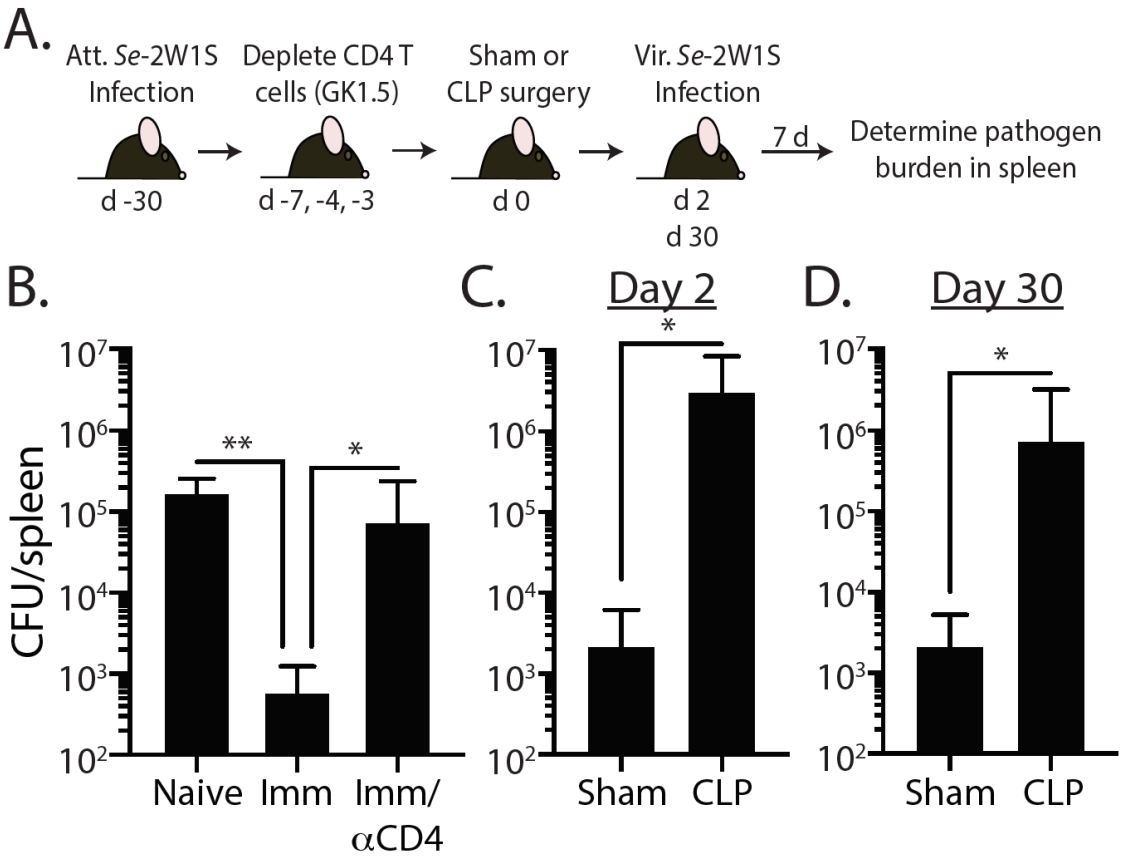

Figure 3-6. Impaired 2W1S-specific memory CD4 T cell-mediated immunity to secondary *Salmonella*-2W1S infection after CLP-induced sepsis. A. Experimental design – B6 mice were immunized with attenuated attenuated *Salmonella enterica* strain BRD509-2W1S (*Se*-2W1S; AroA-; 10^6 CFU i.v.) 30 d before sham or CLP surgery. B. One group of mice (Imm/αCD4) was depleted of CD4 T cells by injecting anti-CD4 mAb GK1.5 i.v. (800 µg on day -7, and 400 µg on days -4 and -3) before second infection with virulent *Salmonella*-2W1S (10^3 CFU i.v.). Bacterial titers in the spleen were determined 7 days later. C. In a separate cohort of attenuated *Se*-2W1S infected mice, sham or CLP surgery was performed. These mice were then challenged with virulent *Se*-2W1S (10^3 CFU i.v.) 2 or 30 days after surgery. Bacterial titers in the spleen were determined 7 days later. Data shown are representative of 3 independent experiments, with at least 5 mice/group in each experiment. * $p < 0.05$, ** $p < 0.01$

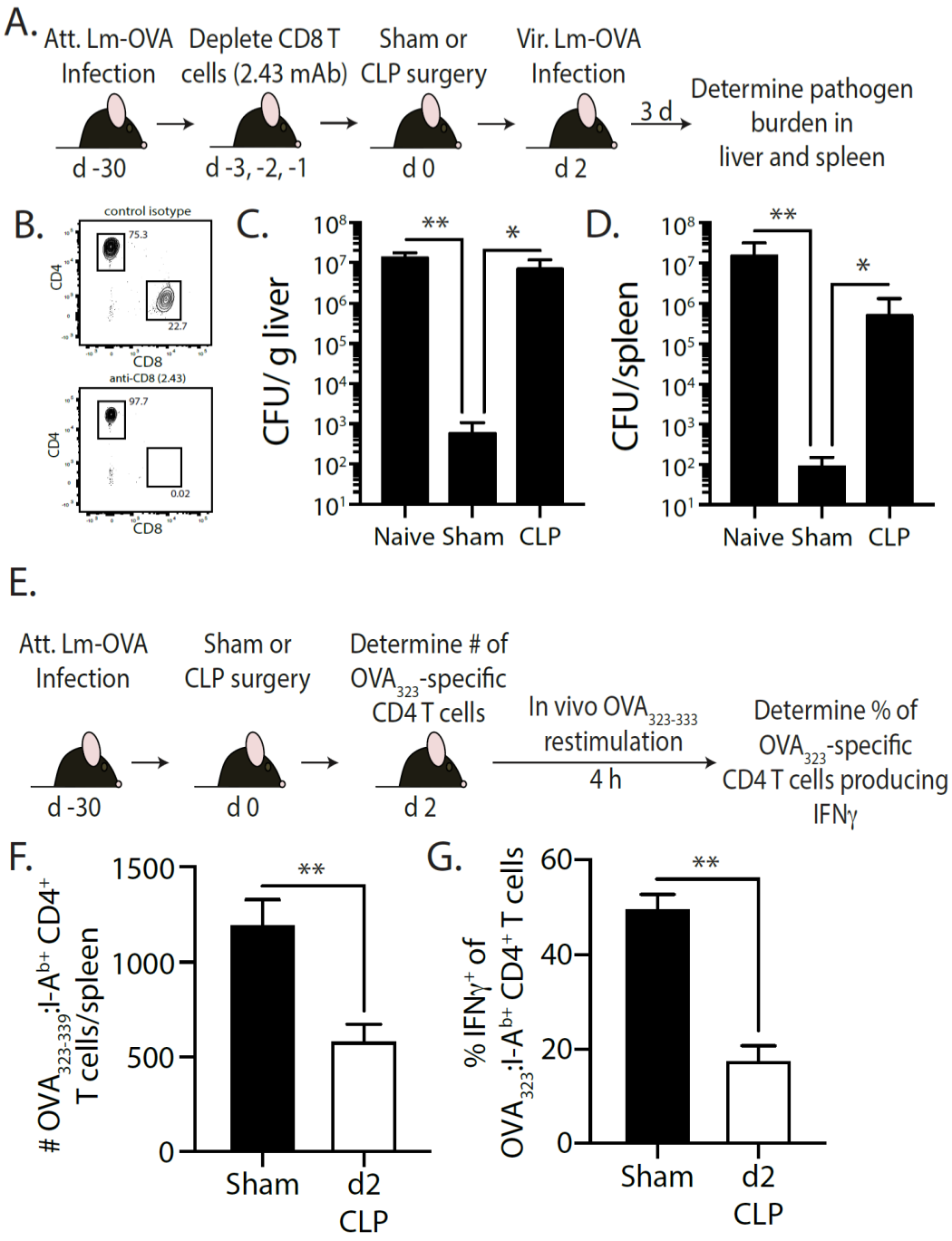

Figure 3-7. Effect of sepsis on OVA$_{323-339}$-specific memory CD4 T cells. A. Experimental design – B6 mice were infected with attenuated *L. monocytogenes*-OVA (LM-OVA; 10^7 CFU i.v.) 30 d before sham or CLP surgery. Mice in the naïve, sham, and CLP groups were depleted of CD8 T cells by injecting 100 µg anti-CD8 mAb (clone 2.43) i.v. 3, 2, and 1 days prior to surgery. B. A small amount of blood was collected from the anti-CD8 mAb-treated mice on the day of surgery and staining for CD4 and CD8 T cells. Representative flow plots show the extent of CD8 T cell depletion

compared to a reference mouse injected with a control isotype mAb. C-D. The mice were infected with virulent LM-OVA (10^4 CFU i.v.) 2 days after surgery. Bacterial titers in the liver and spleen were determined 3 days post-vir LM-OVA infection. Data shown are representative of 2 independent experiments, with at least 5 mice/group in each experiment. * $p < 0.05$, ** $p < 0.01$. E. Experimental design – B6 mice were infected with attenuated *L. monocytogenes*-OVA (LM-OVA; 10^7 CFU i.v.) 30 d before sham or CLP surgery. F. On day 2 post-surgery, the number of $OVA_{323-339}$-specific memory CD4 T cells in the spleen were determined. G. A separate cohort of mice were injected with $OVA_{323-339}$ peptide (100 μg i.v.) 2 days after surgery to restimulate the $OVA_{323-339}$-specific memory CD4 T cells. Spleens were harvested 4 hours later, and the frequency of $IFN\gamma^+$ $OVA_{323-339}$-specific CD4 T cells was determined by flow cytometry. Data shown are representative of 2 independent experiments, with at least 5 mice/group in each experiment. ** $p < 0.01$.

Chapter 4

Maturation status of immune system

in determining outcome to CLP-induced sepsis[3]

[3] This Chapter has been previously published. Cell Reports, Volume 28, Issue 7. Matthew A. Huggins, Frances V. Sjaastad, Mark Pierson, Tamara A. Kucaba, Whitney Swanson, Christopher Staley, Alexa R. Weingarden, Isaac J. Jensen, Derek B. Danahy, Vladimir P. Badovinac, Stephen C. Jameson, Vaiva Vezys, David Masopust, Alexander Khoruts, Thomas S. Griffith and Sara E. Hamilton. Microbial Exposure Enhances Immunity to Pathogens Recognized by TLR2 but Increases Susceptibility to Cytokine Storm through TLR4 Sensitization, pp. 1729-1743 © 2019 Huggins, Sjaastad, Pierson, Kucaba, Swanson, Staley, Weingarden, Jensen, Danahy, Badovinac, Jameson, Vezys, Masopust, Khoruts, Griffith and Hamilton.

Microbial exposures can define an individual's basal immune state. Cohousing specific pathogen-free (SPF) mice with pet store mice, which harbor numerous infectious microbes, results in global changes to the immune system, including increased circulating phagocytes and elevated inflammatory cytokines. How these differences in the basal immune state influence the acute response to systemic infection is unclear. Cohoused mice exhibit enhanced protection from virulent *Listeria monocytogenes* (LM) infection, but increased morbidity and mortality to polymicrobial sepsis. Cohoused mice have more $TLR2^+$ and $TLR4^+$ phagocytes, enhancing recognition of microbes through pattern-recognition receptors. However, the response to a TLR2 ligand is muted in cohoused mice, whereas the response to a TLR4 ligand is greatly amplified, suggesting a basis for the distinct response to *Listeria monocytogenes* and sepsis. Our data illustrate how microbial exposure can enhance the immune response to unrelated challenges but also increase the risk of immunopathology from a severe cytokine storm.

I. Introduction

Mice are one of the most important and heavily used tools in biomedical research, due in part to their well-decoded genetics and their ability to model complex physiological systems in humans[195]. The availability of an extensive array of transgenic and knockout mouse strains, as well as the ease of manipulating the genome to generate novel strains as needed, has made the mouse increasingly valuable for studying functions of the immune system[196]. However, environmental pathogen exposure is an important difference between human and laboratory mouse biology that must be considered when using mouse models to evaluate the fitness of the immune system. Humans and mice are naturally exposed to both commensal and pathogenic microbes on a daily basis from birth. Laboratory mice, in contrast, are often housed under specific pathogen-free (SPF) conditions. While SPF housing has been instrumental in increasing experimental reproducibility, it has also further distanced the mouse model from humans[197]. The immune system of adult humans has been trained and shaped in the context of each infection and vaccination experienced, while the SPF mouse experiences limited microbial exposures[49]. How these interactions between host and microbe might impact future immune responses to acute infection is unknown and prompted the current investigation.

Recent studies have highlighted notable differences in composition and function of the immune systems of SPF mice and mice with increased exposure to naturally transferred murine microbes[50,198]. Natural pathogen transfer by cohousing laboratory mice with “dirty” pet store mice shifts the murine immune system to more closely

resemble that seen in adult humans exposed to microbes through infection and vaccination[50]. The T cell compartment of SPF laboratory mice is dominated by naive cells, whereas the majority of T cells in cohoused and pet store mice have an effector or memory phenotype and corresponding functional capacity. SPF mice have few nonlymphoid tissue-resident T cells, while they are abundant in cohoused mice. Finally, transcriptomic analysis of cells from the blood indicates the basal immune system of an SPF mouse most closely resembles a neonatal human, whereas the cohoused mouse gene expression signature correlates with that of adult humans[50].

Currently, it is poorly understood how natural microbial exposure alters the immune response to future challenges. Microbial exposure can increase resistance to bacterial and parasitic pathogens[50], but the basis for improved control, or whether it extends to other infectious challenges, is unknown. Our ability to incorporate spontaneous microbial exposure allows us to qualitatively address the cumulative effects of natural infections on future immunity. We have leveraged this mouse model where exposure to multiple naturally acquired infections generates an experienced immune system—mimicking a critical aspect of human biology—to investigate the immune response following a systemic inflammatory stimulus. Our data demonstrate substantial differences in the acute immune response after exposure to monomicrobial (using polymicrobial (using the cecal ligation and puncture [CLP] model of sepsis), or sterile (using the classical model of lipopolysaccharides [LPS] endotoxin or Pam3CSK4 challenge) stimuli. Surprisingly, these differences either improved immunity for the host (*Listeria monocytogenes*) or caused a dramatic reduction in survival (CLP and LPS). Our

investigation also identified changes in the microbiome as well as the expression and activation of two pattern-recognition receptors (PRRs), Toll-like receptor 2 (TLR2) and TLR4, following cohousing. A muted response to TLR2 ligands and an exaggerated response to TLR4 ligands indicate a role for infectious history in "training'" the innate immune system. Thus, our results show that an experienced immune system can differentially induce an acute inflammatory response that ultimately benefits or harms the host based on the type of challenge.

II. Materials and Methods

Mice

Female C57BL/6N (B6; 8-10 weeks of age) mice were purchased from Charles River (Wilmington, MA). Female pet store mice were purchased from local pet stores in the Minneapolis-St. Paul, MN metropolitan area. All mice were housed in AALAC-approved animal facilities at the University of Minnesota (BSL-1/BSL-2 for SPF B6 mice, and BSL-3 for cohoused B6 and pet store mice). SPF B6 and pet store mice were cohoused at a ratio of 8:1 in large rat cages for 60 days to facilitate microbe transfer. Littermates were randomly assigned to experimental groups. Experimental procedures were approved by the University of Minneapolis Animal Care and Use Committee and performed following the Office of Laboratory Animal Welfare guidelines and PHS Policy on Human Cancer and Use of Laboratory Animals.

Serology and immune cell phenotyping

Serum was collected prior to and after 60 days of co-housing for serology and cytokine analysis. Serum was screened using EZ-spot and PCR Rodent Infectious Agent (PRIA) array methods (Charles River Laboratories) for sendai virus (SEND), pneumonia virus of mice (PVM), mouse hepatitis virus (MHV), Minute virus of mice (MVM), mouse parvovirus type 1 (MPV-1), mouse parvovirus type 2 (MPV-2), mouse parvovirus-NS1 (NS-1), murine norovirus (MNV), Theiler's murine encephalomyelitis virus (GDVII), reovirus (REO), Rotavirus EDIM (EDIM/ROTA-A), lymphocytic choriomeningitis virus (LCMV), ectromelia virus (ECTRO), mouse adenovirus 1 and 2 (MAV1&2), mouse cytomegalovirus (MCMV), polyoma virus (POLY), mycoplasma pulmonis (MPUL), enchephalitozoon cuniculi (ECUN), cilia-associated respiratory bacillus (CARB), and clostridium piliforme (CPIL). Blood was also collected before and after co-housing to determine the composition and phenotype of circulating immune cells.

Flow cytometry

The following fluorochrome-conjugated mAb were purchased from Biolegend: Ly6C (HK1.4), Nkp46 (29A1.4), MHC II (I:A/I:E) (M5/114.15.2), CD62L (MEL-14), CD45.2 (104), CD44 (IM7), Ly6G (1A8), TLR2 (QA16A01), TLR4-MD2 (MTS510), CD64 (X54-5/7.1, CD14 (Sa14-2) and Tonbo Biosciences: CD8a (53-6.7), CD4 (RM4-5), IFNγ (XMG1.2), Ghost 780 (live/dead).

Measurement of serum cytokines and chemokines

Serum cytokines and chemokines were quantitated with the ProcartaPlex Cytokine & Chemokine 36-plex mouse panel or custom 17-plex panel (CCL5, CCL7,

CXCL1, CXCL5, CXCL10, GM-CSF, IL-1β, IL-2, IL-5, IL-6, IL-10, IL-15/IL-15R, IL-17A, IL-18, IL-28, IFNγ, and TNF; Invitrogen) using a Luminex 200 with Bio-plex Manager Software 5.0.

Listeria infection

Wild-type, virulent *Listeria monocytogenes* (LM) strain 10403s (provided by John Harty, University of Iowa) was grown to log phase in tryptic soy broth containing streptomycin. Mice were infected i.v. with 8×10^4 CFU. Bacterial load in the spleen and liver was determined at the indicated days post-challenge[199].

Cecal ligation and puncture

Sepsis was induced by CLP[47]. Briefly, mice were anesthetized using isoflurane (2.5% gas via inhalation) or Ketamine/xylazine (87.5mg/kg and 12.5mg/kg, respectively, i.p.). The abdomen was shaved and disinfected with 5% povidone-iodine antiseptic. Bupivicaine (6 mg/kg s.c.) was then administered at the site where a midline incision was made. The distal third of the cecum was ligated with 4-0 silk suture and punctured once with a 25-g needle to extrude a small amount of cecal content. The cecum was returned to the abdomen, the peritoneum was closed via continuous suture, and the skin was sealed using surgical glue (Vetbond; 3M, St. Paul, MN). Meloxicam (2 mg/kg) in 1 mL saline was administered at the time of surgery and for 3 additional days for postoperative analgesia and fluid resuscitation. Mice were monitored daily for weight loss and pain for at least 5 days post-surgery. Sham-treated mice underwent the same laparotomy procedure excluding ligation and puncture.

Bacteremia quantitation

Bacterial burden in the blood was assessed at 24 hours after CLP surgery. Heparinized blood was collected via cardiac puncture using aseptic techniques, serially diluted in sterile PBS, and plated on TSA plates. After overnight incubation at 37°C, colonies were counted.

DNA extraction and sequencing

DNA was extracted from single mouse fecal pellets using the DNeasy PowerSoil kit (QIAGEN, Hilden, Germany). The V5-V6 hypervariable regions of the 16S rRNA gene were amplified and paired-end sequenced using the BSF784/1064R primer set[200] by the University of Minnesota Genomics center (UMGC; Minneapolis, MN). Sequencing was done using the Illumina MiSeq platform (Illumina, Inc., San Diego, CA) at a read length of 300 nucleotides (nt). Raw data are deposited in the Sequence Read Archive[201] under BioProject accession number SRP193509.

TLR4 Reporter Cell Assay

Cecal contents were collected and prepared according to previously published protocols (Hilbert et al., 2017). Briefly, SPF and CoH mice were euthanized and cecal contents harvested and weighed. Samples from individual mice were initially mixed with a 5% dextrose solution to create a 40 mg/ml slurry. The cecal slurry was then passed through 70 μm filter to remove large particulates. Slurries were then added at the indicated concentrations to triplicate wells of 96-well flat-bottom plates seeded with 4×10^4 TLR4 reporter cells (HEK-Blue hTLR4; InvivoGen[202]). HEK-Blue hTLR4 were maintained according to manufacturer's recommendations. After 24 h, conditioned media

was collected to measure SEAP activity according to the manufacturer's protocol (QUANTI-Blue Solution, InvivoGen).

Intraperitoneal injection of cecal slurry

Cecal contents from 3-4 donor mice were pooled and mixed with 5% dextrose solution to create a 40 mg/ml cecal slurry. The cecal slurry was then passed through 70 μm filter and then injected i.p. into recipient mice (0.75 or 0.5 mg slurry/g mouse in 300 μl) using a 21G needle. Meloxicam (2 mg/kg) in 1 mL saline was administered at the time of slurry injection and for 3 additional days for postoperative analgesia and fluid resuscitation. Mice were monitored daily for weight loss and pain for at least 5 days post-injection.

Quantitative real-time PCR (qPCR)

Myeloid cells were isolated from the spleens of SPF and CoH mice by plastic adherence[203,204]. Spleens (5 SPF and 5 CoH) were prepared into a single cell suspension in 2 mL HBSS, washed, and resuspended in 10 mL of complete RPMI. Each cell suspension was added to two 10 cm culture dishes and incubated at 37°C for 90 min. Plates were washed twice with 5 mL PBS to remove nonadherent cells. Total RNA was isolated from the remaining adherent myeloid cells using TRIzol reagent (Invitrogen, Carlsbad, CA), and 1 μg was reverse-transcribed using Superscript III (Invitrogen). Resulting cDNA was used as a template for qPCR using TaqMan primer/probe sets for Tlr1, Tlr2, Tlr3, Tlr4, Tlr5, Tlr6, Tlr7, Tlr8, Tlr9, Cd14, Ly96, Myd88, Ticam2, Traf6, Irak1, and 18 s rRNA (Applied Biosystems).

Bioinformatics

Sequence processing was done using mothur (version 1.33.3)[205], as previously described[206]. Briefly, sequences were paired-end join, trimmed for quality, and aligned against the SILVA database (version 123) for clustering. A 2% pre-cluster was used to remove sequences likely to contain errors[207]. Chimeras were identified and removed using UCHIME (version 4.2.40)[208]. Operational taxonomic units (OTUs) were identified at 97% similarity using furthest-neighbor clustering and classified against the Ribosomal Database Project release (version 14). Alpha diversity (within-sample diversity), measured as Good's coverage, Shannon index, and abundance-based coverage estimate (ACE), was calculated in mothur. Differences in beta diversity (between-sample diversity) were calculated using Bray-Curtis dissimilarities[209]. To determine engraftment among CoH mice, SourceTracker (version 0.9.8) was used with default parameters[210]. This program uses a Bayesian algorithm to determine the percent of the community in user-defined sink (co-housed mice) samples that can be attributed to user defined source (SPF and pet store mice) samples.

LPS/Pam3CSK4 challenge

A rodent model of endotoxemia was induced by a single injection of LPS-EB from E. coli O111:B4 (10, 5, or 1 mg/kg body weight i.v.; InvivoGen)[211]. Similarly, some mice were challenged with a single dose (10 mg/kg body weight i.v.) of Pam3CSK4 VacciGrade (InvivoGen).

Quantification and Statistical Analysis

Data shown are presented as mean values ± SEM. GraphPad Prism 8 was used for statistical analysis, where statistical significance was determined using two-tailed

Unpaired, nonparametric Mann-Whitney U test (for 2 individual groups) or group-wise, one-way ANOVA analyses followed by multiple-testing correction using the Holm-Sidak method, with $\alpha = 0.05$. $* p < 0.05$, $** p < 0.01$, $*** p < 0.005$, $**** p < 0.001$. Differences in alpha diversity were determined using ANOVA and differences in relative abundances of genera were determine by Kruskal-Wallis test using the Steel-Dwass-Critchlow-Fligner procedure for pairwise comparisons. Analysis of similarity (ANOSIM) (Clarke, 1993) was used to evaluate differences in community composition, and ordination was done using principal coordinates analysis (PCoA)[212]. Correlation of phyla and genera abundances with axes positions were done using Spearman correlations. ANOVA and Kruskal-Wallis tests were done using XLSTAT software (version 17.06; Addinsoft, Belmont, MA). ANOSIM, PCoA, and correlation analyses were done using mothur. All statistics were evaluated at $\alpha = 0.05$ with Bonferroni correction for multiple comparisons.

Data and Code Availability

The accession number for the raw 16 s rRNA sequencing data reported in this paper is SRA: SRP193509[201].

III. Results

Normalizing Microbial Exposure Creates a More Inflammatory Host Environment

Mice from pet stores carry a number of pathogens normally absent from standard SPF laboratory strains of mice[50]. After cohousing for 60 days, C57BL/6 (B6) mice acquire many of the microbes carried by the pet store mice based on serological assays

(Figure 4-1A). Importantly, this physiological microbial exposure resulted in global changes to the immune status of the cohoused mice. Inflammatory serum cytokine and chemokine levels were elevated in long-term cohoused B6 and pet store mice, relative to SPF B6 mice. For example, the pro-inflammatory cytokines IL-1β, IL-6, IFNγ, and tumor necrosis factor (TNF) were notably higher in the serum of cohoused B6 and pet store mice after 60 days (Figure 4-1B). Similar increases were seen for IL-2, IL-5, IL-9, IL-10, IL-13, IL-15/IL-15R, IL-17A, IL-18, IL-22, IL-23, IL-28, G-CSF, GM-CSF, CCL3, CCL4, CCL5, and CXCL10 (Figures 4-1C and 4-2). Collectively, these data demonstrate that physiological microbial exposure establishes elevated systemic inflammation, marked by the presence of numerous cytokines and chemokines in the serum.

Given the increase in serum cytokines, we next defined the cellular immune composition of cohoused and pet store mice. While the total blood cell numbers were not different among SPF B6, cohoused B6, and pet store mice (Figure 4-3A), cohousing altered the composition of circulating immune cells. The frequency and number of circulating CD4 and CD8 T cells were not changed compared to SPF B6 mice (Figures 4-3B and 4-3C), but consistent with previous data, physiological microbial transfer resulted in increased frequencies of $CD44^{hi}$ and $KLRG1^{+}$ and decreased frequencies of $CD62L^{+}$ CD4 and CD8 T cells (collectively indicating increased frequencies of effector and effector memory T cells[213] and long-lived effector memory T cells[214]) in the blood of cohoused B6 and pet store mice (Figure 4-4)[50]. These data indicate a transition of naive T cells to antigen-stimulated T cells as a result of microbial exposure. The innate immune cell compartment was significantly expanded following cohousing, with

increases in both the frequency and the number of circulating monocytes and neutrophils (Figures 4-3D and 4-3E). In contrast, B cells and natural killer (NK) cells showed modest reductions in the blood after microbial exposure (Figures 4-3F and 4-3G). Collectively, these data demonstrate that physiological microbial exposure establishes numerous elevated cytokines and chemokines in the serum as well as increased circulating phagocytes.

Cohoused mice demonstrate increased resistance to Listeria monocytogenes infection.

Previous data showed cohoused B6 and pet store mice display an increased ability to clear a systemic infection by virulent *Listeria monocytogenes* (LM) – a common bacteria used to assess immune fitness in laboratory mice – at day 3 post-infection relative to SPF B6 mice[50]. While the mechanism of enhanced LM protection was undefined, it is possible LM fails to establish infection in the cohoused mice because the increased circulating monocytes and neutrophils in these mice could mediate very early resistance similar to that shown following murine gammaherpesvirus 68 infection[215]. To more fully define LM resistance after cohousing, we measured the bacterial burden at early timepoints post-challenge. Both SPF and cohoused B6 mice had similar LM burdens in the spleen and liver during the first 8 hours after infection, suggesting the initial establishment of bacterial infection was not impacted by cohousing (Figure 4-5A). While the early bacterial burden was not different, cohoused B6 mice more rapidly and effectively controlled the LM infection. The cohoused B6 mice began to show signs of controlling LM in the liver at 24 hours post-infection. However, 72 hours were needed to observe a significant decrease in LM burdens in the spleens of cohoused mice. By this

timepoint, bacterial loads reached 5190- and 3704-fold lower than SPF B6 mice in the spleens and livers, respectively.

IFNγ plays an important role in the response to intracellular bacteria and effective clearing of LM[216,217]. Because basal IFNγ levels are elevated in cohoused B6 mice (Figure 4-1B), we next examined the cellular source of IFNγ before and after LM infection. We saw a significant increase in the frequency and number of IFNγ-producing cells in the spleen of cohoused B6 mice before and 24 hours after LM infection (Figure 4-5B). In particular, IFNγ-producing CD4 and CD8 T cells were increased in cohoused mice 24 hours post LM infection (Figures 4-5C and 4-5D). The increase was not ubiquitous, as IFNγ-producing NK cells, a well-established early producer of IFNγ during LM infection, were not elevated in cohoused mice after LM infection (Figure 4-5E). Surprisingly, despite the increased frequency of $IFN\gamma^+$ cells in the spleen, the amount of IFNγ detectable in the serum of LM-infected cohoused mice remained constant throughout the 72 hours after infection (Figure 4-5F). In contrast, there was a rapid and robust increase in serum IFNγ of LM-infected SPF mice. As a result, SPF mice had ~100X more IFNγ in the serum 24 hours after systemic virulent LM infection than measured in cohoused mice. A similar trend was seen for TNF and IL-6 (Figure 4-5F). Moreover, the overall serum cytokine/chemokine milieu detected in SPF mice was markedly different 24 hours after LM infection (Figure 4-5G). There was little change, in contrast, seen in cohoused mice when comparing serum cytokine/chemokine levels before and 24 hours after LM infection. Whether these observations are influenced by increased amounts of cytokine produced in the tissues (as opposed to the circulation) in

cohoused mice remains to be determined. Collectively, the data in Figure 4-5 show that cohoused B6 mice exhibit enhanced resistance to LM infection compared to SPF mice with remarkably stable, yet heightened, circulating cytokine/chemokine levels.

Cohoused B6 Mice Exhibit an Exacerbated Cytokine Response and Increased Mortality to CLP-Induced Polymicrobial Sepsis

The data obtained from SPF and cohoused B6 mice after *Listeria monocytogenes* infection, as well as previous data following parasitic infections, suggest that a host with significant microbial exposure can deal with subsequent infections more efficiently[50]. However, the duration, magnitude, and impact of an inflammatory response is pathogen dependent[218], and we reasoned the acute response in SPF and cohoused B6 mice could be similarly influenced by the infecting pathogen(s). To further explore how cohoused mice respond to newly acquired infections, we evaluated the acute response to a systemic polymicrobial infection by gut commensals generated using the CLP model of sepsis[47].

One feature of the CLP model is the ability to modulate the severity of inflammation and mortality based on the amount of cecum ligated and the number and/or size of punctures[47]. Our version of the CLP model induces a septic state in SPF B6 mice defined by modest weight loss that recovers by day 7 post-surgery and ~20% acute mortality[62,153,161,219], which is consistent with clinical rates (Figures 4-6A and 4-6B)[119]. Interestingly, cohoused mice exhibited significantly increased mortality (~75%) compared to SPF mice (~20%) following CLP. Cohoused mice that survived also took longer to regain the weight lost following CLP surgery. The physiological microbial exposure during cohousing alters the cecal microbiome, and this may cause exacerbated

microbial release following CLP surgery; however, there was no difference in bacteremia 24 h post-CLP (Figure 4-6C). Both SPF and cohoused B6 mice had similarly significant reductions in numbers of CD4 and CD8 T cells in the blood by 2 days after CLP-induced sepsis (compared to pre-CLP numbers) that recovered within 1 week (Figure 4-6D), suggesting the increased morbidity and mortality in the cohoused mice was not caused by a substantial deviation in the characteristic acute lymphopenia during CLP-induced sepsis[12,13,29–31,62,64,65,103,117,118,147,161,220].

The acute hyperinflammatory response during sepsis induces a variety of pathophysiological events (e.g., fever, shock, vasodilation, and organ failure) stemming from the rapid and robust production of multiple pro-inflammatory cytokines that must be controlled to prevent an unbridled response and death[98]. The early cytokine storm is likely due to an innate response by a variety of cells within the immune system to multiple pathogen-associated molecular patterns (PAMPs) expressed by the invading microbe(s), as well as the damage-associated molecular patterns (DAMPs) released from dying cells[221]. Consistent with our recent data[118], a transient but relatively modest spike in serum IFNγ was detected in SPF B6 mice after CLP surgery (Figure 4-6E). This was also observed for IL-1β, IL-6, and TNF—cytokines of crucial importance to sepsis pathophysiology[221]—as well as several other cytokines and chemokines (Figure 4-6F). In striking contrast to what we saw in the *Listeria monocytogenes*-infected cohoused mice, the magnitude of this response was markedly increased in cohoused mice subjected to CLP surgery (Figures 4-6E and 4-6F). The exacerbated cytokine storm observed in cohoused mice following CLP surgery, which correlated with the increased morbidity

and acute mortality, contrasted to a muted cytokine response and improved bacterial clearance in *Listeria monocytogenes*-infected cohoused mice (Figure 4-5).

Cohousing of Mice Alters Gut Microbiome Composition

Given the established role for the composition of the gut microbiota in human health and the host resistance to infection[222], we sought to characterize the changes to the microbiome that occur during the cohousing process. Across SPF, cohoused, and pet store mice, a mean Good's coverage of 99.1% ± 0.1% was observed, with a range from 224 to 660 operational taxonomic units (OTUs) identified in individual samples. No differences in alpha diversity parameters were observed due to origin or cohousing (Figure 4-7A; $p = 0.905$ and 0.196 for Shannon and Abundance-based Coverage [ACE] indices, respectively). The predominant phyla in all fecal communities were Bacteroidetes and Firmicutes, and the relative ratios between these did not differ among groups (Figure 4-7B). The relative abundances of Proteobacteria were, however, significantly greater in pet store and cohoused communities compared to SPF (post hoc $p \leq 0.006$), while SPF communities had greater abundances of Verrucomicrobia ($p \leq 0.014$). Some studies suggest Proteobacteria may increase the risk of bacterial translocation and sepsis[223]. At the genus level, communities predominantly comprised Barnesiella, Bacteroides, Prevotella, and Lactobacillus (Figure 4-7B). Communities from SPF mice had significantly greater relative abundances of Barnesiella and Alistipes than cohoused or pet store mice (post hoc $p = 0.019$ and $p \leq 0.006$, respectively). In contrast, cohoused and pet store mice communities had significantly greater abundances of Bacteroides, Phocaeicola (phylum Bacteroidetes), and Parabacteroides ($p \leq 0.038$, $p \leq$

0.026, and $p \leq 0.039$, respectively). Overall, bacterial communities were significantly different in SPF mice compared to cohoused and pet store mice (Figure 4-7C; ANOSIM $R = 0.883$ and 0.952, $p < 0.001$), but cohoused and pet store mouse communities were similar (ANOSIM $R = 0.135$, $p = 0.033$, at Bonferroni-correct $\alpha = 0.017$). SourceTracker analysis revealed a significantly greater similarity to pet store mouse communities than SPF communities ($p < 0.0001$) among cohoused mice (Figure 4-7D). Lastly, cecal contents from SPF and cohoused mice were applied to a TLR4 reporter cell line (HEK-Blue hTLR4) to assay the ability of the differing microbial communities to stimulate this innate pattern-recognition receptor. While there was no increase in abundance of gram-negative bacteria in the cohoused mice compared to SPF ($p = 0.441$), the cecal contents from cohoused mice did display a significantly higher ability to stimulate TLR4, compared to the SPF cecal contents (Figure 4-7E), suggesting an increased endotoxin content in the cohoused cecal material. Thus, the composition of the microbiome following cohousing was differentially able to activate the immune system.

Our data show cohousing SPF laboratory mice with pet store mice skews the composition and maturational status of the host immune system, but it also leads to a shifting of microbial communities in the gut. To assay the relative contribution of these changes toward the heightened sensitivity of cohoused mice to sepsis, we isolated the cecal contents from either SPF or cohoused mice and directly injected them into new hosts to induce an intraperitoneal polymicrobial infection (Figure 4-7F). Injection of cohoused cecal contents resulted in higher mortality compared to SPF cecal contents when transferred to both SPF and cohoused recipients (Figure 4-7G), suggesting the

composition of cohoused mice microbiota induces a more severe septic shock. However, the microbial composition does not solely explain the differences between SPF and cohoused mice. Injection of SPF cecal slurry into cohoused recipients resulted in elevated IL-1β, IFNγ, and TNF 6 h post-transfer, compared to SPF cecal slurry into SPF recipients (Figures 4-7H and 4-8). Our earlier results illustrate that cohoused mice have elevated serum cytokine levels prior to challenge (Figure 4-1). Importantly, following the cecal slurry transfer, IL-1β, IL-6, IFNγ, and TNF were each increased significantly over their baseline levels in both cohoused and SPF recipients (Figure 4-8A). Thus, the differences in cytokine levels following the cecal slurry injection between SPF and cohoused hosts cannot simply be attributed to elevated baseline levels. Similar results were observed when injecting a cohoused cecal slurry into SPF and cohoused recipients, with increased cytokine production in cohoused recipients compared to SPF recipients.

Thus, microbial transfer through cohousing results in an increased sensitivity to sepsis even when the cecal transfer is normalized between the two groups. These results suggest that while the makeup of the gut microbiome does contribute to the severity of sepsis, maturation of the immune system also plays a major role in determining the cytokine response and disease outcome.

Increased Prevalence of TLR2$^+$ and TLR4$^+$ Immune Cells after Normalizing Microbial Exposure

The findings presented in Figure 4-7 suggest there were contributions of both the cecal microbiota and the immunological experience of the mice in dictating susceptibility to sepsis, complicating interpretation. Hence, we moved to models that measured the

response to isolated TLR agonists. TLRs are important pattern-recognition receptors for recognizing bacterial and viral pathogens to mobilize the innate immune response during infection[224,225]. Triacylated and diacylated lipopeptides found in gram-positive bacteria such as *Listeria monocytogenes* are recognized by TLR2/TLR1 and TLR2/TLR6 heterodimers, respectively[226–229]. TLR4 recognizes LPS present in the cell walls of gram-negative bacteria, and both TLR2 and TLR4 have been implicated in inducing septic shock[230–232]. These surface receptors are primarily expressed by circulating innate immune cells (especially phagocytes) and serve to activate the primary immune response[233]. A qPCR analysis of splenic adherent myeloid cells revealed elevated transcription for multiple components of both the TLR2 and TLR4 signaling pathways in cohoused mice relative to SPF mice[203,204]. Both Tlr2 and Tlr4 transcripts, but not other TLRs, were upregulated in cohoused mice compared to SPF mice (Figure 4-9A). Additionally, mRNA for CD14, a co-receptor for TLR4 binding to LPS, as well as the downstream signaling adaptor MyD88, were elevated in the splenic phagocytes following cohousing. These data provide more evidence to suggest cohousing alters the ability of the immune system to recognize and respond to pathogens.

Given the increased frequency and number of circulating monocytes and neutrophils after cohousing (Figure 4-3B), we examined blood cells from SPF and cohoused mice for TLR2 and TLR4 expression as a potential mediator of increased pathogen responsiveness in the cohoused mice. Indeed, cohoused B6 and pet store mice have an increased frequency and total number of $TLR2^+$ and $TLR4^+$ cells circulating in the blood, compared to SPF B6 mice (Figure 4-9B), but no change in the expression

levels of TLR2 or TLR4 as measured by mean fluorescence intensity (MFI; Figures 4-9B and 4-10). The frequency of circulating $CD14^+$ cells is also elevated in cohoused B6 and pet store mice (Figure 4-9C). Following cohousing, monocytes contribute the largest increase in $TLR2^+$ (Figure 4-9D) and $TLR4^+$ cells (Figure 4-9E), as well as a slight, but significant, increase in the number of $TLR2^+$ neutrophils. Both of these cell populations were also numerically expanded in cohoused B6 and pet store mice (see Figures 4-3D and 4-3E). Interestingly, we also noted a modest but significant increase in the number of CD8 T cells expressing TLR4 in the cohoused B6 mice (Figure 4-9E). Thus, these data suggest microbial exposure augments the capacity of the immune system to recognize infection through increased expression of pattern-recognition receptors.

Physiological Microbial Exposure Sensitizes Mice to TLR4, but Not to TLR2, Agonist-Induced Sterile Inflammation

Direct injection of live, virulent *Listeria monocytogenes* establishes an active infection. Similarly, the CLP model of sepsis relies on the disruption of the protective barrier maintained by the intestinal epithelium, releasing a mixture of live microbes into the peritoneum. Injection of the endotoxin LPS is another common model of sepsis, which instead induces a sterile inflammation that mimics the activation of the innate immune system during a septic event[234]. In contrast to plentiful data obtained from LPS endotoxemia models, there is little information regarding the sterile inflammatory response to a purified TLR2 agonist. With the increase in $TLR2^+$ and $TLR4^+$ immune cells (especially monocytes and neutrophils) in mice after physiological microbial exposure, we were interested to see the effect of purified TLR2 or TLR4 agonist

challenge in SPF and cohoused B6 mice. Similar to the data obtained with CLP-induced polymicrobial sepsis, cohoused B6 mice demonstrated an increased susceptibility to LPS challenge and succumbed rapidly to doses (10 and 5 mg/kg intravenous [i.v.]) that were tolerated by SPF mice (Figure 4-11A). Examination of the serum after LPS administration found a rapid increase in IL-6 and IFNγ in both SPF and cohoused B6 mice, but the amount was significantly higher in cohoused B6 mice (Figure 4-11B). This effect was dose dependent, and titration of LPS to 5 mg/kg and 1 mg/kg i.v. reduced cytokine production after challenge. Interestingly, while all SPF and cohoused mice survived after a 1-mg/kg i.v. LPS challenge, there was still an increase in cytokine production at 6 h in cohoused B6 mice relative to B6 SPF (Figure 4-11C). These data show that similar to the live polymicrobial infection seen during CLP, cohoused mice robustly respond to the LPS challenge with rapid pro-inflammatory cytokine production and increased mortality. In contrast to the LPS challenge, injection of the TLR2/TLR1 agonist Pam3CSK4 (10 mg/kg i.v.) was well tolerated in both SPF and cohoused B6 mice (Figure 4-11D). Analysis of the global inflammatory response 6 h after the Pam3CSK4 challenge did reveal some cytokines (e.g., IL-1β, IL-10, IL-15/IL-15R, IL-17A, IL-18, and IL-28) and chemokines (e.g., CCL5, CCL7, CXCL5, and CXCL10) that were elevated in the cohoused mice (Figure 4-11F), but SPF mice had higher amounts of IL-6 and IFNγ in the serum than did cohoused mice (Figure 4-11E), much like what we saw in the *Listeria monocytogenes*-infected mice (see Figure 4-5F). We also find that the TLR3 agonist poly I:C (10 mg/kg i.v.) induces elevated IL-6 and IFNγ in cohoused mice, but the adjuvant was well tolerated by both SPF and cohoused hosts (data not shown). Collectively, these data (when combined with the data in Figure 4-9) suggest the

increased presence of TLR-expressing immune cells following physiological microbial exposure affects the composition and magnitude of an inflammatory response to systemically administered TLR agonists. However, there is also differential responsiveness, such that the TLR2 ligands induce somewhat muted cytokine responses, whereas TLR4 ligands induce dramatic increases in systemic pro-inflammatory cytokines. These distinct responses to TLR stimulation may explain the different responses of cohoused mice to *Listeria monocytogenes* and sepsis, which are major drivers of TLR2 and TLR4, respectively.

IV. Discussion

Animals (including humans) are exposed to commensal and pathogenic microbes throughout their lives, and this physiological microbial exposure has a profound impact on immune competency and overall health[235]. The use of laboratory mice housed under SPF conditions in the vast majority of immunology research has been an important step to improve experimental consistency, but these unusually clean living conditions have inadvertently left the laboratory mice with an underdeveloped immune system—far different from the immune system found in adult humans. The recent description of a mouse model of physiological microbial exposure introduced the important effects of the environment on the basal immune state[50]. The data presented herein have extended those initial findings to demonstrate that microbial exposure alters the inflammatory state of the immune system. Former SPF laboratory mice develop elevated profiles of numerous inflammatory cytokines after microbial transfer through cohousing with outbred pet store mice. In addition, the cellular composition of the immune system is

altered after cohousing to favor increased circulating monocytes and neutrophils expressing TLRs. These changes dramatically altered the responsiveness to future unrelated immune challenges. Intriguingly, the nature of the specific challenge determines whether previous microbial exposure enhances or inhibits effective immune function, pathogen clearance, and ultimately survival of the host. Specifically, cohoused mice demonstrate enhanced bacterial clearance after *Listeria monocytogenes* infection but are more susceptible to death from polymicrobial sepsis and LPS.

Recent studies have drawn attention to the idea that the innate immune system is capable of forming long-term memory in response to stimulation. Mechanisms of this altered responsiveness, or "trained immunity," include changes in expression of pathogen-sensing receptors, signaling proteins, and innate cell numbers[236,237]. In the cohoused mouse model, laboratory mice are exposed to a variety of viral, bacterial, and parasitic microbes, resulting in the activation of innate immune cells through pattern-recognition receptors. Signaling through pattern-recognition receptors induces stable changes in histone methylation[238]. Here, we demonstrate that following cohousing, the "trained" immune system contains increased numbers of TLR2- and TLR4-expressing cells. Furthermore, transcriptional studies by Beura et al. (2016) identified elevated Myd88 mRNA transcripts in cohoused mice, a critical downstream signaling component utilized by most TLRs, including TLR2 and TLR4[224,225,233,237]. We confirm that Myd88 is elevated in cohoused mice (Figure 4-9A) and also show elevated CD14 expression (Figure 4-9C). Thus, innate stimulation through pattern-recognition receptors can be regulated through prior microbial experience to unrelated organisms. The benefit

of these changes is illustrated through enhanced host protection to *Listeria monocytogenes*, but at the cost of increased sensitivity to cytokine storms during polymicrobial sepsis, leading to poorer survival rates. Further studies are required to understand the full landscape of innate changes induced through cohousing and how they potentially synergize to shape the responsiveness to future challenges.

TLR expression on immune cells present in neonatal cord blood is reduced relative to adult blood[239,240]. Furthermore, neonatal T cells and monocytes have a reduced functional capacity to produce cytokines following stimulation[241,242], and the ability of immune cells obtained from infants to produce IFNγ, TNFα, IL-2, and IL-4 is significantly reduced compared to cells from adults[243]. Neonatal blood monocytes are reduced in number compared to adults, and they are less responsive to TLR4 stimulation. This work goes on to demonstrate that neonatal cord blood exposed to malaria in utero causes an elevation in circulating monocytes and responsiveness to TLR4 agonist stimulation. These differences in TLR expression between neonatal and adult humans are consistent with our findings, as we noted substantial increases in the frequency of circulating $TLR2^+$ and $TLR4^+$ cells in cohoused mice (see Figure 4-9) but, intriguingly, not other TLRs (Figure 4-9A). Thus, our study provides additional rationale for using the cohoused murine system to identify the extent that microbial exposure contributes to age-associated differences in the immune system. One hypothesis for the correlation among increasing age, elevation in serum cytokines, and TLR expression (especially in humans) is the increase in microbial exposure through vaccination and natural infection. The cohousing model offers an appealing and unique opportunity to study the impact of

physiological microbial exposure on the immune system in a manner that complements studies using neonatal cord blood and adult human blood.

Cohoused mice are able to more rapidly clear *Listeria monocytogenes* infection than SPF mice (Figure 4-5A)[50]. Our data show SPF and cohoused mice had similar bacterial burdens in both the liver and spleen at 8 h after *Listeria monocytogenes* infection. It was not until 48–72 h post-infection that a reduction in pathogen burden became apparent in the cohoused mice. We observed increased IFNγ production, particularly from CD4+ and CD8+ T cells, after cohousing. Interestingly, the number of NK cells did not increase in cohoused mice (Figure 4-3G), and they were not elevated in their production of IFNγ (Figure 4-5E) as might be expected following immune "training"[237]. Whether this is an indication that specific pathogens are required to train NK cells will require further study. However, since memory T cells can make IFNγ in response to early inflammatory cues in an antigen-independent manner, it is possible that the elevated numbers of antigen-experienced T cells in cohoused mice could lead to improved clearance of *Listeria monocytogenes* and other intracellular bacteria[217,244,245]. These data indicate that the enhanced adaptive immune response may be stimulated via increased TLR expression following microbial exposure. TLR stimulation alerts the host to respond to infectious challenges and recruits T cells to the site of the infection through inflammatory signals[246]. In humans and mice, prior infectious experience can regulate TLR expression and overall immune responsiveness. Humans infected with Plasmodium have increased responsiveness to TLR agonists[247]. TLR expression increases in a feedback loop where IFNγ production enhances TLR

expression and allows the host to more effectively respond to future infectious challenges[248]. This increased responsiveness reveals a "double-edged sword" seen in our cohoused model system, where the host can respond more effectively to TLR2-triggering bacterial infections but is also at a higher risk of pathology from hyper-reactive cytokine responses to TLR4 ligands. We found increased IFNγ-producing cells in the blood 24 h after virulent *Listeria monocytogenes* infection of cohoused mice. Unexpectedly, the amount of IFNγ and a number of other inflammatory cytokines in the serum was relatively unchanged following *Listeria monocytogenes* infection of cohoused mice, though they were markedly elevated in SPF mice. One potential explanation for the reduced numbers of circulating cytokines in the *Listeria monocytogenes*-infected cohoused mice is that memory T cells and "trained" innate cells may be rapidly absorbing the cytokines as they are being produced to facilitate their increased function.

In striking contrast to *Listeria monocytogenes* infection, CLP-induced polymicrobial sepsis results in a dramatic increase in pro-inflammatory cytokines and chemokines in cohoused mice relative to their SPF counterparts. For example, there were exceedingly high amounts of IL-6 (>20,000 pg/ml at 6 h post-CLP) in the serum of cohoused mice after CLP surgery. Previous reports have highlighted the predictive nature of circulating IL-6 levels (i.e., increased mortality with increased IL-6) in regard to mortality in preclinical and clinical settings[116,249,250]. Similar correlations between the amount of IL-1β and TNF and survival have also been made, prompting the clinical testing of various strategies for neutralizing IL-1β and TNF activity[251]. Use of the CLP model has led to a vast expansion of knowledge regarding the intricate changes within the

immune system following a septic event. Recent clinical data using agents (e.g., IL-7 and anti-PD-1 mAb) to manipulate the number and responsiveness of immune cells in sepsis survivors highlight the importance of preclinical experimentation, but the success of these new approaches is atypical[70,252–256]. Over 100 agents (many targeting cytokines) with preclinical efficacy in mouse models of sepsis have been unsuccessful in humans[257]; it is tempting to speculate that the exclusive use of SPF mice in previous preclinical studies may have underestimated the severity of the cytokine response following CLP surgery.

Laboratory mice cohoused with pet store mice not only encounter numerous different pathogenic infections, but also develop changes to the microbiome. The link between microbiome composition and immune status has been increasingly appreciated in the past decade. Immune cell interactions with the diverse components of the microbiome are critical for the development of a healthy immune system[258]. Dysbiosis of a healthy microbiome results in aberrant immune responses and susceptibility to both autoimmunity and inflammatory diseases[259]. Our cohousing experiments demonstrate that the gut microbial contents contribute to the heightened immune response of cohoused mice during sepsis. Cohoused cecal contents injected into the peritoneum of SPF mice induced a more robust cytokine storm, compared to that seen in SPF mice injected with SPF cecal contents. However, our data suggest the gut contents do not fully explain the phenotype, as cohoused recipients displayed an exacerbated cytokine response after injection of either SPF or cohoused cecal slurries. Additional studies are needed to

evaluate how pathogen exposure and variations in commensal microbes influence the maturation and function of the immune system to future infections.

Additionally, we noted similar increases in pro-inflammatory cytokines and increased mortality after exposing cohoused mice to LPS—a potent TLR4 stimulant that induces sterile inflammation. Bolus injection of endotoxin (LPS) is considered a model of sepsis, mostly because of the rapid activation of the innate immune system[260]. Despite having a number of similarities to CLP-induced sepsis (e.g., lethargy, piloerection, and acute leukopenia), there are also a number of important differences, such as the kinetics and magnitude of proinflammatory cytokine (IL-6, TNF) production[234]. Another criticism of LPS endotoxemia as a model of sepsis was based on data suggesting humans to be significantly more sensitive to the effects of the LPS challenge compared to mice[261]. As expected, this conclusion came (in part) from experiments comparing the responsiveness of cells from the blood of adult humans and SPF mice. As now evidenced by data presented herein and previously[50], there are distinct phenotypic and transcriptomic changes within the cells of the immune systems of SPF and cohoused mice that indicate their resemblance to the immune systems of neonate and adult humans, respectively. It stands to reason that the conclusions drawn by Warren et al. (2010) may be the result of comparing the response of the naive, neonate-like immune system of SPF mice to that of the matured, microbially experienced immune system of adult humans. We posit that the differences noted between mice and humans may be more complex than simply a “species-specific” difference, and the underappreciated extent of physiological microbial exposure may have played a more significant role.

In conclusion, we find that mice with normal physiologic exposure to microbes exhibit increased serum cytokine levels and circulating phagocytes, in addition to phenotypic conversion of the CD4 and CD8 T cell compartments. These changes in the basal state of the immune system, however, do not lead to a "blanket" improvement in immunity. Instead, depending on the nature of the immune insult, previous immune history is either beneficial (as in the case of the *Listeria monocytogenes* challenge) or detrimental (as in the case of CLP-induced sepsis). This conclusion differs slightly from previous studies, which have thus far shown improved immune responses after diverse microbial exposure[50,198,262]. The data presented herein suggest that the cumulative microbial exposure of the host defines the expression and differing activation state of individual pattern-recognition receptors. Thus, we cannot exclude the possibility that the more robust immunity acquired via exposure to numerous pathogens could decrease the incidence of sepsis by rapidly controlling pathogens acquired by normal routes of infection—even though our data with cohoused mice clearly develop increased severity of experimental sepsis in the CLP and LPS models. Using the cohousing system, future studies can be designed to differentiate the specific traits influenced by microbial exposure and show how to generate an optimal immune response that minimizes the chances for immunopathology. Applying this cohousing system to diseases that, to date, have been poorly modeled in mice may open new opportunities in preclinical research.

V. Figures

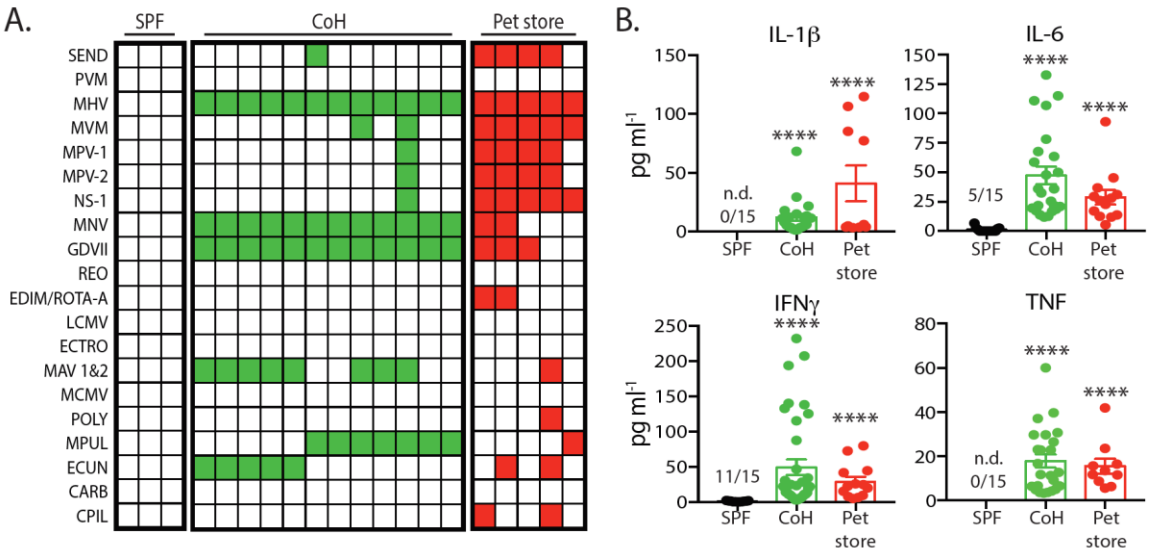

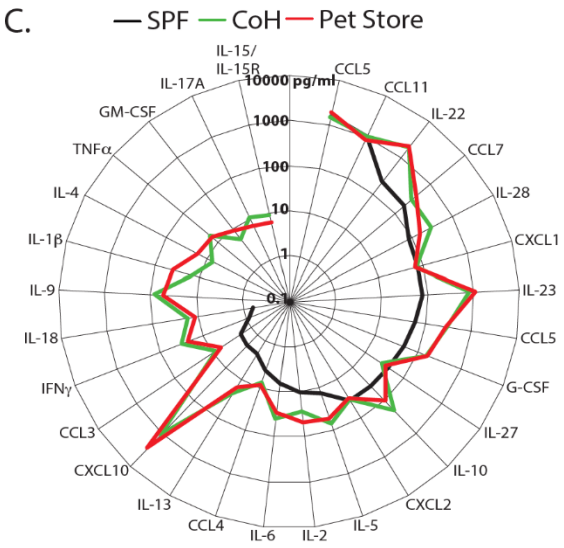

Figure 4-1. Physiological microbial exposure creates a more inflammatory host environment. A. Representative serology from specific pathogen free (SPF) B6, cohoused (CoH) B6, and pet store mice detecting the extent of pathogen exposure. Filled squares indicate a positive serology result for the indicated pathogen. Each column represents an individual mouse. Data are representative of at least 20 independent serology tests conducted. B-C. Serum was collected from SPF B6, cohoused B6, and pet store mice after 60 d. The concentration of cytokines and chemokines was determined by bioplex. B. The number of mice with detectable IL-1β, IL-6, IFNγ, and TNF in the serum are indicated for the SPF group. C. Radar plot comparing the basal serum concentrations of indicated cytokines and chemokines in SPF B6, cohoused B6, and pet store mice. For statistical comparisons, SPF mice with undetectable cytokines were given a value of "0". 10-36 mice/group (pooled from 3 technical replicates) were analyzed in B-C. * Refers to statistical differences in the response of cohoused and pet store mice relative to SPF. * $p < 0.05$, ** $p < 0.01$, *** $p < 0.005$, **** $p < 0.001$, n.d. – none detected. See also Figure 4-2.

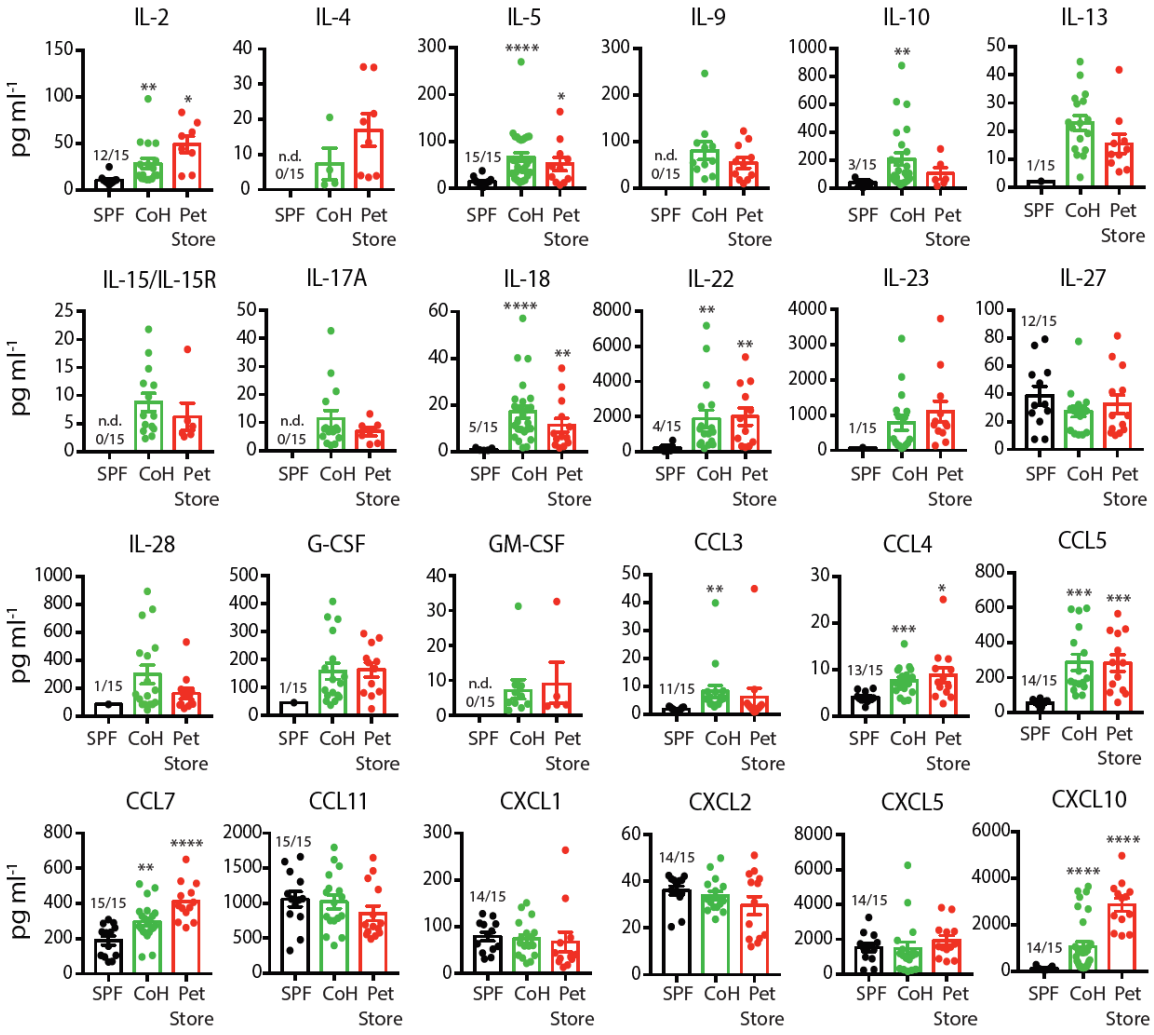

Figure 4-2. Cohousing SPF B6 mice with pet store mice alters serum cytokine and chemokine levels. Related to Figure 4-1. Serum was collected from SPF B6, cohoused (CoH) B6, and pet store mice after 60 d. The level of cytokines and chemokines was determined using bioplex. The number of mice with detectable cytokines in the serum are indicated for the SPF group. For statistical comparisons, SPF mice with undetectable cytokines were given a value of "0". 10- 36 mice/group (pooled from 3 technical replicates) were analyzed. * $p < 0.05$, ** $p < 0.01$, *** $p < 0.005$, **** $p < 0.001$, n.d. – none detected.

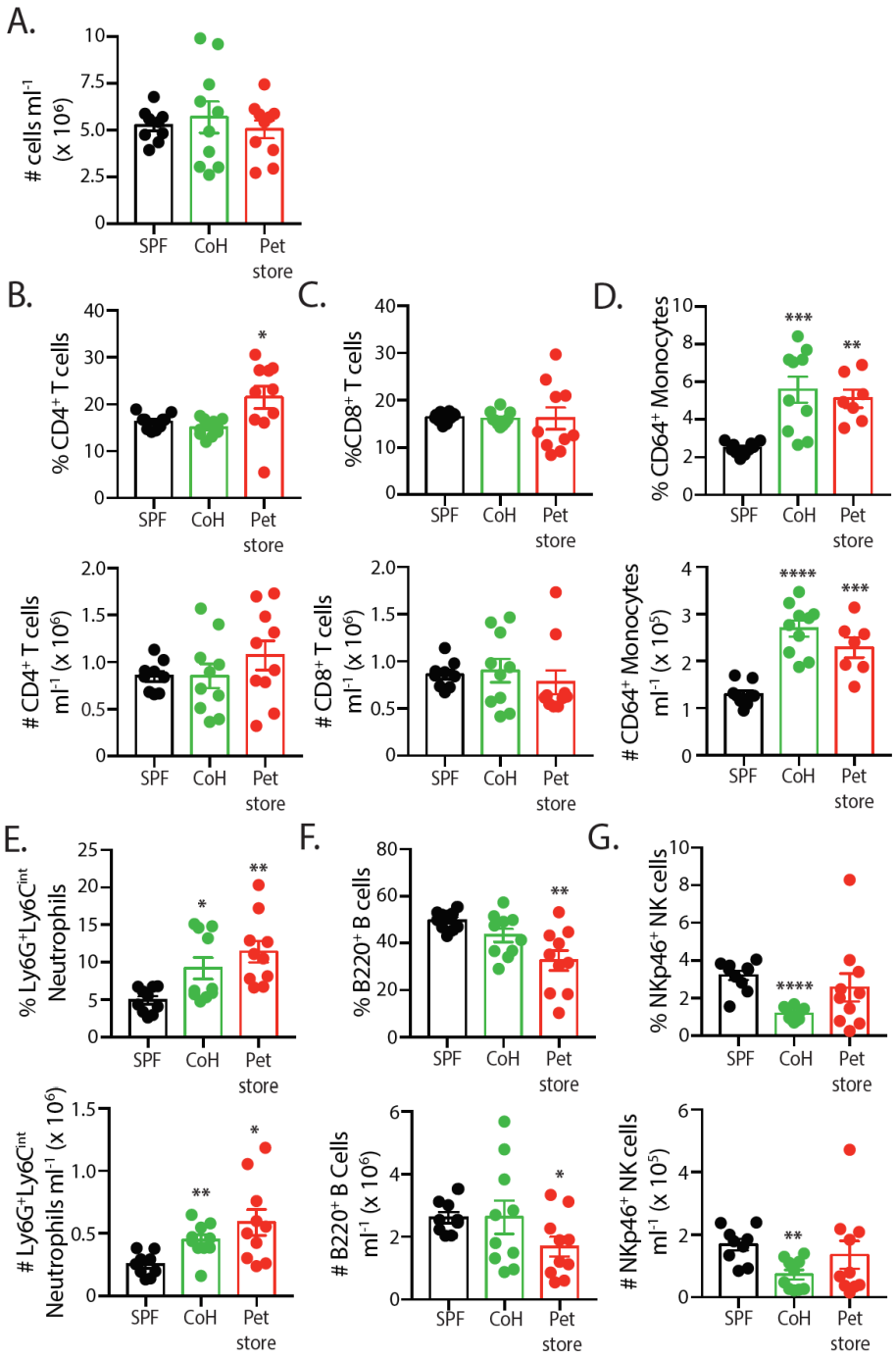

Figure 4-3. Cohoused mice have altered circulating immune cell composition. A. Total circulating immune cell counts from the blood of SPF B6, cohoused (CoH) B6, and pet store mice were determined by flow cytometry. B-F. Frequency and number (cells/ml blood) of B) CD4 T cells, C) CD8 T cells, D) Monocytes, E) Neutrophils, F) B cells, and G) NK cells. 10 mice/group were analyzed, and data are representative of 3 technical replicates. * $p < 0.05$, ** $p < 0.01$, *** $p < 0.005$, **** $p < 0.001$. See also Figure 4-4.

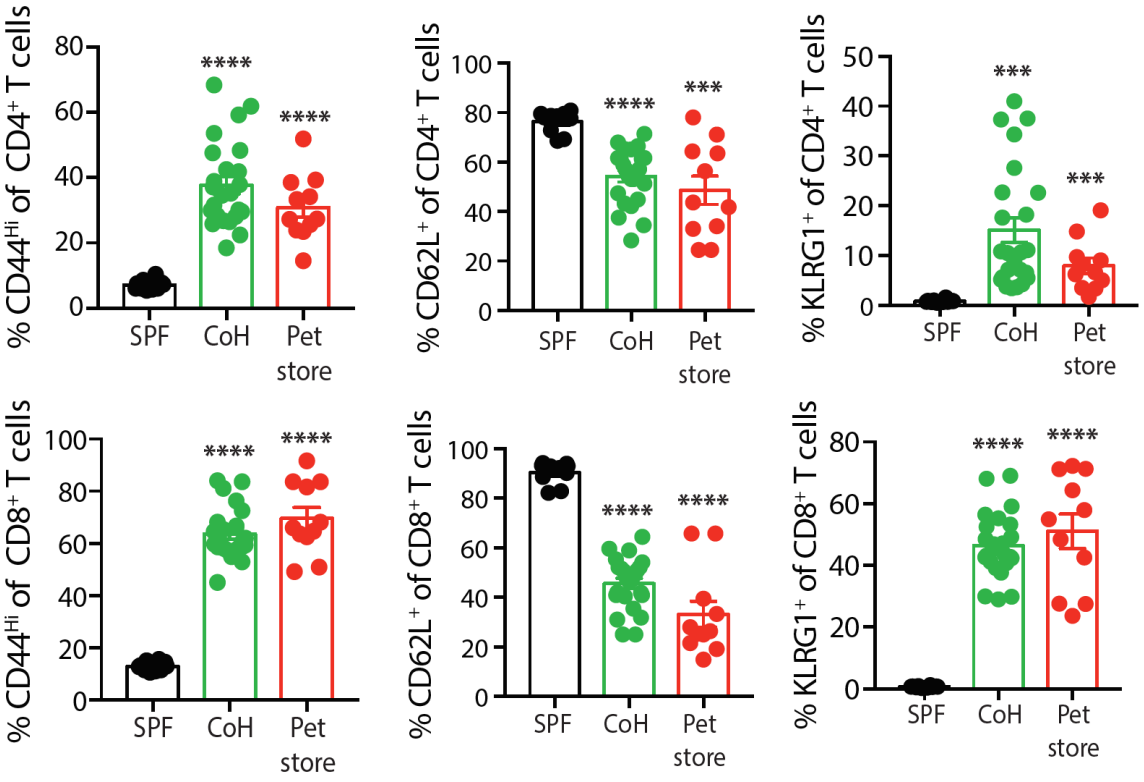

Figure 4-4. Cohoused mice have elevated frequency of antigen-experienced CD4 and CD8 T cells. Related to Figure 4-3. The frequency of CD44^{hi}, CD62L^{+}, and KLRG1^{+} CD4^{+} and CD8^{+} T cells was determined in the blood of SPF B6, cohoused (CoH) B6, and pet store mice was determined after 60 d. 10-24 mice/group pooled from 2 technical replicates. *** $p < 0.005$, **** $p < 0.001$.

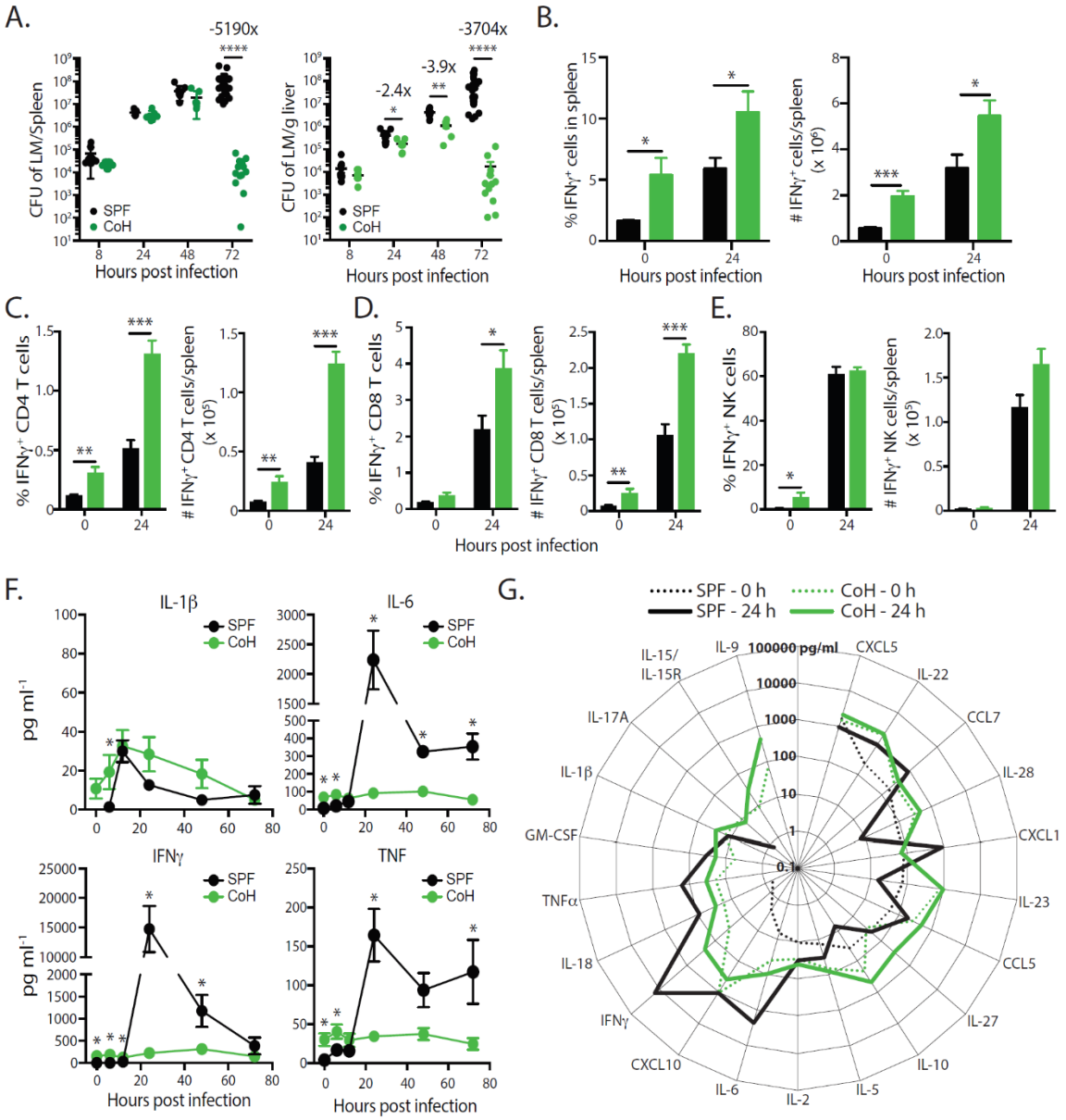

Figure 4-5. Cohoused mice are more 'immune fit' than SPF mice in response to virulent *Listeria* infection. SPF and cohoused (CoH) B6 mice were infected with virulent *L. monocytogenes* (LM; 8 x 104 CFU i.v.). A. Bacterial burden in the spleen and liver was determined after 8, 24, 48, and 72 hours. 7-17 mice/group/time point, pooled from >2 technical replicates. B-E. The frequency and number of IFNγ-producing cells in the spleen before and 24 hours after LM infection were quantified by intracellular cytokine staining flow cytometry. IFNγ-producing B) total cells, C) CD4 T cells, D) CD8 T cells, and E) NK cells were identified. 4-7 mice/group/time point, pooled from two technical replicates. *$p < 0.05$, **$p < 0.01$, *** $p < 0.005$. F. Serum samples from SPF or cohoused B6 mice were obtained at indicated hours after virulent LM infection. The amount of IL-1β, IL-6, IFNγ, and TNF in the serum was determined by bioplex. 4-7

mice/group/time point. * $p < 0.05$, ** $p < 0.01$, *** $p < 0.005$ for SPF vs. cohoused mice at the indicated time points. G. Additional serum cytokine and chemokine levels in SPF (black lines) and cohoused (green lines) B6 mice were determined prior to (dotted lines) and 24 hours post-LM infection (solid lines). No line for given a cytokine indicates levels were below the limit of detection. Data in F and G are representative from two technical replicates.

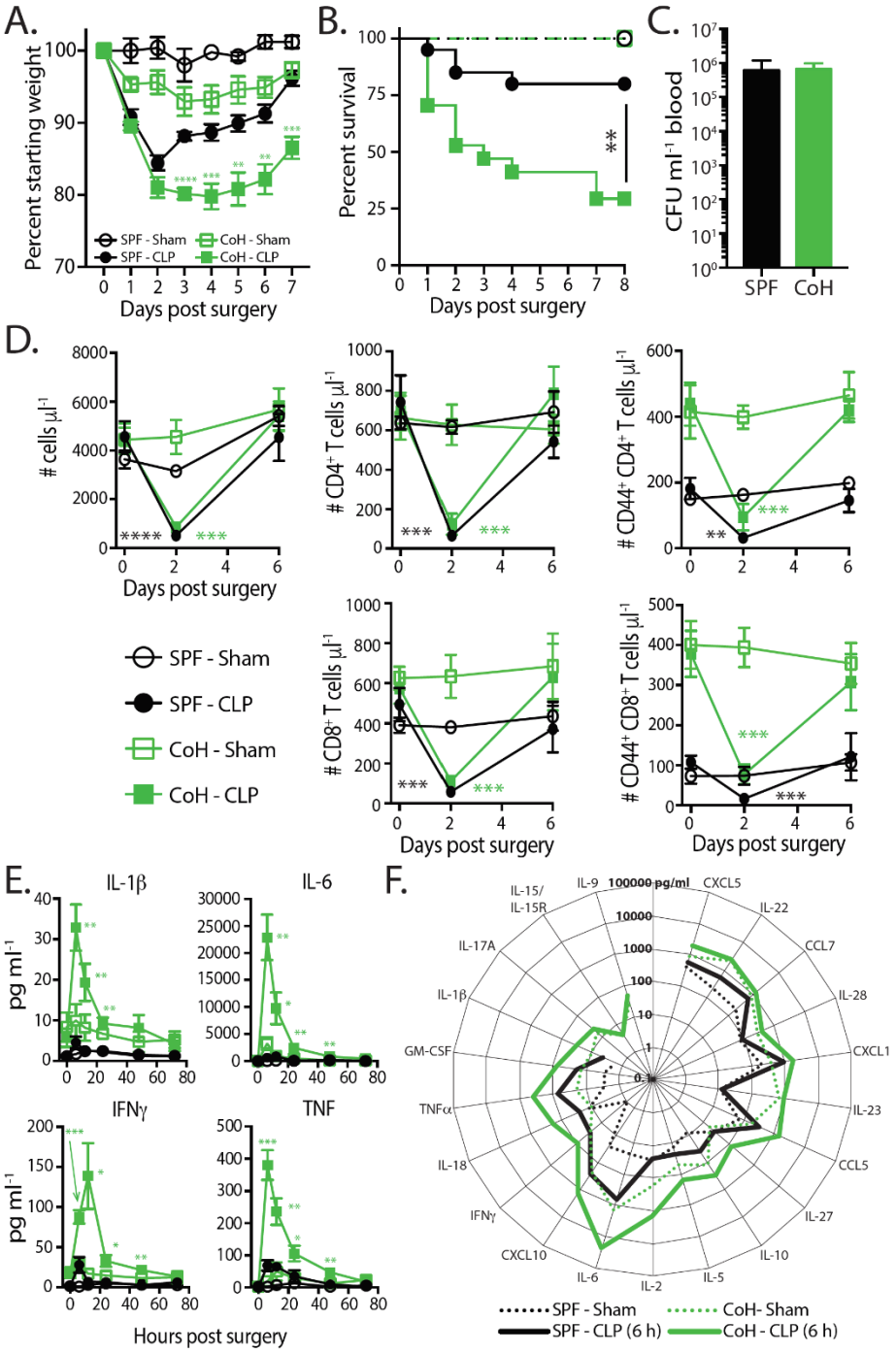

Figure 4-6. Increased morbidity/mortality in CLP-treated cohoused mice correlates with an exacerbated 'cytokine storm'. SPF and cohoused (CoH) B6 mice underwent sham or CLP surgery. Weight loss (A) and survival (B) were monitored over time. 8-17 mice/group, pooled from 2 technical replicates. ** $p < 0.01$, *** $p < 0.005$, **** $p < 0.001$. C. Bacterial CFU in blood at 24 hours post CLP procedure was quantified in SPF and cohoused B6 mice. 9 mice/group, representative of 2 technical replicates. D. The

number of total immune cells, $CD4^+$ T cells, $CD8^+$ T cells, $CD44^+$ $CD4^+$ T cell, and $CD44^+$ $CD8^+$ T cells per µl blood were determined before (day 0) and after (days 2 and 6) sham/CLP surgery. 5-7 mice/group, representative of 3 technical replicates. E. Serum samples from sham- or CLP-treated SPF or CoH B6 mice were obtained at indicated hours after surgery. The amount of IL-1β, IL-6, IFNγ, and TNF in samples was determined by bioplex. F. Additional cytokines and chemokines in the serum 6 hours post-surgery were quantified by bioplex. Data in E and F consist of 4-7 mice/group/time point and are representative of 3 technical replicates. ** $p < 0.01$, *** $p < 0.005$, **** $p < 0.001$ for SPF - CLP vs. cohoused - CLP at the indicated time points.

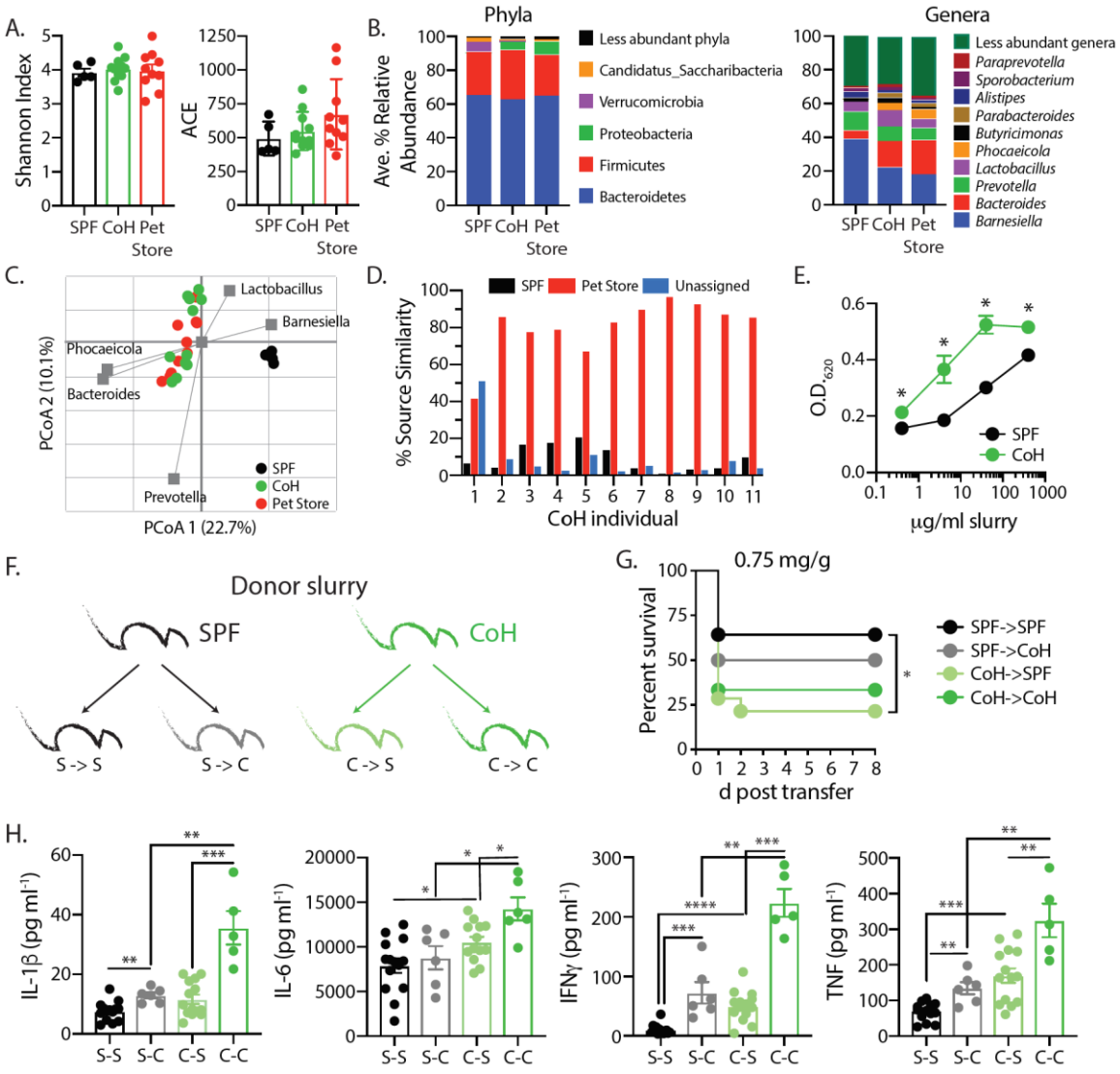

Figure 4-7. Characterization of the microbiome in cohoused mice. A. Mean alpha diversity indices (± S.E.) in mouse fecal samples. Shannon and ACE indices are shown on the left and right, respectively. n = 5 SPF, 11 cohoused (CoH), and 10 pet store samples. B. Distributions of abundant phyla and genera in mouse fecal samples. Less abundant genera accounted for a mean of ≤2.2 % of the community, among all samples. C. PCoA of Bray-Curtis distances (r2 = 0.47). The five most abundant genera were correlated with axes position, where positioning near sample groups indicates greater relative abundance of that genus. D. Similarity of cohoused B6 mice to SPF B6 and pet store mice, determined by SourceTracker. E. Cecal contents from SPF or CoH B6 mice (n = 5 of each) were cultured with the TLR4 reporter cell line, HEK-Blue hTLR4. TLR4 activation was quantified after 24 hours with indicated concentration of cecal material. Data is representative of 3 technical replicates. F. Cecal contents were harvested from SPF or CoH B6 donor mice to challenge recipient mice in the following combinations: S-S, SPF cecal slurry transferred to SPF recipients (n = 14); S-C, SPF cecal slurry

transferred to cohoused recipients (n = 6); C-S, cohoused cecal slurry transferred to SPF recipients (n = 14); and C-C, cohoused cecal slurry transferred to cohoused recipients (n = 6). G. Survival curve of mice after i.p. injection with 0.75 mg/g body weight of cecal slurry as indicated in (F). H. Serum cytokine levels 6 hours post-cecal slurry injection was determined by bioplex. Data in G and H are pooled from 2 technical replicates. * $p < 0.05$, ** $p < 0.01$, *** $p < 0.005$, **** $p < 0.001$. See also Figure 4-8.

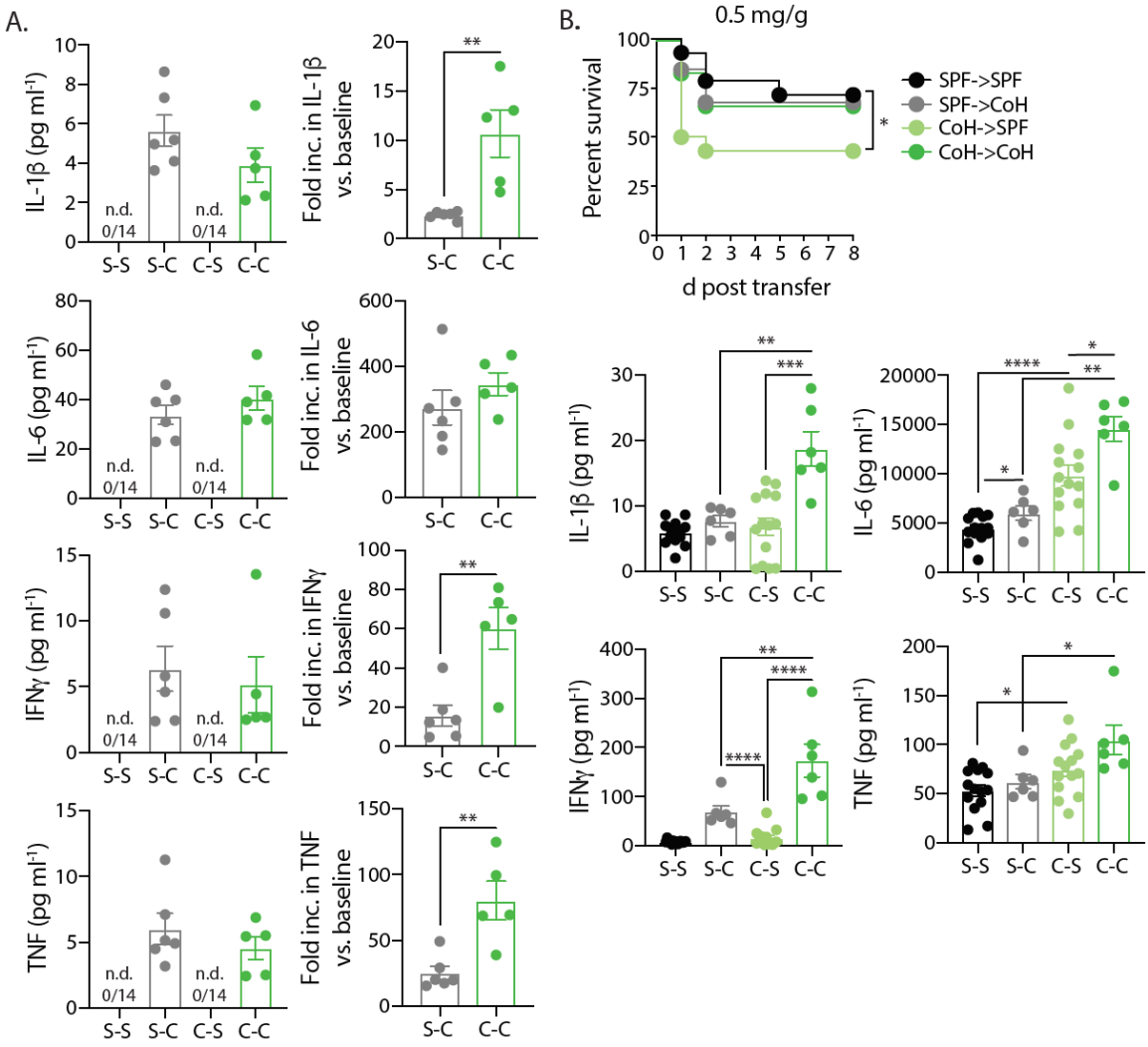

Figure 4-8. Intraperitoneal cecal slurry injection into SPF and cohoused B6 recipient mice. Related to Figure 4-7. A. Baseline serum cytokine levels for mice used in Figure 4-7F-H for IL-1β, IL-6, IFNγ, and TNF. Fold increase 6 hours post cecal injection over baseline levels for IL-1β, IL-6, IFNγ, and TNF was calculated for cohoused recipients. SPF mice not calculated because baseline serum cytokine levels were below detection threshold. B. Survival curve following injection of 0.5 mg/g body weight cecal slurry as outlined in Figure 4-7F. Cecal slurry was harvested from SPF or cohoused donors to challenge recipient mice with varying combinations of host exposure and cecal slurry type. S-S, SPF cecal slurry transferred to SPF host; S-C, SPF cecal slurry transferred to cohoused host; C-S, cohoused cecal slurry transferred to SPF host; C-C, cohoused cecal slurry transferred to cohoused host. IL-1β, IL-6, IFNγ, TNF serum cytokine levels collected 6 hours post cecal slurry injection (0.5 mg/g body weight). Data in A and B is pooled from 2 technical replicates, consisting of 6-14 mice/group.

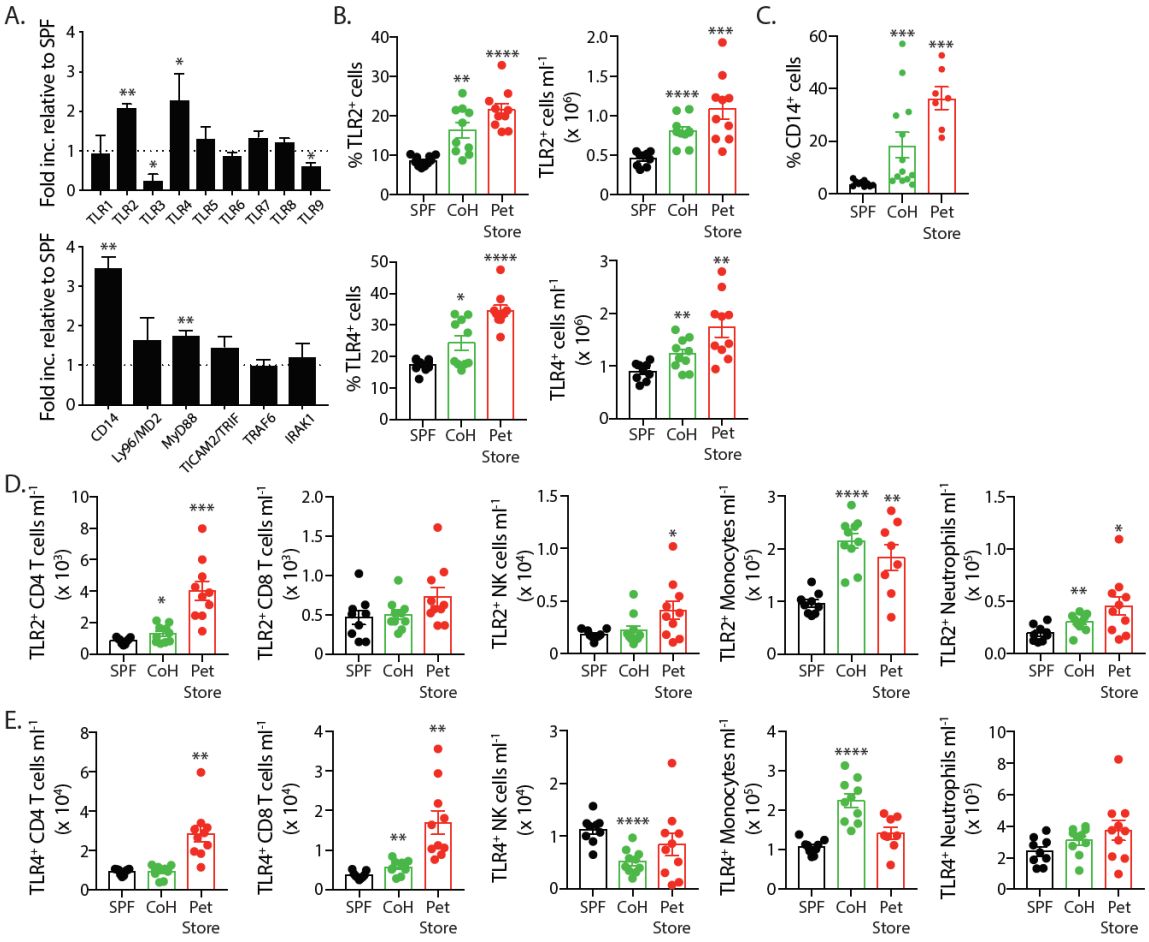

Figure 4-9. TLR2 and TLR4 expression is increased after physiological microbial exposure. A. qPCR analysis of TLRs and TLR signaling pathway components in the adherent myeloid cells isolated from spleens of SPF (n = 5) and cohoused (CoH; n = 5) B6 mice. Data are representative of 2 technical replicates. B. Frequency and number of $TLR2^+$ or $TLR4^+$ cells in the blood of SPF B6, CoH B6, and pet store mice. C. Frequency of $CD14^+$ cells in blood of SPF B6, CoH B6, and pet store mice. D-E. Immune subset quantification of TLR2 (D) and TLR4 (E) expression by CD4 T cells, CD8 T cells, NK cells, monocytes, and neutrophils. Data in B-E consist of 5-10 mice/group and are representative of 3 technical replicates. * $p < 0.05$, ** $p < 0.01$, *** $p < 0.005$. See also Figure 4-10.

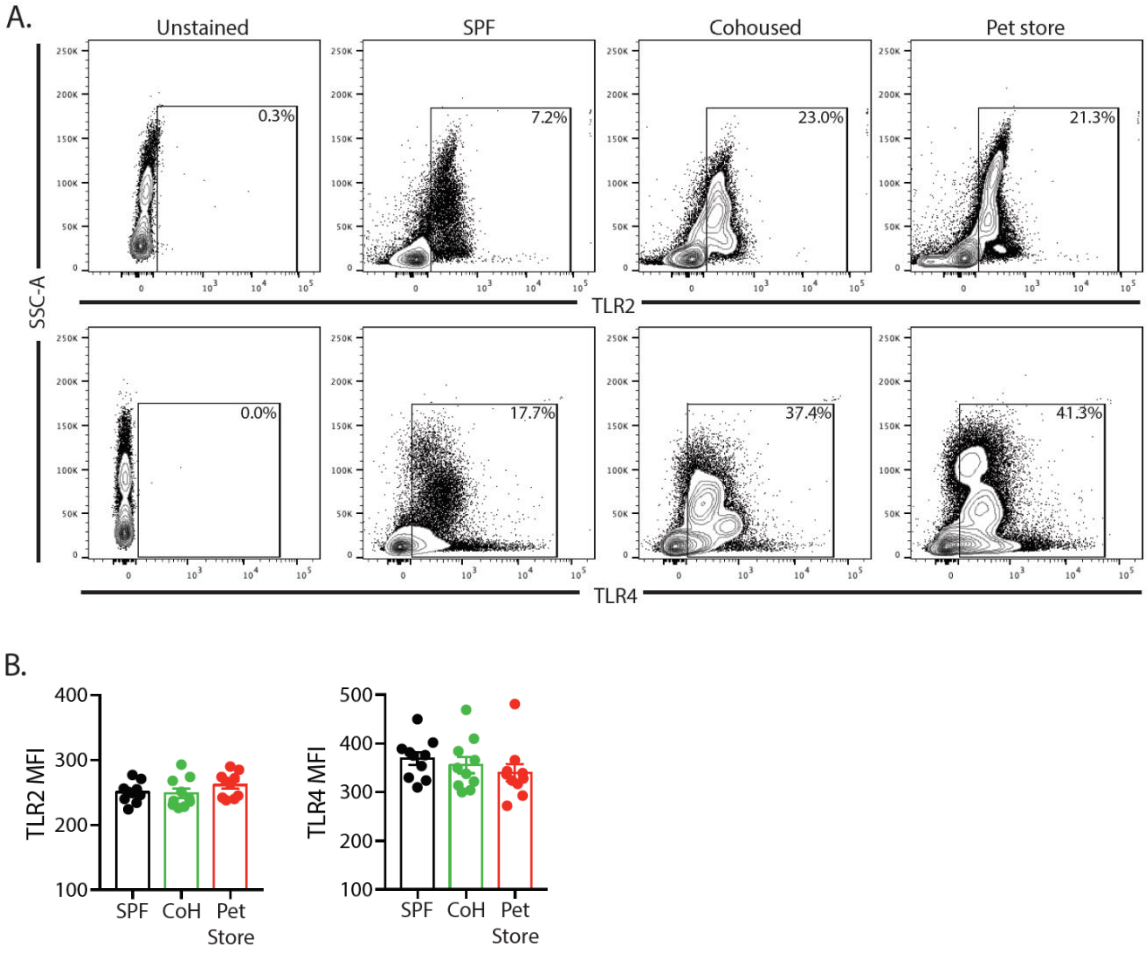

Figure 4-10. Representative TLR2 and TLR4 expression and intensity. Related to Figure 4-9. A. Representative TLR2 and TLR4 staining of blood from SPF B6, cohoused (CoH) B6, and pet store mice. B. Mean fluorescence intensity (MFI) of $TLR2^+$ and $TLR4^+$ cells from blood of SPF B6, CoH B6, and pet store mice. 10 mice/group (pooled from 3 technical replicates) were analyzed.

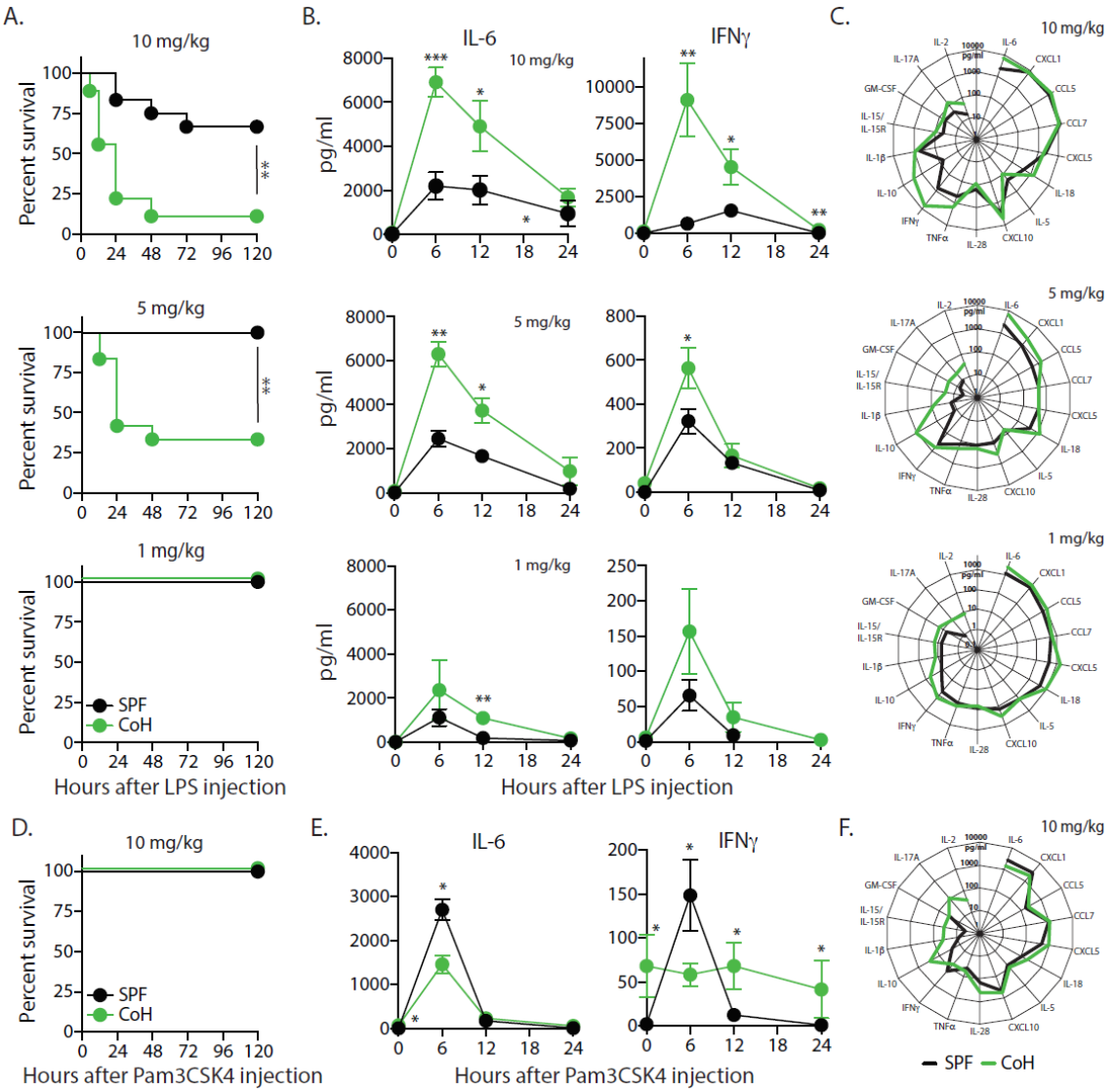

Figure 4-11. Increased cytokine production in cohoused mice after LPS injection correlates with increased mortality. SPF and cohoused (CoH) B6 mice were injected with LPS (10, 5, or 1 mg/kg i.v.). A. Survival after LPS injection. B-C. Serum samples were obtained at indicated hours after LPS injection, and the amount of IL-6 and IFNγ was determined by bioplex. C. Additional cytokines and chemokines in the serum 6 hours post-LPS injection were quantified by bioplex. D-F. SPF and CoH B6 mice were injected with Pam3CSK4 (10 mg/kg i.v.). Survival was monitored, and the amounts of various cytokines and chemokines in the serum 6 hours post-Pam3CKS4 injection were quantified by bioplex. Survival data (A and D) consist of 12-21 mice/group and are pooled from 3 technical replicates. Cytokine data (B, C, E, and F) consist of 4-7 mice/group/time point and are representative of 3 technical replicates. * $p < 0.05$, ** $p < 0.01$ for SPF vs. cohoused at the indicated time points.

Chapter 5: Conclusions

The primary focus of my thesis is identifying how sepsis alters CD4 T cell number and function. Specifically, I am interested in understanding how sepsis affects T cell-dependent B cell responses following immunization and the impact on CD4 T cell responses to secondary infections. Previous work from the Griffith lab has shown that while the total CD4 T cell population recovers numerically, the recovery of individual antigen-specific populations occurs asymmetrically resulting in holes in the naive T cell compartment[62,64]. I have investigated how this dynamic recovery might impact future responses to immunization, specifically T cell-dependent B cell responses and hypothesized that it would result in reduced class switching, Tfh-dependent somatic hypermutation, and affinity maturation. To test this, I immunized mice following CLP-induced sepsis with antigen containing linked CD4 T cell and B cell epitopes and tracked the antigen specific cells and antibody production. My experiments demonstrate prolonged impairments in Tfh and B cell number and function post sepsis[31]. These findings suggest that patients with a history of sepsis lack the immune function to mount a sufficient response to vaccination and may get little benefit from typical vaccination protocols.

Publications from the Griffith lab show that 2W1S-specific naive CD4 T cells are numerically and functionally depleted after sepsis and do not recover by 30 days post sepsis[62]. In contrast, OVA_{323}-specific naive CD4 T cells are reduced in number and function immediately after sepsis but recover numerically and functionally by 30 days post CLP[62]. Compared to naïve cells, memory T cells exist at higher numbers and can

more rapidly respond during re-challenge[24,183]. Additionally, memory T cells are known to be resistant to apoptosis[183,263], prompting me to question how sepsis might impact the 2W1S-specific and OVA_{323}-specific populations of memory CD4 T cells. To build on these findings, I infected mice with attenuated *Listeria monocytogenes* or *Salmonella enterica* expressing 2W1S or OVA_{323} to generate memory populations of 2W1S- and OVA_{323}-specific CD4 T cells, a majority being Th1s. Then I performed CLPs 30 days after infection and tracked the 2W1S-specific cells. The number of 2W1S-specific memory CD4 T cells was significantly reduced immediately after sepsis induction but recovered by day 14. The ability to produce effector cytokines and clear secondary did not recover by day 30 post sepsis. The OVA_{323}-specific population showed numerical reductions at day 2 post sepsis and deficits in cytokine production as well as pathogen clearance. These experiments demonstrate prolonged impairments in Th1, Tfh and B cell responses to both primary and secondary challenges post sepsis. Additionally, these findings suggest that patients with a history of sepsis may get little benefit from vaccinations typically administered to healthy individuals and will have increased risk of secondary infections for which CD4 T cells are critical for pathogen control. Future studies could examine yearly influenza vaccination responses in sepsis survivors.

The CLP mouse model of sepsis is commonly referred to as the “gold standard” of sepsis and accurately recapitulates many aspects of human sepsis. Despite being a widely accepted model in the field of sepsis research, key differences between laboratory mice and humans suffering from sepsis, including pathogen exposure and immune status, have limited the use of the CLP model in the development of new and effective sepsis

therapies. Previously it has been reported that immune experienced COH mice have increased numbers of total and memory CD4 and CD8 T cells and, without previous exposure, have improved survival compared to SPF mice when challenged with a lethal dose of *Listeria monocytogenes*[50]. I wanted to know if COH mice might have improved responses to sepsis and determine how physiological pathogen exposure and immune experience alter inflammatory responses and immune suppression after sepsis. To explore this question, I examined the inflammatory status of COH mice before and after sepsis. I found that in non-septic mice, immune experience results in elevated numbers of circulating monocytes, upregulation of TLR4 on monocytes, and elevated serum levels of various inflammatory cytokines, suggesting evidence of innate immune training. Following sepsis, COH mice displayed significantly elevated levels of inflammatory cytokines in serum and reduced survival. Using LPS challenge and the cecal slurry model of sepsis, our team was able to determine that the elevated inflammatory response and mortality observed in the COH mice was the result of both heightened immune activation and the pathogenicity of the COH intestinal microbiome. These findings shed light on the impact of pathogen exposure and innate immune training on inflammatory responses and immunopathology in sepsis. Further, these data suggest that using the COH model to study human inflammatory diseases, which historically have been controversially modeled in mice, may improve preclinical research and lead to the development of new effective therapies for sepsis and other inflammatory diseases[264–266].

References

1. Van Der Poll T, Van De Veerdonk FL, Scicluna BP, Netea MG (2017) The immunopathology of sepsis and potential therapeutic targets. *Nat Rev Immunol* **17**: 407–420.

2. Shankar-Hari M, Phillips GS, Levy ML, Seymour CW, Liu VX, Deutschman CS, Angus DC, Rubenfeld GD, Singer M (2016) Developing a newdefinition and assessing newclinical criteria for Septic shock: For the third international consensus definitions for sepsis and septic shock (sepsis-3). *JAMA - J Am Med Assoc* **315**: 775–787.

3. Rhee C, Dantes R, Epstein L, Murphy DJ, Seymour CW, Iwashyna TJ, Kadri SS, Angus DC, Danner RL, Fiore AE, et al. (2017) Incidence and trends of sepsis in US hospitals using clinical vs claims data, 2009-2014. *JAMA* **318**: 1241–1249.

4. Delano MJ, Ward PA (2016) The immune system's role in sepsis progression, resolution, and long-term outcome. *Immunol Rev* **274**: 330–353.

5. Angus DC, Linde-Zwirble WT, Lidicker J, Clermont G, Carcillo J, Pinsky MR (2001) Epidemiology of severe sepsis in the United States: analysis of incidence, outcome, and associated costs of care. *Crit Care Med* **29**: 1303–1310.

6. Coopersmith CM, Wunsch H, Fink MP, Linde-Zwirble WT, Olsen KM, Sommers MS, Anand KJ, Tchorz KM, Angus DC, Deutschman CS (2012) A comparison of critical care research funding and the financial burden of critical illness in the United States. *Crit Care Med* **40**: 1072–1079.

7. Heyland DK, Hopman W, Coo H, Tranmer J, McColl MA (2000) Long-term health-related quality of life in survivors of sepsis. Short Form 36: a valid and reliable measure of health-related quality of life. *Crit Care Med* **28**: 3599–3605.

8. Delano MJ, Ward PA (2016) Sepsis-induced immune dysfunction: Can immune therapies reduce mortality? *J Clin Invest* **126**: 23–31.

9. Hotchkiss RS, Monneret G, Payen D (2013) Immunosuppression in sepsis: A novel understanding of the disorder and a new therapeutic approach. *Lancet Infect Dis* **13**: 260–268.

10. Hotchkiss RS, Moldawer LL, Opal SM, Reinhart K, Turnbull IR, Vincent JL (2016) Sepsis and septic shock. *Nat Rev Dis Prim* **2**: 16045.

11. Angus DC, van der Poll T (2013) Severe Sepsis and Septic Shock. *N Engl J Med* **369**: 840–851.

12. Jensen IJ, Sjaastad F V, Griffith TS, Badovinac VP (2018) Sepsis-Induced T Cell Immunoparalysis: The Ins and Outs of Impaired T Cell Immunity. *J Immunol* **200**: 1543–1553.

13. Strother RK, Danahy DB, Kotov DI, Kucaba TA, Zacharias ZR, Griffith TS, Legge KL, Badovinac VP (2016) Polymicrobial Sepsis Diminishes Dendritic Cell Numbers and Function Directly Contributing to Impaired Primary CD8 T Cell Responses In Vivo. *J*

Immunol **197**: 4301–4311.

14. Hall MJ, Williams SN, DeFrances CJ, Golosinskiy A (2011) Inpatient care for septicemia or sepsis: a challenge for patients and hospitals. *NCHS Data Brief* 1–8.

15. Hotchkiss RS, Swanson PE, Freeman BD, Tinsley KW, Cobb JP, Matuschak GM, Buchman TG, Karl IE (1999) Apoptotic cell death in patients with sepsis, shock, and multiple organ dysfunction. *Crit Care Med* **27**: 1230–1251.

16. Hotchkiss RS, Tinsley KW, Swanson PE, Schmieg RE, Hui JJ, Chang KC, Osborne DF, Freeman BD, Cobb JP, Buchman TG, et al. (2001) Sepsis-induced apoptosis causes progressive profound depletion of B and CD4+ T lymphocytes in humans. *J Immunol* **166**: 6952–6963.

17. Unsinger J, Kazama H, McDonough JS, Griffith TS, Hotchkiss RS, Ferguson TA (2010) Sepsis-induced apoptosis leads to active suppression of delayed-type hypersensitivity by CD8+ regulatory T cells through a TRAIL-dependent mechanism. *J Immunol* **184**: 6766–6772.

18. Hotchkiss RS, Tinsley KW, Swanson PE, Grayson MH, Osborne DF, Wagner TH, Cobb JP, Coopersmith C, Karl IE (2002) Depletion of Dendritic Cells, But Not Macrophages, in Patients with Sepsis. *J Immunol* **168**: 2493–2500.

19. Otto GP, Sossdorf M, Claus RA, Rodel J, Menge K, Reinhart K, Bauer M, Riedemann NC (2011) The late phase of sepsis is characterized by an increased microbiological burden and death rate. *Crit Care* **15**: R183.

20. Luyt CE, Combes A, Deback C, Aubriot-Lorton MH, Nieszkowska A, Trouillet JL, Capron F, Agut H, Gibert C, Chastre J (2007) Herpes simplex virus lung infection in patients undergoing prolonged mechanical ventilation. *Am J Respir Crit Care Med* **175**: 935–942.

21. Limaye AP, Kirby KA, Rubenfeld GD, Leisenring WM, Bulger EM, Neff MJ, Gibran NS, Huang ML, Santo Hayes TK, Corey L, et al. (2008) Cytomegalovirus reactivation in critically ill immunocompetent patients. *JAMA* **300**: 413–422.

22. Ranieri VM, Thompson BT, Barie PS, Dhainaut JF, Douglas IS, Finfer S, Gårdlund B, Marshall JC, Rhodes A, Artigas A, et al. (2012) Drotrecogin alfa (activated) in adults with septic shock. *N Engl J Med* **366**: 2055–2064.

23. Abraham E, Reinhart K, Opal S, Demeyer I, Doig C, López Rodriguez A, Beale R, Svoboda P, Laterre PF, Simon S, et al. (2003) Efficacy and Safety of Tifacogin (Recombinant Tissue Factor Pathway Inhibitor) in Severe Sepsis: A Randomized Controlled Trial. *J Am Med Assoc* **290**: 238–247.

24. Murphy K, Weaver C (2017) *Janeway's Immunbiology*. Garland Science, Taylor & Francis Group, New York.

25. Rittirsch D, Flierl MA, Ward PA (2008) Harmful molecular mechanisms in sepsis. *Nat Rev Immunol* **8**: 776–787.

26. de Stoppelaar SF, van 't Veer C, van der Poll T (2014) The role of platelets in sepsis. *Thromb Haemost* **20**: 3494.

27. Bone RC (1992) Sepsis and coagulation. An important link. *Chest* **101**: 594–596.

28. Levi M, van der Poll T (2017) Coagulation and sepsis. *Thromb Res* **149**: 38–44.

29. Duong S, Condotta SA, Rai D, Martin MD, Griffith TS, Badovinac VP (2014) Polymicrobial sepsis alters antigen-dependent and -independent memory CD8 T cell functions. *J Immunol* **192**: 3618–3625.

30. Jensen IJ, Winborn CS, Fosdick MG, Shao P, Tremblay MM, Shan Q, Tripathy SK, Snyder CM, Xue HH, Griffith TS, et al. (2018) Polymicrobial sepsis influences NK-cell-mediated immunity by diminishing NK-cell-intrinsic receptor-mediated effector responses to viral ligands or infections. *PLoS Pathog* **14**: e1007405.

31. Sjaastad F V, Condotta SA, Kotov JA, Pape KA, Dail C, Danahy DB, Kucaba TA, Tygrett LT, Murphy KA, Cabrera-Perez J, et al. (2018) Polymicrobial Sepsis Chronic Immunoparalysis Is Defined by Diminished Ag-Specific T Cell-Dependent B Cell Responses. *Front Immunol* **9**: 2532.

32. Meakins JL, Pietsch JB, Bubenick O, Kelly R, Rode H, Gordon J, MacLean LD (1977) Delayed hypersensitivity: indicator of acquired failure of host defenses in sepsis and trauma. *Ann Surg* **186**: 241–250.

33. Milne CA, Guttmann RD, Meakins JL (1982) Short-term implications of delayed-type hypersensitivity responses in renal transplant recipients. *Transplant Proc* **14**: 673–675.

34. Christou N V., Meakins JL, Gordon J, Yee J, Hassan-Zahraee M, Nohr CW, Shizgal HM, MacLean LD (1995) The delayed hypersensitivity response and host resistance in surgical patients. 20 years later. *Ann Surg* **222**: 534–546; discussion 546-8.

35. Hotchkiss RS, Osmon SB, Chang KC, Wagner TH, Coopersmith CM, Karl IE (2005) Accelerated lymphocyte death in sepsis occurs by both the death receptor and mitochondrial pathways. *J Immunol* **174**: 5110–5118.

36. Hotchkiss RS, Swanson PE, Knudson CM, Chang KC, Cobb JP, Osborne DF, Zollner KM, Buchman TG, Korsmeyer SJ, Karl IE (1999) Overexpression of Bcl-2 in transgenic mice decreases apoptosis and improves survival in sepsis. *J Immunol* **162**: 4148–4156.

37. Iwata A, Stevenson VM, Minard A, Tasch M, Tupper J, Lagasse E, Weissman I, Harlan JM, Winn RK (2003) Over-Expression of Bcl-2 Provides Protection in Septic Mice by a trans Effect . *J Immunol* **171**: 3136–3141.

38. Hotchkiss RS, Tinsley KW, Swanson PE, Chang KC, Cobb JP, Buchman TG, Korsmeyer SJ, Karl IE (1999) Prevention of lymphocyte cell death in sepsis improves survival in mice. *Proc Natl Acad Sci U S A* **96**: 14541–14546.

39. Hotchkiss RS, Chang KC, Swanson PE, Tinsley KW, Hui JJ, Klender P, Xanthoudakis S, Roy S, Black C, Grimm E, et al. (2000) Caspase inhibitors improve survival in sepsis: a critical role of the lymphocyte. *Nat Immunol* **1**: 496–501.

40. Efron PA, Mohr AM, Moore FA, Moldawer LL (2015) The future of murine sepsis and trauma research models. *J Leukoc Biol* **98**: 945–952.

41. Dejager L, Pinheiro I, Dejonckheere E, Libert C (2011) Cecal ligation and puncture: The gold standard model for polymicrobial sepsis? *Trends Microbiol* **19**: 198–208.

42. Hilbert T, Steinhagen F, Senzig S, Cramer N, Bekeredjian-Ding I, Parcina M, Baumgarten G, Hoeft A, Frede S, Boehm O, et al. (2017) Vendor effects on murine gut microbiota influence experimental abdominal sepsis. *J Surg Res* **211**: 126–136.

43. Wichterman KA, Baue AE, Chaudry IH (1980) Sepsis and septic shock--a review of laboratory models and a proposal. *J Surg Res* **29**: 189–201.

44. Baker CC, Chaudry IH, Gaines HO, Baue AE (1983) Evaluation of factors affecting mortality rate after sepsis in a murine cecal ligation and puncture model. *Surgery* **94**: 331–335.

45. Imamura M, Clowes GHA (1975) Hepatic blood flow and oxygen consumption in starvation, sepsis and septic shock. *Surg Gynecol Obstet* **141**: 27–34.

46. Parker SJ, Watkins PE (2001) Experimental models of gram-negative sepsis. *Br J Surg* **88**: 22–30.

47. Rittirsch D, Huber-Lang MS, Flierl MA, Ward PA (2009) Immunodesign of experimental sepsis by cecal ligation and puncture. *Nat Protoc* **4**: 31–36.

48. Hotchkiss RS, Nicholson DW (2006) Apoptosis and caspases regulate death and inflammation in sepsis. *Nat Rev Immunol* **6**: 813–822.

49. Foster HL (1959) Housing of disease-free vertebrates. *Ann N Y Acad Sci* **78**: 80–88.

50. Beura LK, Hamilton SE, Bi K, Schenkel JM, Odumade OA, Casey KA, Thompson EA, Fraser KA, Rosato PC, Filali-Mouhim A, et al. (2016) Normalizing the environment recapitulates adult human immune traits in laboratory mice. *Nature* **532**: 512–516.

51. Pepper M, Jenkins MK (2011) Origins of CD4(+) effector and central memory T cells. *Nat Immunol* **12**: 467–471.

52. Dupage M, Bluestone JA (2016) Harnessing the plasticity of CD4+ T cells to treat immune-mediated disease. *Nat Rev Immunol* **16**: 149–163.

53. McHeyzer-Williams MG, Davis MM (1995) Antigen-Specific Development of Primary and Memory T Cells in Vivo. *Science (80-)* **268**: 106–111.

54. Ahmed R, Gray D (1996) Immunological memory and protective immunity: Understanding their relation. *Science (80-)* **272**: 54–60.

55. Dutton, R. W., Bradley, L. M., Swain SL (1998) T cell memory. *Curr Top Microbiol Immunol* **16**: 201–23.

56. Venet F, Davin F, Guignant C, Larue, Audrey Darbon R, Allombert C, Mougin B, Malcus C, Lepape A, Monneret G (2010) Early assessment of leukocyte alterations at diagnosis of septic shock. *Shock* **34**: 358–363.

57. Inoue S, Suzuki-Utsunomiya K, Okada Y, Taira T, Iida Y, Miura N, Tsuji T, Yamagiwa T, Morita S, Chiba T, et al. (2013) Reduction of immunocompetent T cells followed by prolonged lymphopenia in severe sepsis in the elderly. *Crit Care Med* **41**: 810–819.

58. Gouel-Cheron A, Venet F, Allaouchiche B, Monneret G (2012) CD4+ T-lymphocyte alterations in trauma patients. *Crit Care* **16**: 432.

59. Chen X, Ye J, Ye J (2011) Analysis of peripheral blood lymphocyte subsets and prognosis in patients with septic shock. *Microbiol Immunol* **55**: 736–742.

60. Roger PM, Hyvernat H, Ticchioni M, Kumar G, Dellamonica J, Bernardin G (2012) The early phase of human sepsis is characterized by a combination of apoptosis and proliferation of T cells. *J Crit Care* **27**: 384–393.

61. Francois B, Jeannet R, Daix T, Walton AH, Shotwell MS, Unsinger J, Monneret G, Rimmele T, Blood T, Morre M, et al. (2018) Interleukin-7 restores lymphocytes in septic shock: the IRIS-7 randomized clinical trial. *JCI Insight* **3**: e98960.

62. Cabrera-Perez J, Condotta SA, James BR, Kashem SW, Brincks EL, Rai D, Kucaba TA, Badovinac VP, Griffith TS (2015) Alterations in antigen-specific naive CD4 T cell precursors after sepsis impairs their responsiveness to pathogen challenge. *J Immunol* **194**: 1609–1620.

63. Xie J, Chen CW, Sun Y, Laurie SJ, Zhang W, Otani S, Martin GS, Coopersmith CM, Ford ML (2019) Increased attrition of memory T cells during sepsis requires 2B4. *JCI Insight* **4**: e126030.

64. Cabrera-Perez J, Babcock JC, Dileepan T, Murphy KA, Kucaba TA, Badovinac VP, Griffith TS (2016) Gut Microbial Membership Modulates CD4 T Cell Reconstitution and Function after Sepsis. *J Immunol* **197**: 1692–1698.

65. Cabrera-Perez J, Condotta SA, Badovinac VP, Griffith TS (2014) Impact of sepsis on CD4 T cell immunity. *J Leukoc Biol* **96**: 767–777.

66. Boomer JS, To K, Chang KC, Ii SDJ, Kreisel D, Takasu O, Osborne DF, Walton AH, Bricker TL, Jarman 2nd SD, et al. (2011) Immunsuppression in Patients Who Die of Sepsis and Multiple Organ Failure. *JAMA - J Am Med Assoc* **306**: 2594–2605.

67. De AK, Kodys KM, Pellegrini J, Yeh B, Furse RK, Bankey P, Miller-Graziano CL (2000) Induction of global anergy rather than inhibitory Th2 lymphokines mediates posttrauma T cell immunodepression. *Clin Immunol* **96**: 52–66.

68. Iv WFC, Cavassani KA, Ito T, Schaller M, Ishii M, Dou Y, Kunkel SL, Carson IV WF, Cavassani KA, Ito T, et al. (2010) Impaired CD4+ T-cell proliferation and effector function correlates with repressive histone methylation events in a mouse model of severe sepsis. *Eur J Immunol* **40**: 998–1010.

69. Guignant C, Lepape A, Huang X, Kherouf H, Denis L, Poitevin F, Malcus C, Chéron A, Allaouchiche B, Gueyffier F, et al. (2011) Programmed death-1 levels correlate with increased mortality, nosocomial infection and immune dysfunctions in septic shock patients. *Crit Care* **15**: R99.

70. Spec A, Shindo Y, Burnham CD, Wilson S, Ablordeppey EA, Beiter ER, Chang K, Drewry AM, Hotchkiss RS (2016) T cells from patients with Candida sepsis display a suppressive immunophenotype. *Crit Care* **20**: 15.

71. Boomer JS, Shuherk-Shaffer J, Hotchkiss RS, Green JM (2012) A prospective analysis of lymphocyte phenotype and function over the course of acute sepsis. *Crit Care* **16**: R112.

72. Cavassani KA, Carson WF th, Moreira AP, Wen H, Schaller MA, Ishii M, Lindell DM,

Dou Y, Lukacs NW, Keshamouni VG, et al. (2010) The post sepsis-induced expansion and enhanced function of regulatory T cells create an environment to potentiate tumor growth. *Blood* **115**: 4403–4412.

73. Gaborit BJ, Roquilly A, Louvet C, Sadek A, Tessoulin B, Broquet A, Jacqueline C, Vourc M, Chaumette T, Chauveau M (2020) Regulatory T Cells Expressing Tumor Necrosis Factor Receptor Type 2 Play a Major Role in CD4 T-Cell Impairment During Sepsis. *J Infect Dis* jiaa225.

74. Nascimento DC, Melo PH, Piñeros AR, Ferreira RG, Colón DF, Donate PB, Castanheira F V., Gozzi A, Czaikoski PG, Niedbala W, et al. (2017) IL-33 contributes to sepsis-induced long-Term immunosuppression by expanding the regulatory T cell population. *Nat Commun* **8**: 14919.

75. Venet F, Filipe-Santos O, Lepape A, Malcus C, Poitevin-Later F, Grives A, Plantier N, Pasqual N, Monneret G (2013) Decreased T-cell repertoire diversity in sepsis: a preliminary study. *Crit Care Med* **41**: 111–119.

76. Yang A, Farmer E, Lin J, Wu TC, Hung CF (2017) The current state of therapeutic and T cell-based vaccines against human papillomaviruses. *Virus Res* **231**: 148–165.

77. Dey A, Molodecky NA, Verma H, Sharma P, Yang JS, Saletti G, Ahmad M, Bahl SK, Wierzba TF, Nandy RK, et al. (2016) Human circulating antibody-producing B cell as a predictive measure of mucosal immunity to poliovirus. *PLoS One* **11**: 1–14.

78. Auladell M, Jia X, Hensen L, Chua B, Fox A, Nguyen THO, Doherty PC, Kedzierska K (2019) Recalling the future: Immunological memory toward unpredictable influenza viruses. *Front Immunol* **10**: 1400.

79. Bali P, Rafi A (2011) Immunological mechanisms of vaccination. *Nat Immunol* **12**: 509–517.

80. Pape KA, Jenkins MK (2018) Do memory B cells form secondary germinal centers?: It depends. *Cold Spring Harb Perspect Biol* **10**: a029116.

81. Crotty S (2011) Follicular helper CD4 T cells (TFH). *Annu Rev Immunol* **29**: 621–663.

82. Priyamvada L (2016) B Cell Responses during Secondary Dengue Virus Infection Are. *J Virol* **90**: 5574–5585.

83. Shankar-Hari M, Fear D, Lavender P, Mare T, Beale R, Swanson C, Singer M, Spencer J (2017) Activation-Associated accelerated apoptosis of memory B cells in critically III patients with sepsis. *Crit Care Med* **45**: 875–882.

84. Suzuki K, Inoue S, Kametani Y, Komori Y, Chiba S, Sato T, Inokuchi S, Ogura S (2016) Reduced Immunocompetent B Cells and Increased Secondary Infection in Elderly Patients with Severe Sepsis. *Shock* **46**: 270–278.

85. Nicolai O, Pötschke C, Schmoeckel K, Darisipudi MN, van der Linde J, Raafat D, Bröker BM (2020) Antibody Production in Murine Polymicrobial Sepsis—Kinetics and Key Players. *Front Immunol* **11**: 828.

86. Mohr A, Polz J, Martin EM, Grießl S, Kammler A, Pötschke C, Lechner A, Bröker BM, Mostböck S, Männel DN (2012) Sepsis leads to a reduced antigen-specific primary

antibody response. *Eur J Immunol* **42**: 341–352.

87. Heesters BA, van der Poel CE, Das A, Carroll MC (2016) Antigen Presentation to B Cells. *Trends Immunol* **37**: 844–854.

88. Casadevall A (1998) Antibody-mediated protection against intracellular pathogens. *Trends Microbiol* **6**: 102–107.

89. Dorner T, Radbruch A (2007) Antibodies and B cell memory in viral immunity. *Immunity* **27**: 384–392.

90. Noelle RJ, Snow EC (1991) T helper cell-dependent B cell activation. *FASEB J* **5**: 2770–2776.

91. Weinstein JS, Hernandez SG, Craft J (2012) T cells that promote B-Cell maturation in systemic autoimmunity. *Immunol Rev* **247**: 160–171.

92. Yates JL, Racine R, McBride KM, Winslow GM (2013) T cell-dependent IgM memory B cells generated during bacterial infection are required for IgG responses to antigen challenge. *J Immunol* **191**: 1240–1249.

93. Noelle RJ, Ledbetter JA, Aruffo A (1992) CD40 and its ligand, an essential ligand-receptor pair for thymus-dependent B-cell activation. *Immunol Today* **13**: 431–433.

94. Noelle RJ, Roy M, Shepherd DM, Stamenkovic I, Ledbetter JA, Aruffo A (1992) A 39-kDa protein on activated helper T cells binds CD40 and transduces the signal for cognate activation of B cells. *Proc Natl Acad Sci U S A* **89**: 6550–6554.

95. MacLennan IC, Liu YJ, Johnson GD (1992) Maturation and dispersal of B-cell clones during T cell-dependent antibody responses. *Immunol Rev* **126**: 143–161.

96. Reth M (1992) Antigen receptors on B lymphocytes. *Annu Rev Immunol* **10**: 97–121.

97. Crotty S (2014) T follicular helper cell differentiation, function, and roles in disease. *Immunity* **41**: 529–542.

98. Hotchkiss RS, Karl IE (2003) The pathophysiology and treatment of sepsis. *N Engl J Med* **348**: 138–150.

99. Sepsis: Data & Reports, Last updated 2017, Accessed on 2017.

100. Gaieski DF, Edwards JM, Kallan MJ, Carr BG (2013) Benchmarking the incidence and mortality of severe sepsis in the United States. *Crit Care Med* **41**: 1167–1174.

101. Donnelly JP, Hohmann SF, Wang HE (2015) Unplanned Readmissions After Hospitalization for Severe Sepsis at Academic Medical Center–Affiliated Hospitals*. *Crit Care Med* **43**: 1916–1927.

102. Hotchkiss RS, Monneret G, Payen D (2013) Sepsis-induced immunosuppression: from cellular dysfunctions to immunotherapy. *Nat Rev Immunol* **13**: 862–874.

103. Condotta SA, Rai D, James BR, Griffith TS, Badovinac VP (2013) Sustained and incomplete recovery of naive CD8+ T cell precursors after sepsis contributes to impaired CD8+ T cell responses to infection. *J Immunol* **190**: 1991–2000.

104. Pape KA, Taylor JJ, Maul RW, Gearhart PJ, Jenkins MK (2011) Different B cell populations mediate early and late memory during an endogenous immune response. *Science (80-)* **331**: 1203–1207.

105. Taylor JJ, Pape KA, Steach HR, Jenkins MK (2015) Apoptosis and antigen affinity limit effector cell differentiation of a single naive B cell. *Science (80-)* **347**: 784–787.

106. Taylor JJ, Pape KA, Jenkins MK (2012) A germinal center-independent pathway generates unswitched memory B cells early in the primary response. *J Exp Med* **209**: 597–606.

107. Yang JA, Tubo NJ, Gearhart MD, Bardwell VJ, Jenkins MK (2015) Cutting edge: Bcl6-interacting corepressor contributes to germinal center T follicular helper cell formation and B cell helper function. *J Immunol* **194**: 5604–5608.

108. Moon JJ, Chu HH, Pepper M, McSorley SJ, Jameson SC, Kedl RMM, Jenkins MK (2007) Naive CD4(+) T cell frequency varies for different epitopes and predicts repertoire diversity and response magnitude. *Immunity* **27**: 203–213.

109. Moon JJ, Chu HH, Hataye J, Pagan AJ, Pepper M, McLachlan JB, Zell T, Jenkins MK (2009) Tracking epitope-specific T cells. *Nat Protoc* **4**: 565–581.

110. Pepper M, Pagan AJ, Igyarto BZ, Taylor JJ, Jenkins MK (2011) Opposing signals from the Bcl6 transcription factor and the interleukin-2 receptor generate T helper 1 central and effector memory cells. *Immunity* **35**: 583–595.

111. O'Sullivan ST, Lederer JA, Horgan AF, Chin DH, Mannick JA, Rodrick ML (1995) Major injury leads to predominance of the T helper-2 lymphocyte phenotype and diminished interleukin-12 production associated with decreased resistance to infection. *Ann Surg* **222**: 482.

112. Pachot A, Monneret G, Voirin N, Leissner P, Venet F, Bohé J, Payen D, Bienvenu J, Mougin B, Lepape A, et al. (2005) Longitudinal study of cytokine and immune transcription factor mRNA expression in septic shock. *Clin Immunol* **114**: 61–69.

113. Potschke C, Kessler W, Maier S, Heidecke CD, Broker BM (2013) Experimental sepsis impairs humoral memory in mice. *PLoS One* **8**: e81752.

114. Eskandari MK, Bolgos G, Miller C, Nguyen DT, DeForge LE, Remick DG (1992) Anti-tumor necrosis factor antibody therapy fails to prevent lethality after cecal ligation and puncture or endotoxemia. *J Immunol* **148**: 2724–2730.

115. Villa P, Sartor G, Angelini M, Sironi M, Conni M, Gnocchi P, Isetta AM, Grau G, Buurman W, van Tits LJ, et al. (1995) Pattern of cytokines and pharmacomodulation in sepsis induced by cecal ligation and puncture compared with that induced by endotoxin. *Clin Diagn Lab Immunol* **2**: 549–553.

116. Remick DG, Bolgos GR, Siddiqui J, Shin J, Nemzek JA (2002) Six at six: interleukin-6 measured 6 h after the initiation of sepsis predicts mortality over 3 days. *Shock* **17**: 463–467.

117. Gurung P, Rai D, Condotta SA, Babcock JC, Badovinac VP, Griffith TS (2011) Immune unresponsiveness to secondary heterologous bacterial infection after sepsis induction is

TRAIL dependent. *J Immunol* **187**: 2148–2154.

118. Danahy DB, Anthony SM, Jensen IJ, Hartwig SM, Shan Q, Xue HH, Harty JT, Griffith TS, Badovinac VP (2017) Polymicrobial sepsis impairs bystander recruitment of effector cells to infected skin despite optimal sensing and alarming function of skin resident memory CD8 T cells. *PLoS Pathog* **13**: e1006569.

119. Levy MM, Artigas A, Phillips GS, Rhodes A, Beale R, Osborn T, Vincent JL, Townsend S, Lemeshow S, Dellinger RP (2012) Outcomes of the Surviving Sepsis Campaign in intensive care units in the USA and Europe: a prospective cohort study. *Lancet Infect Dis* **12**: 919–924.

120. Rudensky Ay, Rath S, Preston-Hurlburt P, Murphy DB, Janeway Jr. CA (1991) On the complexity of self. *Nature* **353**: 660–662.

121. Wang C, Collins M, Kuchroo VK (2015) Effector T cell differentiation: are master regulators of effector T cells still the masters? *Curr Opin Immunol* **37**: 6–10.

122. Jogdand GM, Mohanty S, Devadas S (2016) Regulators of Tfh Cell Differentiation. *Front Immunol* **7**: 520.

123. HogenEsch H (2002) Mechanisms of stimulation of the immune response by aluminum adjuvants. *Vaccine* **20**: S34-9.

124. Brewer JM (2006) (How) do aluminium adjuvants work? *Immunol Lett* **102**: 10–15.

125. Chu RS, Targoni OS, Krieg AM, Lehmann P V, Harding C V (1997) CpG oligodeoxynucleotides act as adjuvants that switch on T helper 1 (Th1) immunity. *J Exp Med* **186**: 1623–1631.

126. Adderson E (2012) Infectious complications of antibody deficiency. In Long SS, Pickering LK, Prober CG (eds.), *Principles and Practice of Pediatric Infctious Diseases* pp 609–615. Elsevier Saunders, Philadelphia.

127. Krautz C, Maier SL, Brunner M, Langheinrich M, Giamarellos-Bourboulis EJ, Gogos C, Armaganidis A, Kunath F, Grutzmann R, Weber GF (2018) Reduced circulating B cells and plasma IgM levels are associated with decreased survival in sepsis - A meta-analysis. *J Crit Care* **45**: 71–75.

128. Glazer AN, Hixson CS (1977) Subunit structure and chromophore composition of rhodophytan phycoerythrins. Porphyridium cruentum B-phycoerythrin and b-phycoerythrin. *J Biol Chem* **252**: 32–42.

129. Wiethaus J, Busch AW, Dammeyer T, Frankenberg-Dinkel N (2010) Phycobiliproteins in Prochlorococcus marinus: biosynthesis of pigments and their assembly into proteins. *Eur J Cell Biol* **89**: 1005–1010.

130. Trama AM, Moody MA, Alam SM, Jaeger FH, Lockwood B, Parks R, Lloyd KE, Stolarchuk C, Scearce R, Foulger A, et al. (2014) HIV-1 envelope gp41 antibodies can originate from terminal ileum B cells that share cross-reactivity with commensal bacteria. *Cell Host Microbe* **16**: 215–226.

131. Duchmann R, May E, Heike M, Knolle P, Neurath M, Meyer zum Buschenfelde KH (1999) T cell specificity and cross reactivity towards enterobacteria, bacteroides,

bifidobacterium, and antigens from resident intestinal flora in humans. *Gut* **44**: 812–818.

132. Su LF, Kidd BA, Han A, Kotzin JJ, Davis MM (2013) Virus-specific CD4(+) memory-phenotype T cells are abundant in unexposed adults. *Immunity* **38**: 373–383.

133. Teng F, Klinger CN, Felix KM, Bradley CP, Wu E, Tran NL, Umesaki Y, Wu HJ (2016) Gut Microbiota Drive Autoimmune Arthritis by Promoting Differentiation and Migration of Peyer's Patch T Follicular Helper Cells. *Immunity* **44**: 875–888.

134. Hegazy AN, West NR, Stubbington MJT, Wendt E, Suijker KIM, Datsi A, This S, Danne C, Campion S, Duncan SH, et al. (2017) Circulating and Tissue-Resident CD4(+) T Cells With Reactivity to Intestinal Microbiota Are Abundant in Healthy Individuals and Function Is Altered During Inflammation. *Gastroenterology* **153**: 1320-1337 e16.

135. Bae JS, Lee W, Son HN, Lee YM, Kim IS (2014) Anti-transforming growth factor beta-induced protein antibody ameliorates vascular barrier dysfunction and improves survival in sepsis. *Acta Physiol* **212**: 306–315.

136. Deenick EK, Hasbold J, Hodgkin PD (1999) Switching to IgG3, IgG2b, and IgA is division linked and independent, revealing a stochastic framework for describing differentiation. *J Immunol* **163**: 4707–4714.

137. Cazac BB, Roes J (2000) TGF-beta receptor controls B cell responsiveness and induction of IgA in vivo. *Immunity* **13**: 443–451.

138. Kutza AST, Muhl E, Hackstein H, Kirchner H, Bein G (1998) High Incidence of Active Cytomegalovirus Infection Among Septic Patients. *Clin Infect Dis* **26**: 1076–1082.

139. Walton AH, Muenzer JT, Rasche D, Boomer JS, Sato B, Brownstein BH, Pachot A, Brooks TL, Deych E, Shannon WD, et al. (2014) Reactivation of multiple viruses in patients with sepsis. *PLoS One* **9**: 1–13.

140. Recommended immunization schedule for adults aged 19 years or older, United States, 2018, Last updated 2018, Accessed on 2018.

141. Brun-Buisson C, Doyon F, Carlet J, Dellamonica P, Gouin F, Lepoutre A, Mercier JC, Offenstadt G, Regnier B (1995) Incidence, risk factors, and outcome of severe sepsis and septic shock in adults. A multicenter prospective study in intensive care units. French ICU Group for Severe Sepsis. *JAMA* **274**: 968–974.

142. Levy MM, Fink MP, Marshall JC, Abraham E, Angus D, Cook D, Cohen J, Opal SM, Vincent JL, Ramsay G, et al. (2001) 2001 SCCM/ESICM/ACCP/ATS/SIS International Sepsis Definitions Conference. *Intensive Care Med* **29**: 530–538.

143. Sasser SM, Varghese M, Joshipura M, Kellermann A (2006) Preventing death and disability through the timely provision of prehospital trauma care. *Bull World Heal Organ* **84**: 507.

144. Probst C, Pape HC, Hildebrand F, Regel G, Mahlke L, Giannoudis P, Krettek C, Grotz MR (2009) 30 years of polytrauma care: An analysis of the change in strategies and results of 4849 cases treated at a single institution. *Injury* **40**: 77–83.

145. Probst C, Zelle BA, Sittaro NA, Lohse R, Krettek C, Pape HC (2009) Late death after multiple severe trauma: when does it occur and what are the causes? *J Trauma* **66**: 1212–

1217.

146. Gentile LF, Cuenca AG, Efron PA, Ang D, Bihorac A, McKinley BA, Moldawer LL, Moore FA (2012) Persistent inflammation and immunosuppression: a common syndrome and new horizon for surgical intensive care. *J Trauma Acute Care Surg* **72**: 1491–1501.

147. Unsinger J, Kazama H, McDonough JS, Hotchkiss RS, Ferguson TA (2009) Differential lymphopenia-induced homeostatic proliferation for CD4+ and CD8+ T cells following septic injury. *J Leukoc Biol* **85**: 382–390.

148. Kaech SM, Wherry EJ, Ahmed R (2002) Effector and memory T-cell differentiation: implications for vaccine development. *Nat Rev Immunol* **2**: 251–262.

149. Harty JT, Badovinac VP (2008) Shaping and reshaping CD8+ T-cell memory. *Nat Rev Immunol* **8**: 107–119.

150. Schenkel JM, Masopust D (2014) Tissue-resident memory T cells. *Immunity* **41**: 886–897.

151. Beura LK, Fares-Frederickson NJ, Steinert EM, Scott MC, Thompson EA, Fraser KA, Schenkel JM, Vezys V, Masopust D (2019) CD4(+) resident memory T cells dominate immunosurveillance and orchestrate local recall responses. *J Exp Med* **216**: 1214–1229.

152. Taylor JJ, Jenkins MK (2011) CD4+ memory T cell survival. *Curr Opin Immunol* **23**: 319–323.

153. Condotta SA, Cabrera-Perez J, Badovinac VP, Griffith TS (2013) T-cell-mediated immunity and the role of TRAIL in sepsis-induced immunosuppression. *Crit Rev Immunol* **33**: 23–40.

154. Huggins MA, Sjaastad F V, Pierson M, Kucaba TA, Swanson W, Staley C, Weingarden AR, Jensen IJ, Danahy DB, Badovinac VP, et al. (2019) Microbial Exposure Enhances Immunity to Pathogens Recognized by TLR2 but Increases Susceptibility to Cytokine Storm through TLR4 Sensitization. *Cell Rep* **28**: 1729-1743 e5.

155. Goldberg MF, Roeske EK, Ward LN, Pengo T, Dileepan T, Kotov DI, Jenkins MK (2018) Salmonella Persist in Activated Macrophages in T Cell-Sparse Granulomas but Are Contained by Surrounding CXCR3 Ligand-Positioned Th1 Cells. *Immunity* **49**: 1090-1102 e7.

156. Pagan AJ, Pepper M, Chu HH, Green JM, Jenkins MK (2012) CD28 promotes CD4+ T cell clonal expansion during infection independently of its YMNM and PYAP motifs. *J Immunol* **189**: 2909–2917.

157. Nelson RW, McLachlan JB, Kurtz JR, Jenkins MK (2013) CD4+ T cell persistence and function after infection are maintained by low-level peptide:MHC class II presentation. *J Immunol* **190**: 2828–2834.

158. Brown R, Bancewicz J, Hamid J, Patel NJ, Ward CA, Farrand RJ, Pumphrey RS, Irving M (1982) Failure of delayed hypersensitivity skin testing to predict postoperative sepsis and mortality. *Br Med J (Clin Res Ed)* **284**: 851–853.

159. Meakins JL, Christou N V, Bohnen J, MacLean LD (1982) Failure of delayed hypersensitivity skin testing to predict postoperative sepsis and mortality. *Br Med J (Clin Res Ed)* **285**: 1207–1208.

160. Vissinga C, Nagelkerken L, Zijlstra J, Hertogh-Huijbregts A, Boersma W, Rozing J (1990) A decreased functional capacity of CD4+ T cells underlies the impaired DTH reactivity in old mice. *Mech Ageing Dev* **53**: 127–139.

161. Condotta SA, Khan SH, Rai D, Griffith TS, Badovinac VP (2015) Polymicrobial Sepsis Increases Susceptibility to Chronic Viral Infection and Exacerbates CD8+ T Cell Exhaustion. *J Immunol* **195**: 116–125.

162. McDermott DS, Varga SM (2011) Quantifying antigen-specific CD4 T cells during a viral infection: CD4 T cell responses are larger than we think. *J Immunol* **187**: 5568–5576.

163. Kotov DI, Kotov JA, Goldberg MF, Jenkins MK (2018) Many Th Cell Subsets Have Fas Ligand-Dependent Cytotoxic Potential. *J Immunol* **200**: 2004–2012.

164. Benoun JM, Peres NG, Wang N, Pham OH, Rudisill VL, Fogassy ZN, Whitney PG, Fernandez-Ruiz D, Gebhardt T, Pham QM, et al. (2018) Optimal protection against Salmonella infection requires noncirculating memory. *Proc Natl Acad Sci U S A* **115**: 10416–10421.

165. Hess J, Ladel C, Miko D, Kaufmann SH (1996) Salmonella typhimurium aroA- infection in gene-targeted immunodeficient mice: major role of CD4+ TCR-alpha beta cells and IFN-gamma in bacterial clearance independent of intracellular location. *J Immunol* **156**: 3321–3326.

166. Monack DM, Mueller A, Falkow S (2004) Persistent bacterial infections: the interface of the pathogen and the host immune system. *Nat Rev Microbiol* **2**: 747–765.

167. Johanns TM, Ertelt JM, Lai JC, Rowe JH, Avant RA, Way SS (2010) Naturally occurring altered peptide ligands control Salmonella-specific CD4+ T cell proliferation, IFN-gamma production, and protective potency. *J Immunol* **184**: 869–876.

168. Johanns TM, Ertelt JM, Rowe JH, Way SS (2010) Regulatory T cell suppressive potency dictates the balance between bacterial proliferation and clearance during persistent Salmonella infection. *PLoS Pathog* **6**: e1001043.

169. Marzo AL, Vezys V, Williams K, Tough DF, Lefrancois L (2002) Tissue-level regulation of Th1 and Th2 primary and memory CD4 T cells in response to Listeria infection. *J Immunol* **168**: 4504–4510.

170. Delano MJ, Thayer T, Gabrilovich S, Kelly-Scumpia KM, Winfield RD, Scumpia PO, Cuenca AG, Warner E, Wallet SM, Wallet MA, et al. (2011) Sepsis induces early alterations in innate immunity that impact mortality to secondary infection. *J Immunol* **186**: 195–202.

171. Condotta SA, Richer MJ, Badovinac VP, Harty JT (2012) Probing CD8 T cell responses with Listeria monocytogenes infection. *Adv Immunol* **113**: 51–80.

172. Brocke S, Hahn H (1991) Heat-killed Listeria monocytogenes and L. monocytogenes soluble antigen induce clonable CD4+ T lymphocytes with protective and chemotactic activities in vivo. *Infect Immun* **59**: 4531–4539.

173. Harty JT, Schreiber RD, Bevan MJ (1992) CD8 T cells can protect against an intracellular bacterium in an interferon gamma-independent fashion. *Proc Natl Acad Sci U S A* **89**:

11612–11616.

174. Bhardwaj V, Kanagawa O, Swanson PE, Unanue ER (1998) Chronic Listeria infection in SCID mice: requirements for the carrier state and the dual role of T cells in transferring protection or suppression. *J Immunol* **160**: 376–384.

175. Vincent JL, Marshall JC, Namendys-Silva SA, Francois B, Martin-Loeches I, Lipman J, Reinhart K, Antonelli M, Pickkers P, Njimi H, et al. (2014) Assessment of the worldwide burden of critical illness: the intensive care over nations (ICON) audit. *Lancet Respir Med* **2**: 380–386.

176. Cohen J, Vincent JL, Adhikari NK, Machado FR, Angus DC, Calandra T, Jaton K, Giulieri S, Delaloye J, Opal S, et al. (2015) Sepsis: a roadmap for future research. *Lancet Infect Dis* **15**: 581–614.

177. Le Gros G, Ben-Sasson SZ, Seder R, Finkelman FD, Paul WE (1990) Generation of interleukin 4 (IL-4)-producing cells in vivo and in vitro: IL-2 and IL-4 are required for in vitro generation of IL-4-producing cells. *J Exp Med* **172**: 921–929.

178. Hsieh CS, Heimberger AB, Gold JS, O'Garra A, Murphy KM (1992) Differential regulation of T helper phenotype development by interleukins 4 and 10 in an alpha beta T-cell-receptor transgenic system. *Proc Natl Acad Sci U S A* **89**: 6065–6069.

179. Baker CC, Miller CL, Trunkey DD, Lim Jr. RC (1979) Identity of mononuclear cells which compromise the resistance of trauma patients. *J Surg Res* **26**: 478–487.

180. Hansbrough JF, Bender EM, Zapata-Sirvent R, Anderson J (1984) Altered helper and suppressor lymphocyte populations in surgical patients. A measure of postoperative immunosuppression. *Am J Surg* **148**: 303–307.

181. Uzzaman A, Cho SH (2012) Chapter 28: Classification of hypersensitivity reactions. *Allergy Asthma Proc* **33 Suppl 1**: S96-9.

182. Hamilton SE, Badovinac VP, Beura LK, Pierson M, Jameson SC, Masopust D, Griffith TS (2020) New Insights into the Immune System Using Dirty Mice. *J Immunol* **205**: 3–11.

183. Grayson JM, Harrington LE, Lanier JG, Wherry EJ, Ahmed R (2002) Differential sensitivity of naive and memory CD8+ T cells to apoptosis in vivo. *J Immunol* **169**: 3760–3770.

184. Unsinger J, McGlynn M, Kasten KR, Hoekzema AS, Watanabe E, Muenzer JT, McDonough JS, Tschoep J, Ferguson TA, McDunn JE, et al. (2010) IL-7 promotes T cell viability, trafficking, and functionality and improves survival in sepsis. *J Immunol* **184**: 3768–3779.

185. Serbanescu MA, Ramonell KM, Hadley A, Margoles LM, Mittal R, Lyons JD, Liang Z, Coopersmith CM, Ford ML, McConnell KW (2016) Attrition of memory CD8 T cells during sepsis requires LFA-1. *J Leukoc Biol* **100**: 1167–1180.

186. Danahy DB, Strother RK, Badovinac VP, Griffith TS (2016) Clinical and Experimental Sepsis Impairs CD8 T-Cell-Mediated Immunity. *Crit Rev Immunol* **36**: 57–74.

187. Inoue S, Unsinger J, Davis CG, Muenzer JT, Ferguson TA, Chang K, Osborne DF, Clark AT, Coopersmith CM, McDunn JE, et al. (2010) IL-15 Prevents Apoptosis, Reverses

Innate and Adaptive Immune Dysfunction, and Improves Survival in Sepsis. *J Immunol* **184**: 1401–1409.

188. Stieglitz D, Schmid T, Chhabra NF, Echtenacher B, Männel DN, Mostböck S (2015) TNF and regulatory T cells are critical for sepsis-induced suppression of T cells. *Immun Inflamm Dis* **3**: 374–385.

189. Rimmelé T, Payen D, Cantaluppi V, Marshall J, Gomez H, Gomez A, Murray P, Kellum JA (2016) Immune cell phenotype and function in sepsis. *Shock* **45**: 282–291.

190. Hall MW, Knatz NL, Vetterly C, Tomarello S, Wewers MD, Volk HD, Carcillo JA (2011) Immunoparalysis and nosocomial infection in children with multiple organ dysfunction syndrome. *Intensive Care Med* **37**: 525–532.

191. Goldenberg NM, Leligdowicz A, Slutsky AS, Friedrich JO, Lee WL (2014) Is nosocomial infection really the major cause of death in sepsis? **18**: 540.

192. Daviaud F, Grimaldi D, Dechartres A, Charpentier J, Geri G, Marin N, Chiche J, Cariou A, Mira J, Pène F (2015) Timing and causes of death in septic shock. *Ann Intensive Care* **5**: 16.

193. Zhao G, Li D, Zhao Q, Song J, Chen X, Hong G, Li M, Wu B, Lu Z (2016) Incidence , risk factors and impact on outcomes of secondary infection in patients with septic shock : an 8-year retrospective study. *Nat Publ Gr* **64**: 1–9.

194. Robertson CM, Perrone EE, McConnell KW, Dunne WM, Boody B, Brahmbhatt T, Diacovo MJ, Van Rooijen N, Hogue LA, Cannon CL, et al. (2008) Neutrophil Depletion Causes a Fatal Defect in Murine Pulmonary Staphylococcus aureus clearance. *J Surg Res* **150**: 278–285.

195. Muller B, Grossniklaus U (2010) Model organisms--A historical perspective. *J Proteomics* **73**: 2054–2063.

196. Doudna JA, Charpentier E (2014) Genome editing. The new frontier of genome engineering with CRISPR-Cas9. *Science (80-)* **346**: 1258096.

197. Masopust D, Sivula CP, Stephen C, Masopust D, Sivula CP, Jameson SC (2020) Of Mice, Dirty Mice, and Men: Using Mice To Understand Human Immunology. **199**: 383–388.

198. Reese TA, Bi K, Kambal A, Filali-Mouhim A, Beura LK, Burger MC, Pulendran B, Sekaly RP, Jameson SC, Masopust D, et al. (2016) Sequential Infection with Common Pathogens Promotes Human-like Immune Gene Expression and Altered Vaccine Response. *Cell Host Microbe* **19**: 713–719.

199. Hamilton SE, Wolkers MC, Schoenberger SP, Jameson SC (2006) The generation of protective memory-like CD8+ T cells during homeostatic proliferation requires CD4+ T cells. *Nat Immunol* **7**: 475–481.

200. Claesson MJ, Wang Q, O'Sullivan O, Greene-Diniz R, Cole JR, Ross RP, O'Toole PW (2010) Comparison of two next-generation sequencing technologies for resolving highly complex microbiota composition using tandem variable 16S rRNA gene regions. *Nucleic Acids Res* **38**: e200.

201. Leinonen R, Sugawara H, Shumway M, International Nucleotide Sequence Database C

(2011) The sequence read archive. *Nucleic Acids Res* **39**: D19-21.

202. Simons MP, Moore JM, Kemp TJ, Griffith TS (2007) Identification of the mycobacterial subcomponents involved in the release of tumor necrosis factor-related apoptosis-inducing ligand from human neutrophils. *Infect Immun* **75**: 1265–1271.

203. Inaba K, Swiggard WJ, Steinman RM, Romani N, Schuler G, Brinster C (2001) Isolation of dendritic cells. *Curr Protoc Immunol* Chapter 3:Unit 3.7.

204. Steinman RM, Kaplan G, Witmer MD, Cohn ZA (1979) Identification of a novel cell type in peripheral lymphoid organs of mice: V. Purification of spleen dendritic cells, new surface markers, and maintenance in vitro. *J Exp Med* **149**: 1–16.

205. Schloss PD, Westcott SL, Ryabin T, Hall JR, Hartmann M, Hollister EB, Lesniewski RA, Oakley BB, Parks DH, Robinson CJ, et al. (2009) Introducing mothur: Open-source, platform-independent, community-supported software for describing and comparing microbial communities. *Appl Environ Microbiol* **75**: 7537–7541.

206. Staley C, Kaiser T, Vaughn BP, Graiziger CT, Hamilton MJ, Rehman TU, Song K, Khoruts A, Sadowsky MJ (2018) Predicting recurrence of Clostridium difficile infection following encapsulated fecal microbiota transplantation. *Microbiome* **6**: 166.

207. Huse SM, Welch DM, Morrison HG, Sogin ML (2010) Ironing out the wrinkles in the rare biosphere through improved OTU clustering. *Environ Microbiol* **12**: 1889–1898.

208. Edgar RC, Haas BJ, Clemente JC, Quince C, Knight R (2011) UCHIME improves sensitivity and speed of chimera detection. *Bioinformatics* **27**: 2194–2200.

209. Bray JR, Curtis JT (1957) An Ordination of the Upland Forest Communities of Southern Wisconsin. *Ecol Monogr* **27**: 325–349.

210. Knights D, Kuczynski J, Charlson ES, Zaneveld J, Mozer MC, Collman RG, Bushman FD, Knight R, Kelley ST (2011) Bayesian community-wide culture-independent microbial source tracking. *Nat Methods* **8**: 761–763.

211. Markwart R, Condotta SA, Requardt RP, Borken F, Schubert K, Weigel C, Bauer M, Griffith TS, Forster M, Brunkhorst FM, et al. (2014) Immunosuppression after sepsis: systemic inflammation and sepsis induce a loss of naive T-cells but no enduring cell-autonomous defects in T-cell function. *PLoS One* **9**: e115094.

212. Anderson MJ, Willis TJ (2003) Canonical analysis of principal coordinates: A useful method of constrained ordination for ecology. *Ecology* **84**: 511–525.

213. Wherry EJ, Teichgraber V, Becker TC, Masopust D, Kaech SM, Antia R, von Andrian UH, Ahmed R (2003) Lineage relationship and protective immunity of memory CD8 T cell subsets. *Nat Immunol* **4**: 225–234.

214. Olson JA, McDonald-Hyman C, Jameson SC, Hamilton SE (2013) Effector-like CD8(+) T cells in the memory population mediate potent protective immunity. *Immunity* **38**: 1250–1260.

215. Barton ES, White DW, Cathelyn JS, Brett-McClellan KA, Engle M, Diamond MS, Miller VL, Virgin IV HW (2007) Herpesvirus latency confers symbiotic protection from bacterial infection. *Nature* **447**: 326–329.

216. Harty JT, Bevan MJ (1995) Specific immunity to Listeria monocytogenes in the absence of IFN gamma. *Immunity* **3**: 109–117.

217. Lertmemongkolchai G, Cai G, Hunter CA, Bancroft GJ (2001) Bystander Activation of CD8 + T Cells Contributes to the Rapid Production of IFN-γ in Response to Bacterial Pathogens. *J Immunol* **166**: 1097–1105.

218. Haring JS, Badovinac VP, Harty JT (2006) Inflaming the CD8+ T cell response. *Immunity* **25**: 19–29.

219. Danahy DB, Jensen IJ, Griffith TS, Badovinac VP (2019) Cutting Edge: Polymicrobial Sepsis Has the Capacity to Reinvigorate Tumor-Infiltrating CD8 T Cells and Prolong Host Survival. *J Immunol* **202**: 2843–2848.

220. Cabrera-Perez J, Badovinac VP, Griffith TS (2017) Enteric immunity, the gut microbiome, and sepsis: Rethinking the germ theory of disease. *Exp Biol Med* **242**: 127–139.

221. Chousterman BG, Swirski FK, Weber GF (2017) Cytokine storm and sepsis disease pathogenesis. *Semin Immunopathol* **39**: 517–528.

222. Thiemann S, Smit N, Roy U, Lesker TR, Gálvez EJC, Helmecke J, Basic M, Bleich A, Goodman AL, Kalinke U, et al. (2017) Enhancement of IFNγ Production by Distinct Commensals Ameliorates Salmonella-Induced Disease. *Cell Host Microbe* **21**: 682-694.e5.

223. Mai V, Torrazza RM, Ukhanova M, Wang X, Sun Y, Li N, Shuster J, Sharma R, Hudak ML, Neu J (2013) Distortions in Development of Intestinal Microbiota Associated with Late Onset Sepsis in Preterm Infants. *PLoS One* **8**: e52876.

224. Beutler BA (2009) TLRs and innate immunity. *Blood* **113**: 1399–1407.

225. Kawasaki T, Kawai T (2014) Toll-like receptor signaling pathways. *Front Immunol* **5**: 461.

226. Akira S, Takeda K, Kaisho T (2001) Toll-like receptors: critical proteins linking innate and acquired immunity. *Nat Immunol* **2**: 675–680.

227. Takeda K, Akira S (2001) Regulation of innate immune responses by Toll-like receptors. *Jpn J Infect Dis* **54**: 209–219.

228. Takeda K, Akira S (2001) Roles of Toll-like receptors in innate immune responses. *Genes Cells* **6**: 733–742.

229. Takeda K, Kaisho T, Akira S (2003) Toll-Like Receptors. *Annu Rev Immunol* **21**: 335–376.

230. Heipertz EL, Harper J, Lopez CA, Fikrig E, Hughes ME, Walker WE (2018) Circadian Rhythms Influence the Severity of Sepsis in Mice via a TLR2-Dependent, Leukocyte-Intrinsic Mechanism. *J Immunol* **201**: 193–201.

231. Lima CX, Souza DG, Amaral FA, Fagundes CT, Rodrigues IPS, Alves-Filho JC, Kosco-Vilbois M, Ferlin W, Shang L, Elson G, et al. (2015) Therapeutic effects of treatment with anti-TLR2 and anti-TLR4 monoclonal antibodies in polymicrobial sepsis. *PLoS One* **10**:

e0132336.

232. Oliveira-Nascimento L, Massari P, Wetzler LM (2012) The role of TLR2 ininfection and immunity. *Front Immunol* **3**: 79.

233. Kawai T, Akira S (2011) Toll-like Receptors and Their Crosstalk with Other Innate Receptors in Infection and Immunity. *Immunity* **34**: 637–650.

234. Remick DG, Newcomb DE, Bolgos GL, Call DR (2000) Comparison of the mortality and inflammatory response of two models of sepsis: lipopolysaccharide vs. cecal ligation and puncture. *Shock* **13**: 110–116.

235. Huggins MA, Jameson SC, Hamilton SE (2019) Embracing microbial exposure in mouse research. *J Leukoc Biol* **105**: 73–79.

236. Foster SL, Hargreaves DC, Medzhitov R (2007) Gene-specific control of inflammation by TLR-induced chromatin modifications. *Nature* **447**: 972–978.

237. Netea MG, Joosten LAB, Latz E, Mills KHG, Natoli G, Stunnenberg HG, O'Neill LAJ, Xavier RJ (2016) Trained immunity: A program of innate immune memory in health and disease. *Science (80-)* **352**: aaf1098.

238. Quintin J, Saeed S, Martens J, Giamarellos-Bourboulis E, Ifrim D, Logie C, Kullberg B, Joosten L, Xavier R, Stunnenberg H, et al. (2012) Candida albicans induces monocyte training via epigenetic reprogramming through a dectin-1-dependent pathway. *Cell Host Microbe* **12**: 10.

239. Kollmann TR, Crabtree J, Rein-Weston A, Blimkie D, Thommai F, Wang XY, Lavoie PM, Furlong J, Fortuno ES, Hajjar AM, et al. (2009) Neonatal Innate TLR-Mediated Responses Are Distinct from Those of Adults. *J Immunol* **183**: 7150–7160.

240. Pedraza-Sańchez S, Hise AG, Ramachandra L, Arechavaleta-Velasco F, King CL (2013) Reduced frequency of a CD14+ CD16+ monocyte subset with high toll-like receptor 4 expression in cord blood compared to adult blood contributes to lipopolysaccharide hyporesponsiveness in newborns. *Clin Vaccine Immunol* **20**: 962–971.

241. Chipeta J, Komada Y, Zhang XL, Deguchi T, Sugiyama K, Azuma E, Sakurai M (1998) CD4+ and CD8+ cell cytokine profiles in neonates, older children, and adults: increasing T helper type 1 and T cytotoxic type 1 cell populations with age. *Cell Immunol* **183**: 149–156.

242. Gasparoni A, Ciardelli L, Avanzini A, Castellazzi AM, Carini R, Rondini G, Chirico G (2003) Age-related changes in intracellular TH1/TH2 cytokine production, immunoproliferative T lymphocyte response and natural killer cell activity in newborns, children and adults. *Biol Neonate* **84**: 297–303.

243. Hartel C, Adam N, Strunk T, Temming P, Muller-Steinhardt M, Schultz C (2005) Cytokine responses correlate differentially with age in infancy and early childhood. *Clin Exp Immunol* **142**: 446–453.

244. Berg RE, Crossley E, Murray S, Forman J (2003) Memory CD8+ T cells provide innate immune protection against Listeria monocytogenes in the absence of cognate antigen. *J Exp Med* **198**: 1583–1593.

245. Berg RE, Crossley E, Murray S, Forman J (2005) Relative contributions of NK and CD8 T cells to IFN-gamma mediated innate immune protection against Listeria monocytogenes. *J Immunol* **175**: 1751–1757.

246. Akira S, Uematsu S, Takeuchi O (2006) Pathogen recognition and innate immunity. *Cell* **124**: 783–801.

247. McCall MBB, Netea MG, Hermsen CC, Jansen T, Jacobs L, Golenbock D, van der Ven AJAM, Sauerwein RW (2007) Plasmodium falciparum Infection Causes Proinflammatory Priming of Human TLR Responses. *J Immunol* **179**: 162–171.

248. Franklin BS, Parroche P, Ataíde MA, Lauw F, Ropert C, De Oliveira RB, Pereira D, Tada MS, Nogueira P, Da Silva LHP, et al. (2009) Malaria primes the innate immune response due to interferon-γ induced enhancement of toll-like receptor expression and function. *Proc Natl Acad Sci U S A* **106**: 5789–5794.

249. Hack CE, De Groot ER, Felt-Bersma RJ, Nuijens JH, Strack Van Schijndel RJ, Eerenberg-Belmer AJ, Thijs LG, Aarden LA (1989) Increased plasma levels of interleukin-6 in sepsis. *Blood* **74**: 1704–1710.

250. Waage A, Brandtzaeg P, Halstensen A, Kierulf P, Espevik T (1989) The complex pattern of cytokines in serum from patients with meningococcal septic shock. Association between interleukin 6, interleukin 1, and fatal outcome. *J Exp Med* **169**: 333–338.

251. Zanotti S, Kumar A, Kumar A (2002) Cytokine modulation in sepsis and septic shock. *Expert Opin Investig Drugs* **11**: 1061–1075.

252. Shindo Y, Fuchs AG, Davis CG, Eitas T, Unsinger J, Burnham CD, Green JM, Morre M, Bochicchio G V, Hotchkiss RS (2017) Interleukin 7 immunotherapy improves host immunity and survival in a two-hit model of Pseudomonas aeruginosa pneumonia. *J Leuk Biol* **101**: 543–554.

253. Shindo Y, Unsinger J, Burnham C, Green JM, Hotchkiss RS (2015) Interleukin 7 and anti-programmed cell death 1 antibody have differing effects to reverse sepsis-induced immunosuppression. *Shock* **43**: 334–343.

254. Venet F, Demaret J, Blaise BJ, Rouget C, Girardot T, Idealisoa E, Rimmelé T, Mallet F, Lepape A, Textoris J, et al. (2017) IL-7 Restores T Lymphocyte Immunometabolic Failure in Septic Shock Patients through mTOR Activation. *J Immunol* **199**: 1606–1615.

255. Venet F, Foray AP, Villars-Mechin A, Malcus C, Poitevin-Later F, Lepape A, Monneret G, Fabienne Venet, Anne-Perrine Foray, Astrid Villars-Méchin, Christophe Malcus, Françoise Poitevin-Later AL and GM (2012) IL-7 restores lymphocyte functions in septic patients. *J Immunol* **189**: 5073–5081.

256. West EE, Jin H-T, Rasheed A-U, Penaloza-MacMaster P, Ha S-J, Tan WG, Youngblood B, Freeman GJ, Smith K. A, Ahmed R (2013) PD-L1 blockade synergizes with IL-2 therapy in reinvigorating exhausted T cells. *J Clin Invest* **123**: 2604–2615.

257. Fink MP (2014) Animal models of sepsis. *Virulence* **5**: 143–153.

258. Belkaid Y, Hand TW (2014) Role of the microbiota in immunity and inflammation. *Cell* **157**: 121–141.

259. Kamada N, Seo SU, Chen GY, Núñez G (2013) Role of the gut microbiota in immunity and inflammatory disease. *Nat Rev Immunol* **13**: 321–335.

260. Stortz JA, Raymond SL, Mira JC, Moldawer LL, Mohr AM, Efron PA (2017) Murine Models of Sepsis and Trauma: Can We Bridge the Gap? *ILAR J* **58**: 90–105.

261. Warren HS, Fitting C, Hoff E, Adib-Conquy M, Beasley-Topliffe L, Tesini B, Liang X, Valentine C, Hellman J, Hayden D, et al. (2010) Resilience to bacterial infection: Difference between species could Be due to proteins in serum. *J Infect Dis* **201**: 223–232.

262. Rosshart SP, Vassallo BG, Angeletti D, Hutchinson DS, Morgan AP, Takeda K, Hickman HD, McCulloch JA, Badger JH, Ajami NJ, et al. (2017) Wild Mouse Gut Microbiota Promotes Host Fitness and Improves Disease Resistance. *Cell* **171**: 1015-1028.E13.

263. Gupta S, Bi R, Gollapudi S (2005) Central memory and effector memory subsets of human CD4+ and CD8+ T cells display differential sensitivity to TNF-α-induced apoptosis. *Ann N Y Acad Sci* **1050**: 108–114.

264. Takao K, Miyakawa T (2015) Genomic responses in mouse models greatly mimic human inflammatory diseases. *Proc Natl Acad Sci U S A* **112**: 1167–1172.

265. Seok J, Warren HS, Cuenca AG, Mindrinos MN, Baker H V, Xu W, Richards DR, McDonald-Smith GP, Gao H, Hennessy L, et al. (2013) Genomic responses in mouse models poorly mimic human inflammatory diseases. *Proc Natl Acad Sci U S A* **110**: 3507–3512.

266. Guillon A, Preau S, Aboab J, Azabou E, Jung B, Silva S, Textoris J, Uhel F, Vodovar D, Zafrani L, et al. (2019) Preclinical septic shock research: why we need an animal ICU. *Ann Intensive Care* **9**: 66.